Dissertation

Comprehensive studies of Yukawa couplings on magnetized toroidal orbifolds

Yoshiyuki TATSUTA

February, 2017

Dissertation

Comprehensive studies of Yukawa couplings on magnetized toroidal orbifolds

Waseda University

Graduate School of Advanced Science and Engineering,

Department of Pure and Applied Physics,

Research on Theoretical Particle Physics

Yoshiyuki TATSUTA

February, 2017

Acknoledgement

First, I would like to sincerely thank Prof. Hiroyuki Abe for his generous hospitality as my supervisor and fruitful discussions. I would also like to sincerely thank Prof. Tatsuo Kobayashi, Prof. Makoto Sakamoto, Prof. Tetsutaro Higaki, Hiroshi Ohki, Kenji Nishiwaki, Yusuke Shimizu, Yukihiro Fujimoto, Keigo Sumita, Akio Tomiya and Shohei Uemura for valuable correspondences during the research collaborations.

I am quite grateful for Prof. Wilfried Buchmüller, Prof. Stephen King, Prof. Joe Sato, Prof. Fuminobu Takahashi, Yutaka Ookouchi, Prof. Masahiro Ibe, Prof. Yutaka Sakamura, Masafumi Kurachi, Shinya Matsuzaki, Koji Tsumura, Prof. Yuji Omura, Kyu Jung Bae, Hiroyuki Ishida, Natsumi Nagata, Tomohiro Fujita, Keisuke Harigaya, Teppei Kitahara, Kyohei Mukaida, Takahiro Terada, Yuta Hamada, Masaki Yamada and Yuichiro Tada for useful comments and discussions in various workshops, conferences and JSPS meetings and so forth.

In particular, I would like to thank Emeritus Prof. Shin'ichi Ishiwata for his very kind supports to my request of changing departments.

I acknowledge Emeritus Prof. Ichiro Ohba, Prof. Hiromichi Nakazato and Prof. Kazuya Yuasa for comments in our laboratory's journal clubs, spring and summer schools.

Abstract

Superstring theory is a unique known candidate for consistent unified theory including gravitational interactions and has no theoretical inconsistency so far. It is known to be defined in ten-dimensional spacetime (10D), and this predicts that there exist extra six dimensions compactified on some compact space. It is also known that geometrical properties of compact six dimensions determine masses and couplings in the four-dimensional effective field theory (4D EFT) after dimensional reductions.

We study magnetized 10D supersymmetric Yang–Mills theory appearing as the low-energy effective field theory of type IIB superstring theory and assume that extra six dimensions are compactificated on a product of multiple two dimensional tori, toroidal orbifolds or their combination(s). Toroidal orbifold is the 'mainifold' with extra boundary condition(s) in addition to toroidal periodic boundary conditions. Thanks to magnetic fluxes in such compact spaces, chiral matters, their family replications and hierarchical Yukawa couplings appear in the 4D EFT. Thus, it is quite important to be familiar with geometrical properties of magnetized toroidal orbifolds, and also to reveal their phenomenological aspects for the purpose of theoretical model buildings. Accordingly, we pursuit the possibility of realizing promising phenomenological models, e.g., the standard model (SM) of particle physics and the minimal supersymmetric standard model (MSSM), which can lead to realizations of much more realistic observables.

Dedicated to my parents and grand mothers.

Contents

1 Overture **1**

2 Brief reviews of magnetic fluxes **5**
2.1 Toroidal compactification and magnetic fluxes 5
2.2 Extensions to toroidal orbifolds 13

3 Classification of three-generation models **19**
3.1 Strategy for classification 19
3.2 Results of the classification 23

4 Systematic analysis of Yukawa hierarchies **29**
4.1 Motivation for investigating Yukawa hierarchies 29
4.2 One-Higgs-pair case 31
4.3 Two-Higgs-pair case 38

5 Gaussian Froggatt–Nielsen mechanism **45**
5.1 Supersymmetry 45
5.2 Model construction 46
5.3 Gaussian Froggatt–Nielsen mechanism 51
5.4 10D embedding and D-term contributions 60
5.5 The other configurations for the Gaussian FN mechanism 63

6 Coda **67**

A Explicit expressions of the expansion coefficients **69**
A T^2/Z_2 69
A.1 $(\alpha, \beta) = (0, 0)$ case 70
A.2 $(\alpha, \beta) = (\frac{1}{2}, 0)$ case 70
A.3 $(\alpha, \beta) = (0, \frac{1}{2})$ case 70
A.4 $(\alpha, \beta) = (\frac{1}{2}, \frac{1}{2})$ case 70
B T^2/Z_3 71
C T^2/Z_4 72
D T^2/Z_6 73

B The full results of systematic search on the T^2/Z_2 orbifold 75

Chapter 1

Overture

The standard model (SM) of elementary particle physics has been completed by the discovery of the Higgs boson [1, 2], and it is known that the SM is a quite successful theory which can explain almost all of phenomena around the electroweak scale with great accuracy.

The SM gauge group is $SU(3)_C \times SU(2)_L \times U(1)_Y$, and their gauge theories can describe the phenomena related to three types of forces, i.e., the strong force between quarks in protons, the weak force in the beta decay and the electromagnetic force between electromagnetically charged matters. In spite of the brilliant success of the SM of elementary particle physics, there are several phenomena which can not be explained in the framework of the SM. For example,

- *the dark matter: there is no candidate for the dark matter in the SM particles,*
- *the gauge hierarchy problem: the electroweak scale is not stable under large loop corrections to the Higgs boson mass,*
- *the flavor puzzle: the origin of the flavor structures among the SM quarks and leptons is still unrevealed,*

and so forth. In order to solve the above problems, various phenomenological models have been proposed and investigated constantly in a long history since the SM was proposed. Also, there still exist several theoretical difficulties in the SM. In particular, it is difficult to understand the origin(s) of the SM structures, e.g., the SM gauge group, the family replications of quarks and leptons and the concrete values of the Yukawa coupling constants. Indeed, the SM can describe almost all of phenomena among the three-generations of quarks and leptons with great accuracy, however, the reason that there exist such *"replicas"* of the SM quarks and leptons carrying the same charges under the SM gauge group is still unknown within the framework of the SM. The mysterious replicas of quarks and charged leptons have large hierarchical masses and non-trivial mixing angles between their generations according to more recent experimental data [3]. In fact, almost all input parameters in the SM of elementary particles are known to be coupling constants in the

Yukawa-type interaction terms among quarks, leptons and the Higgs boson. Such Yukawa coupling constants are directly incorporated into the mass matrices among the SM quarks and leptons after the Higgs boson acquires its (non-zero) vacuum expectation value (VEV) at the bottom of a wine-bottle-type Higgs potential, and the Yukawa coupling constants should lead to the observed masses and mixing angles of quarks and leptons in the SM. However, concrete structures in the mass matrices, i.e., the values of the Yukawa coupling constants are still experimentally unrevealed and ambiguous so far. This is called *"the flavor puzzle"* or *"the flavor problem"*. Indeed, there are many approaches to explain the concrete structures in the mass matrices of the SM fermions in bottom-up approaches of four dimensional (4D) spacetime.

For example, many people have studied the *"texture zero"* analysis and the flavor symmetries and so on. In the former case, they assume the zeros in the mass matrices as many as possible, e.g., four or five zeros. One famous ansatz of the texture zero analysis is known as *"the Fritzsch mass matrix"* [4, 5] where we assume the zeros in $(1,1)$, $(1,3)$, $(2,2)$ and $(3,1)$ entries of the mass matrices. In 1978, this marvelous parametrization of the quark mass matrices was proposed by Fritzsch [4]. The Hermitian Fritzsch mass matrix, has only minimal non-vanishing elements and also a strong predictability to the quark flavor structure, i.e., the mass hierarchies of up-type and down-type quarks and the small mixing angles. Indeed, it relates the quark mass hierarchies to the small quark mixings due to the strong predictability, and it has been focused on by many researchers. In 1993, the Fritzsch mass matrix was used to explain the lepton flavor structure [6].[1] The Fritzsch mass matrix explained also the lepton large mixings without any extension of the original matrix. Subsequently, a few years later it was shown by numerical calculation that the Fritzsch mass matrix can realize the hierarchy of charged lepton masses and the large lepton mixing angles, simultaneously. However, many experiments have reported the marvelous observations with great accuracy in the quarks, e.g., the Cabbibo angle $\sin\theta_{12} = 0.225$ in the quark sector. According to the recent accurate experiments of the quarks, the Fritzsch mass matrix has been ruled out only in the quarks (See the latest results of the lepton sector in Ref. [10]).

Another famous ansatz for dealing with the flavor puzzle is to use the flavor symmetries. The flavor symmetries play an important role in revealing the origin of the flavor structures of both the quarks and leptons. In 1978, Froggatt and Nielsen introduced a $U(1)$ flavor symmetry in the quark mass matrices [11]. By selecting appropriate $U(1)$ charge assignments among the different generations of the quarks, the quark mass hierarchies and the Cabbibo–Kobayashi–Maskawa (CKM) matrix [12] were simultaneously explained. The Froggatt–Nielsen mechanism was applied to the lepton sector in the long history. As well as the (continuous) $U(1)$ symmetry, *"non-Abelian discrete flavor symmetries"* have been focused on.[2] In the early 2000's, it turned out that some of the non-Abelian discrete flavor symmetries can easily lead to the large mixing angles in the

[1] See also Refs. [7, 8, 9]

[2] See for review [13].

lepton sector, e.g., tri-bimaximal (TBM) [14] and bimaximal (BM) mixing patterns.[3] At that time, people ardently liked and used the specific non-Abelian discrete flavor symmetries $S_3, D_4, A_4, S_4, \Delta(27), \Delta(54)$ and so on in order to especially realize the TBM mixing pattern. In accordance with such discrete symmetries, various model buildings have been investigated before the discovery of the non-vanishing reactor angle θ_{13} in 2012 [16]. Some people still study the discrete flavor symmetries in order to realize much more realistic patterns of the lepton mixing angles. Furthermore, several extensions with/without the non-Abelian discrete flavor symmetries are adapted in many works, e.g., *"stitching the Yukawa quilt"* [17], *"Occam's razor"* [18, 19, 20, 21] and *"repressing anarchy"* [22].

As the other directions in explaining the origin of the flavor structures, there are other promising approaches toward the solutions to the flavor puzzle. One of them is a hypothesis to assume *"extra dimensions"*. Then, total dimensions under consideration are $4+d$, i.e., the 4D spacetime that we feel plus extra d (space) dimensions are assumed. It is plausible that the extra d dimensions would be compactified on some compact space. The reason can be seen as follows. If the extra dimensions spread out on infinite coordinates like the three-dimensional space out of 4D Minkowski spacetime, we would directly recognize the presence of the extra dimensions. The extra dimensions still constitute one of the hypotheses in the elementally particle physics. In the presence of compactified extra spaces, their geometry and topology affect the phenomenological properties appearing in the low energy effective action, e.g., chiral matters, their family structures and hierarchical Yukawa couplings. Thus, it is important to study the structures of the extra dimensions from the phenomenological point of view. For instance, the extra dimensional models can solve the phenomenological problems in the SM and its extensions, for example, the gauge hierarchy problem [23, 24], (non-vanishing) tiny neutrino masses [25] and the flavor puzzle [26, 27] and so forth.

In addition to the possibilities of solving the flavor puzzle, it is also attractive to look at the string theory. As is well known, the SM does not describe gravitational interactions of the particles that affect the beginning of our universe. The superstring theory formulated in ten dimensional (10D) spacetime is almost the only known candidate of the unified theory including quantum gravitational interactions. Indeed, the supersymmetric Yang–Mills (SYM) theory in higher dimensional spacetime appears as a low energy effective field theory of the superstring theory. This is quite interesting from the phenomenological as well as theoretical viewpoint. (See for a review, Ref. [28].) It is an interesting possibility that the SM is embedded in one of such SYM theories, namely, the SM is realized as a low energy effective theory of the superstring theory. In such string model buildings, it is quite important to break higher dimensional supersymmetry (SUSY) in order to obtain 4D chiral spectra, e.g., the SM spectra. People usually consider nontrivial background geometry for the extra-dimensional compact space and/or boundary conditions of fields in it, with which, the $\mathcal{N} = 1$ SUSY can be obtained in accordance with the partial supersymmetry breaking as $\mathcal{N} = 4$ into $\mathcal{N} = 0, 1$ or 2 caused by them.

As well as the geometry and boundary condition(s), recently the assumption of non-

[3] The various mixings are summarized in Refs. [13, 15]

vanishing magnetic fluxes in the extra dimensions has been attracted much attentions, which can also break SUSY fully or partially in higher-dimensional SYM theories. Indeed, various phenomenological studies with the magnetic fluxes have been done, for example, computations of zero-mode wavefunctions and Yukawa coupling constants on a two-dimensional (2D) torus T^2 [29], their extensions to toroidal orbifolds T^2/Z_N ($N = 2, 3, 4, 6$) [30, 31, 32], constructions of three-generation models [33], the minimal supersymmetric standard model (MSSM) and its extended models [34], analysis of non-Abelian discrete flavor symmetries [35, 36] and the other researches [37, 38, 39, 40, 41]. It is interesting that the flavor puzzle can be also addressed within such a framework, by interpreting the SM flavor structure in terms of the boundary conditions of fields and the existence of magnetic fluxes on T^2. With respect to the non-vanishing magnetic fluxes, it is interesting that the Yukawa couplings can be analytically calculated from the overlap integrals of zero-mode wavefunctions on the 2D torus [29]. The recent studies [31, 32] have researched that the viable informations on the 2D torus were extended to the toroidal orbifolds T^2/Z_N ($N = 2, 3, 4, 6$), The extensions involving the toroidal orbifolds are applicable to the phenomenological model buildings.

One of subjects of this thesis is to comprehensively investigate a phenomenological aspect of the Yukawa couplings on magnetized toroidal orbifolds. We will systematically analyze the eigenvalues of mass matrices which are obtained in terms of the VEVs of the Higgs fields. Then, we will reveal whether such Yukawa couplings can be suitable for the model constructions including, e.g., quark-Higgs interactions.

This thesis is organized as follows. In the next chapter, we briefly review general magnetized ten dimensional Yang–Mills theory compactified on a product of multiple two dimensional tori, two dimensional toroidal orbifolds or their combination(s), and see that the phenomenological ingredients appear via the existence of non-vanishing magnetic fluxes. Chapter 3 is based on Ref. [42]. In Chapter 3, we pursuit the possibility of constructing three-generation models of the quarks and charged leptons on magnetized toroidal orbifolds. We show the results by systematically searching all the allowed configurations of magnetic fluxes, Scherk–Schwartz twisting phases and Z_N parities. Chapter 4 is based on Ref. [43]. In Chapter 4, we classify the mass hierarchies of the three-generation models obtained in Chapter 3. Then, we examine whether sufficiently large hierarchies between mass eigenvalues in the mass matrices are obtained or not. Chapter 5 is based on Ref. [44]. In Chapter 5, we propose a phenomenological model by assuming an appropriate configuration of magnetic fluxes on T^2/Z_2 orbifold. Furthermore, we show new textures of Yukawa couplings possessing the ability to explain the experimental data of quarks and leptons, e.g., mass ratios and mixing angles. We investigate their dependences on theoretical input parameters in order to discuss the validity of the Yukawa textures. Chapter 6 is devoted to the summary. In Appendices A and B, we show some details for the mode analysis and the model building, respectively, which are omitted in the main chapters.

Chapter 2

Brief reviews of magnetic fluxes

2.1 Toroidal compactification and magnetic fluxes

In this section, we give a brief review of the toroidal compactification with magnetic fluxes, mainly based on Ref. [42].

First of all, we start with higher dimensional supersymmetric Yang–Mills (SYM) theory defined on ten dimensional (10D) spacetime, which consists of four dimensional (4D) Minkowski spacetime M^4 and a product of three two dimensional (2D) tori $T^2 \times T^2 \times T^2$.[1] An action of the 10D SYM theory is given as

$$S = \int_{M^4} d^4x \int_{(T^2)^3} d^6z \sqrt{-G}\, \mathrm{Tr} \left[-\frac{1}{4} F_{MN} F^{MN} + \frac{i}{2} \bar{\lambda} \Gamma^M D_M \lambda \right], \tag{2.1}$$

where indices M and N run over $0, 1, 2, ..., 9$, which can be decomposed into 4D part $\mu = 0, 1, 2, 3$ and extra dimensional parts $i = 1, 2, 3$. The 10D metric G_{MN} consists of a 4D Minkowski metric and an extra dimensional metric whose the i-th 2D torus part is expressed as

$$g^{(i)} = (2\pi R^{(i)}) \begin{pmatrix} 1 & \mathrm{Re}\, \tau^{(i)} \\ \mathrm{Re}\, \tau^{(i)} & |\tau^{(i)}|^2 \end{pmatrix}, \tag{2.2}$$

respectively, and G denotes a determinant of the 10D metric G_{MN}. The i-th part of the 10D metric includes a toroidal radius $R^{(i)}$ and a complex structure modulus $\tau^{(i)}$, respectively.[2] The i-th two dimensional torus is expressed by a complex coordinate $z_i \equiv y_{2i+2} + \tau^{(i)} y_{2i+3}$ and its complex conjugation $\bar{z}_i \equiv y_{2i+2} - \bar{\tau}^{(i)} y_{2i+3}$ with totally six Cartesian coordinates $y_m\, (m = 4, 5, 6, 7, 8, 9)$ of extra dimensions. Since we consider the toroidal compactification of extra six dimensions, a geometry of extra dimensions should reflect on toroidal periodicities for two directions, such that the complex coordinates are identified

[1] The superfield description of the higher dimensional SYM theories has been studied in Refs. [45, 46, 38]. However, in this thesis, we focus on the component action of the SYM theory.

[2] Note that the toroidal radius is associated with a compactification scale, $M_C \sim 1/2\pi R^{(i)}$.

as $z_i \sim z_i + 1 \sim z_i + \tau^{(i)}$. In the above expression of the SYM action, we define an abbreviated notation $d^6z = \prod_{i=1}^{3} dz_i d\bar{z}_i$. Note that the SYM action holds $\mathcal{N} = 1$ SUSY in 10D spacetime, corresponding to $\mathcal{N} = 4$ in 4D spacetime, unless we put non-vanishing magnetic fluxes on tori. As we will show later, a presence of non-vanishing magnetic flues can break $\mathcal{N} = 4$ SUSY into $\mathcal{N} = 0, 1$ or 2 SUSY in 4D spacetime.

In the above expression of the SYM action, it is found that the SYM theory in the 10D spacetime consists only of a 10D vector field A_M and its superpartner, i.e., a 10D Majorana–Weyl spinor gaugino field λ. The definitions of covariant derivative and field strength are explicitly written as

$$D_M\lambda = \partial_M - ig[A_M, \lambda], \tag{2.3}$$
$$F_{MN} = \partial_M A_N - \partial_N A_M - ig[A_M, A_N], \tag{2.4}$$

where g denotes an only parameter in the SYM theory, i.e., a 10D gauge coupling constant.

Next, we expand the 10D vector and gaugino fields by Kaluza–Klein (KK) decompositions as

$$\lambda(x, \{z_i, \bar{z}_i\}) = \sum_{l,m,n} \chi_{lmn}(x) \otimes \psi_l^{(1)}(z_1, \bar{z}_1) \otimes \psi_m^{(2)}(z_2, \bar{z}_2) \otimes \psi_n^{(3)}(z_3, \bar{z}_3), \tag{2.5}$$
$$A_M(x, \{z_i, \bar{z}_i\}) = \sum_{l,m,n} \varphi_{lmn,M}(x) \otimes \phi_{l,M}^{(1)}(z_1, \bar{z}_1) \otimes \phi_{m,M}^{(2)}(z_2, \bar{z}_2) \otimes \phi_{n,M}^{(3)}(z_3, \bar{z}_3), \tag{2.6}$$

where l, m, n are labels of KK-modes and $\psi_l^{(i)}$ ($\phi_{l,M}^{(i)}$) denotes a 2D Weyl spinor (a 2D vector) expressing the l-the KK-mode on the i-th torus, respectively. In the following, we only concentrate on massless zero-modes, i.e., $l, m, n = 0$, and suppress the KK indices in the KK-expanded 10D fields in the following. It is important to be noted that the 2D spinor carries a 2D chirality distinguished by $+$ or $-$,

$$\psi^{(i)} = \begin{pmatrix} \psi_+^{(i)} \\ \psi_-^{(i)} \end{pmatrix}, \tag{2.7}$$

where we adopt the gamma matrices,

$$\tilde{\Gamma}^{2i+2} = \begin{pmatrix} 0 & 1 \\ 1 & 0 \end{pmatrix}, \qquad \tilde{\Gamma}^{2i+3} = \begin{pmatrix} 0 & -i \\ i & 0 \end{pmatrix}. \tag{2.8}$$

Now, we assume non-vanishing vacuum expectation values for A_M,

$$A^{(b)}(\{z_i, \bar{z}_i\}) = \sum_{i=1}^{3} \frac{\pi}{g\mathrm{Im}\,\tau^{(i)}} \begin{pmatrix} M_1^{(i)}\mathrm{Im}[(\bar{z}_i + \bar{C}_1^{(i)})dz_i]\,\mathbf{1}_{N_1} & & \\ & \ddots & \\ & & M_n^{(i)}\mathrm{Im}[(\bar{z}_i + \bar{C}_n^{(i)})dz_i]\,\mathbf{1}_{N_n} \end{pmatrix}$$
$$\equiv \sum_{i=1}^{3} (A_{z_i}^{(b)}(\bar{z}_i)dz_i + A_{\bar{z}_i}^{(b)}(z_i)d\bar{z}_i), \tag{2.9}$$

where $M_k^{(i)}\,(k=1,2,...,n)$ denote magnetic fluxes on the i-th torus, and they must be integers owing to the Dirac's quantization condition that the Lagrangian compactified on 2D tori should be single-valued for toroidal periodic boundary identifications $z_i \sim z_i+1 \sim z_i+\tau^{(i)}\,(i=1,2,3)$. Additionally, $C_k^{(i)}\,(k=1,2,...,n)$ denote the Wilson line phases on the i-th torus. Note that the (continuous) Wilson line phases can take arbitrary values on 2D tori. As we will explain later, when we treat toroidal orbifolds $T^2/Z_N\,(N=2,3,4,6)$, then values of the Wilson line phases are restricted to several specific discrete values. Note that for the other values of N, the toroidal periodicity is inconsistent with extra-dimensional crystallography [47]. The above magnetic background breaks the non-Abelian gauge group which the SYM theory possess into its subgroups as $U(N)\to\sum_{k=1}^n U(N_k)$, where $N=\sum_{k=1}^n N_k$. After the gauge symmetry breaking, we obtain the following correlation conditions between toroidal periodic conditions and gauge transformations of the vector potential $A^{(b)}$,

$$A^{(b)}(\{z_i+\delta_{ij},\bar{z}_i+\delta_{ij}\})=A^{(b)}(\{z_i,\bar{z}_i\})+d_j\chi_1(\{z_i\}), \tag{2.10}$$

$$A^{(b)}(\{z_i+\delta_{ij}\tau^{(j)},\bar{z}_i+\delta_{ij}\bar{\tau}^{(j)}\})=A^{(b)}(\{z_i,\bar{z}_i\})+d_j\chi_\tau(\{z_i\}), \tag{2.11}$$

where χ_1 and χ_τ are given by

$$\chi_1(\{z_i\})=\sum_{i=1}^3\chi_{1_i}(z_i)\equiv\sum_{i=1}^3\frac{\pi}{g\mathrm{Im}\,\tau^{(i)}}\begin{pmatrix}M_1^{(i)}\mathbf{1}_{N_1} & & \\ & \ddots & \\ & & M_n^{(i)}\mathbf{1}_{N_n}\end{pmatrix}\mathrm{Im}\,dz_i, \tag{2.12}$$

$$\chi_\tau(\{z_i\})=\sum_{i=1}^3\chi_{\tau_i}(z_i)\equiv\sum_{i=1}^3\frac{\pi}{g\mathrm{Im}\,\tau^{(i)}}\begin{pmatrix}M_1^{(i)}\mathbf{1}_{N_1} & & \\ & \ddots & \\ & & M_n^{(i)}\mathbf{1}_{N_n}\end{pmatrix}\mathrm{Im}\,(\bar{\tau}^{(i)}dz_i). \tag{2.13}$$

The single-valuedness of the SYM action requires the gaugino field should satisfy the following transformation laws under the toroidal periodic conditions,

$$\lambda(x,\{z_i+\delta_{ij},\bar{z}_i+\delta_{ij}\})=U_{1_j}(z_j)\lambda(x,\{z_i,\bar{z}_i\})U_{1_j}(z_j)^\dagger, \tag{2.14}$$

$$\lambda(x,\{z_i+\delta_{ij}\tau^{(j)},\bar{z}_i+\delta_{ij}\tau^{(j)}\})=U_{\tau_j}(z_j)\lambda(x,\{z_i,\bar{z}_i\})U_{\tau_j}(z_j)^\dagger, \tag{2.15}$$

for $j=1,2,3$. Unitary matrices $U_{1_i}(z_i)$ and $U_{\tau_i}(z_i)$ associated with the gauge transformation are defined by

$$U_{1_i}(z_i)\equiv e^{ig\chi_{1_i}(z_i)+2\pi i\boldsymbol{\alpha}^{(i)}}, \tag{2.16}$$

$$U_{\tau_i}(z_i)\equiv e^{ig\chi_{\tau_i}(z_i)+2\pi i\boldsymbol{\beta}^{(i)}}, \tag{2.17}$$

where $\boldsymbol{\alpha}^{(i)}$ and $\boldsymbol{\beta}^{(i)}$ denote the Scherk–Schwartz phases related to compactification twists,

whose definitions are given as

$$\boldsymbol{\alpha}^{(i)} \equiv \begin{pmatrix} \alpha_1^{(i)} \mathbf{1}_{N_1} & & \\ & \ddots & \\ & & \alpha_n^{(i)} \mathbf{1}_{N_n} \end{pmatrix}, \tag{2.18}$$

$$\boldsymbol{\beta}^{(i)} \equiv \begin{pmatrix} \beta_1^{(i)} \mathbf{1}_{N_1} & & \\ & \ddots & \\ & & \beta_n^{(i)} \mathbf{1}_{N_n} \end{pmatrix}. \tag{2.19}$$

These Scherk–Schwartz phases $\alpha_k^{(i)}$ and $\beta_k^{(i)}$ $(k = 1, 2, ..., n)$ can take arbitrary continuous values on 2D tori, like the Wilson line phases. On toroidal orbifolds T^2/Z_N $(N = 2, 3, 4, 6)$, possible values of the Scherk–Schwartz (SS) phases are also restricted to several discrete values, as we see in the next section.

In the remainder of this section, we explain explicit examples of how to use magnetic fluxes in phenomenological model buildings. For simplicity, we show in detail a specific example of flux background,

$$A^{(b)}(\{z_i, \bar{z}_i\}) = \sum_{i=1}^{3} \frac{\pi}{g \mathrm{Im}\, \tau^{(i)}} \begin{pmatrix} M_a^{(i)} \mathrm{Im}[(\bar{z}_i + \bar{C}_a^{(i)}) dz_i] \, \mathbf{1}_{N_a} & 0 \\ 0 & M_b^{(i)} \mathrm{Im}[(\bar{z}_i + \bar{C}_b^{(i)}) dz_i] \, \mathbf{1}_{N_b} \end{pmatrix}. \tag{2.20}$$

Thanks to this two-block diagonal flux, the non-Abelian gauge group in the SYM theory breaks into its subgroups as $U(N) \to U(N_a) \times U(N_b)$. Accordingly, the 10D gaugino field splits into four parts as follows,

$$\lambda(x, \{z_i, \bar{z}_i\}) = \begin{pmatrix} \lambda^{aa}(x, \{z_i, \bar{z}_i\}) & \lambda^{ab}(x, \{z_i, \bar{z}_i\}) \\ \lambda^{ba}(x, \{z_i, \bar{z}_i\}) & \lambda^{bb}(x, \{z_i, \bar{z}_i\}) \end{pmatrix}. \tag{2.21}$$

Since we KK-expand the 10D gaugino field in a direct-product form (2.6), the decomposed 2D Weyl parts of the 10D gaugino field are also separated into four parts,

$$\psi^{(i)}(x, \{z_i, \bar{z}_i\}) = \begin{pmatrix} \psi^{(i)aa}(\{z_i, \bar{z}_i\}) & \psi^{(i)ab}(\{z_i, \bar{z}_i\}) \\ \psi^{(i)ba}(\{z_i, \bar{z}_i\}) & \psi^{(i)bb}(\{z_i, \bar{z}_i\}) \end{pmatrix}. \tag{2.22}$$

The diagonal parts λ^{aa} and λ^{bb} correspond to gaugino fields under the unbroken gauge groups $U(N_a) \times U(N_b)$, respectively. On the other hand, the off diagonal parts λ^{ab} and λ^{ba} behave as bi-fundamental representations $(N_a, \bar{N}_b)$ and $(\bar{N}_a, N_b)$ under the unbroken gauge groups. Thus, we obtain bi-fundamental representations thanks to inputting non-vanishing magnetic fluxes. For the above separated parts, we can write down zero-mode

equations which zero-modes of λ^{aa} ($\lambda^{ab}, \lambda^{ba}, \lambda^{bb}$) should satisfy respectively:

$$\begin{pmatrix} \partial_{\bar{z}_i}\psi_+^{(i)aa} & [\partial_{\bar{z}_i} + \frac{\pi}{2\mathrm{Im}\,\tau^{(i)}}(M_{ab}^{(i)}z_i + C_{ab}^{(i)})]\psi_+^{(i)ab} \\ [\partial_{\bar{z}_i} + \frac{\pi}{2\mathrm{Im}\,\tau^{(i)}}(M_{ba}^{(i)}z_i + C_{ba}^{(i)})]\psi_+^{(i)ba} & \partial_{\bar{z}_i}\psi_+^{(i)bb} \end{pmatrix} = 0, \quad (2.23)$$

$$\begin{pmatrix} \partial_{z_i}\psi_-^{(i)aa} & [\partial_{z_i} - \frac{\pi}{2\mathrm{Im}\,\tau^{(i)}}(M_{ab}^{(i)}\bar{z}_i + \bar{C}_{ab}^{(i)})]\psi_-^{(i)ab} \\ [\partial_{z_i} - \frac{\pi}{2\mathrm{Im}\,\tau^{(i)}}(M_{ba}^{(i)}\bar{z}_i + \bar{C}_{ba}^{(i)})]\psi_-^{(i)ba} & \partial_{z_i}\psi_-^{(i)bb} \end{pmatrix} = 0, \quad (2.24)$$

for $i = 1, 2, 3$, where we have introduced abbreviations of notations, $M_{ab}^{(i)} \equiv M_a^{(i)} - M_b^{(i)}$ and $C_{ab}^{(i)} \equiv C_a^{(i)} - C_b^{(i)}$ and so forth. One can easily find that the diagonal gaugino fields $\psi^{(i)aa}$ and $\psi^{(i)bb}$ are not affected by magnetic fluxes and Wilson line phases, while only the off diagonal bi-fundamental fields $\psi^{(i)ab}$ and $\psi^{(i)ba}$ receive additional terms dependent on the magnetic fluxes as well as the Wilson-line phases in their zero-mode equations. Note that the difference between the equations (2.23) and (2.24) is originated from a 2D chirality (+ or −) on the i-th torus. When we try to solve the zero-mode equations, it should be important to take into account boundary conditions on the tori. Since the toroidal periodic conditions are connected with the gauge transformations of flux background each other, by using (2.14) and (2.15) with the two block-diagonal flux, we easily write down boundary conditions for separated spinor fields,

$$\psi_{s^{(i)}}^{(i)aa}(z_i + 1, \bar{z}_i + 1) = \psi_{s^{(i)}}^{(i)aa}(z_i, \bar{z}_i), \quad (2.25)$$

$$\psi_{s^{(i)}}^{(i)bb}(z_i + 1, \bar{z}_i + 1) = \psi_{s^{(i)}}^{(i)bb}(z_i, \bar{z}_i), \quad (2.26)$$

$$\psi_{s^{(i)}}^{(i)ab}(z_i + 1, \bar{z}_i + 1) = e^{i\frac{\pi s^{(i)}}{\mathrm{Im}\,\tau^{(i)}}\mathrm{Im}\,(M_{ab}^{(i)}z_i + C_{ab}^{(i)}) + 2\pi i\alpha_{ab}^{(i)}}\psi_{s^{(i)}}^{(i)ab}(z_i, \bar{z}_i), \quad (2.27)$$

$$\psi_{s^{(i)}}^{(i)ba}(z_i + 1, \bar{z}_i + 1) = e^{i\frac{\pi s^{(i)}}{\mathrm{Im}\,\tau^{(i)}}\mathrm{Im}\,(M_{ba}^{(i)}z_i + C_{ba}^{(i)}) + 2\pi i\alpha_{ba}^{(i)}}\psi_{s^{(i)}}^{(i)ba}(z_i, \bar{z}_i), \quad (2.28)$$

and

$$\psi_{s^{(i)}}^{(i)aa}(z_i + \tau^{(i)}, \bar{z}_i + \bar{\tau}^{(i)}) = \psi_{s^{(i)}}^{(i)aa}(z_i, \bar{z}_i), \quad (2.29)$$

$$\psi_{s^{(i)}}^{(i)bb}(z_i + \tau^{(i)}, \bar{z}_i + \bar{\tau}^{(i)}) = \psi_{s^{(i)}}^{(i)bb}(z_i, \bar{z}_i), \quad (2.30)$$

$$\psi_{s^{(i)}}^{(i)ab}(z_i + \tau^{(i)}, \bar{z}_i + \bar{\tau}^{(i)}) = e^{i\frac{\pi s^{(i)}}{\mathrm{Im}\,\tau^{(i)}}\mathrm{Im}\,(M_{ab}^{(i)}z_i + C_{ab}^{(i)}) + 2\pi i\beta_{ab}^{(i)}}\psi_{s^{(i)}}^{(i)ab}(z_i, \bar{z}_i), \quad (2.31)$$

$$\psi_{s^{(i)}}^{(i)ba}(z_i + \tau^{(i)}, \bar{z}_i + \bar{\tau}^{(i)}) = e^{i\frac{\pi s^{(i)}}{\mathrm{Im}\,\tau^{(i)}}\mathrm{Im}\,(M_{ba}^{(i)}z_i + C_{ba}^{(i)}) + 2\pi i\beta_{ba}^{(i)}}\psi_{s^{(i)}}^{(i)ba}(z_i, \bar{z}_i), \quad (2.32)$$

where we define abbreviations of notations, $\alpha_{ab}^{(i)} \equiv \alpha_a^{(i)} - \alpha_b^{(i)}$ and $\beta_{ab}^{(i)} \equiv \beta_a^{(i)} - \beta_b^{(i)}$ and $s^{(i)}$ denotes a 2D chirality on the i-th torus, i.e., $s^{(i)} = \pm 1$.

The solutions of the zero-mode equations including non-vanishing magnetic fluxes are characterized by both magnitudes and signs of them. First, let us consider a case of $M_{ab}^{(i)} > 0$. Only $\psi_+^{(i)ab}$ and $\psi_-^{(i)ba}$ possess (convergent) normalizable zero-mode wavefunctions. On the other hand, $\psi_+^{(i)ba}$ and $\psi_-^{(i)ab}$ can not be convergent and not normalizable, thus we regard that $\psi_+^{(i)ba}$ and $\psi_-^{(i)ab}$ possess no zero-mode wavefunctions in our scenario. Then, by

solving the zero-mode equations including magnetic fluxes with the above pseudo periodic boundary conditions, we find that analytic forms of the zero-mode wavefunctions are given as

$$\psi_+^{(i)ab}(z_i) = \Theta^{(I+\alpha_{ab}^{(i)},\beta_{ab}^{(i)})}_{M_{ab}^{(i)},a_{ab}^{(i)}}(z_i,\tau^{(i)}), \tag{2.33}$$

$$\psi_-^{(i)ba}(\bar{z}_i) = \Theta^{(I+\alpha_{ba}^{(i)},\beta_{ba}^{(i)})}_{M_{ba}^{(i)},\bar{a}_{ba}^{(i)}}(\bar{z}_i,\bar{\tau}^{(i)}), \tag{2.34}$$

for $I = 0, 1, ..., M_{ab}^{(i)} - 1$, where the Wilson line phase is divided by magnetic fluxes for later convenience, i.e., $a_{ab}^{(i)} \equiv C_{ab}^{(i)}/M_{ab}^{(i)}$, and each of the zero-mode wavefunctions can be expressed in terms of the Jacobi theta function as

$$\Theta^{(I+\alpha_{ab}^{(i)},\beta_{ab}^{(i)})}_{M_{ab}^{(i)},a_{ab}^{(i)}}(z_i,\tau^{(i)}) = \mathcal{N}_{ab}\cdot e^{i\pi M_{ab}^{(i)}(z_i+a_{ab}^{(i)})\frac{\mathrm{Im}(z_i+a_{ab}^{(i)})}{\mathrm{Im}\,\tau^{(i)}}}\cdot\vartheta\begin{bmatrix}\frac{I+\alpha_{ab}^{(i)}}{M_{ab}^{(i)}}\\ -\beta_{ab}^{(i)}\end{bmatrix}(M_{ab}^{(i)}(z_i+a_{ab}^{(i)}), M_{ab}^{(i)}\tau_i), \tag{2.35}$$

$$\Theta^{(I+\alpha_{ba}^{(i)},\beta_{ba}^{(i)})}_{M_{ba}^{(i)},\bar{a}_{ba}^{(i)}}(\bar{z}_i,\bar{\tau}^{(i)}) = \mathcal{N}_{ba}\cdot e^{i\pi M_{ba}^{(i)}(\bar{z}_i+\bar{a}_{ba}^{(i)})\frac{\mathrm{Im}(\bar{z}_i+\bar{a}_{ba}^{(i)})}{\mathrm{Im}\,\bar{\tau}^{(i)}}}\cdot\vartheta\begin{bmatrix}\frac{I+\alpha_{ba}^{(i)}}{M_{ba}^{(i)}}\\ -\beta_{ba}^{(i)}\end{bmatrix}(M_{ba}^{(i)}(\bar{z}_i+\bar{a}_{ba}^{(i)}), M_{ba}^{(i)}\bar{\tau}_i), \tag{2.36}$$

with normalization factors of the zero-mode wavefunctions $\mathcal{N}_{ab}$ and $\mathcal{N}_{ba}$. As will be shown, the normalization factors are determined by the normalization and orthogonal condition of zero-mode wavefunctions. The Jacobi theta function is analytically defined by

$$\vartheta\begin{bmatrix}a\\ b\end{bmatrix}(\nu,\tau) = \sum_{l=-\infty}^{\infty} e^{\pi i(a+l)^2\tau}e^{2\pi i(a+l)(\nu+b)}. \tag{2.37}$$

Note that the Jacobi theta function possesses four arguments, a, b, ν and τ. The parameters a and b take real values, and ν and τ are complex parameters. It should be noted that this elliptic function only converges if $\mathrm{Im}\,\tau > 0$, otherwise this function is not well defined. The Jacobi theta function possesses quasi-periodic properties among a and b,

$$\vartheta\begin{bmatrix}a+1\\ b\end{bmatrix}(\nu,\tau) = \vartheta\begin{bmatrix}a\\ b\end{bmatrix}(\nu,\tau), \tag{2.38}$$

$$\vartheta\begin{bmatrix}a\\ b+1\end{bmatrix}(\nu,\tau) = e^{2\pi i a}\,\vartheta\begin{bmatrix}a\\ b\end{bmatrix}(\nu,\tau), \tag{2.39}$$

and ν,

$$\vartheta\begin{bmatrix}a\\ b\end{bmatrix}(\nu+1,\tau) = e^{2\pi i a}\,\vartheta\begin{bmatrix}a\\ b\end{bmatrix}(\nu,\tau), \tag{2.40}$$

$$\vartheta\begin{bmatrix}a\\ b\end{bmatrix}(\nu+\tau,\tau) = e^{-2\pi i(b+\nu+\tau/2)}\,\vartheta\begin{bmatrix}a\\ b\end{bmatrix}(\nu,\tau). \tag{2.41}$$

These periodic properties in the Jacobi theta function can be interpreted as the remnant of the toroidal periodic boundary conditions. It is easily found that bi-fundamental fields $\psi_+^{(i)ab}(z_i)$ and $\psi_-^{(i)ba}(\bar{z}_i)$ have (degenerate) $|M_{ab}^{(i)}|$ zero-mode solutions. This degeneracy of the zero-mode wavefunctions corresponds to nothing but the family replication of matter fields, e.g., three-generations among the SM quarks and leptons. This implies that we can realize the three-generation structure of a matter field $(N_a, \bar{N}_b)$ by imposing $|M_{ab}^{(i)}| = 3$. Next, we consider a case of $M_{ab}^{(i)} < 0$. Then opposite modes of the 2D spinor fields survive as

$$\psi_+^{(i)ba}(z_i) = \Theta^{(I+\alpha_{ba}^{(i)},\beta_{ba}^{(i)})}_{M_{ba}^{(i)},a_{ba}^{(i)}}(z_i,\tau^{(i)}), \tag{2.42}$$

$$\psi_-^{(i)ab}(\bar{z}_i) = \Theta^{(I+\alpha_{ab}^{(i)},\beta_{ab}^{(i)})}_{M_{ab}^{(i)},\bar{a}_{ab}^{(i)}}(\bar{z}_i,\bar{\tau}^{(i)}). \tag{2.43}$$

The wavefunctions of $\psi_+^{(i)ba}(z_i)$ and $\psi_-^{(i)ab}(\bar{z}_i)$ are expressed in the same way as the case of $M_{ab}^{(i)} > 0$. Finally, in a case of $M_{ab}^{(i)} = 0$, also the off diagonal parts are not affected by magnetic fluxes, then, all of $\psi_\pm^{(i)aa}$, $\psi_\pm^{(i)ab}$, $\psi_\pm^{(i)ba}$ and $\psi_\pm^{(i)bb}$ should be constantly located on the i-th torus and independent of the torus coordinates z_i and $\bar{z}_i$. The normalization factors $\mathcal{N}_{ab}$ and $\mathcal{N}_{ba}$ are detemined by the orthonormality conditions for a complete set of the zero-mode wavefunctions on the torus,

$$\int d^2z_i \left(\Theta^{(I+\alpha_{ab}^{(i)},\beta_{ab}^{(i)})}_{M_{ab}^{(i)},a_{ab}^{(i)}}(z_i,\tau^{(i)})\right)^* \Theta^{(J+\alpha_{ab}^{(i)},\beta_{ab}^{(i)})}_{M_{ab}^{(i)},a_{ab}^{(i)}}(z_i,\tau^{(i)}) = \delta_{IJ} \qquad (M_{ab}^{(i)} > 0), \tag{2.44}$$

$$\int d^2z_i \left(\Theta^{(I+\alpha_{ba}^{(i)},\beta_{ba}^{(i)})}_{M_{ba}^{(i)},\bar{a}_{ba}^{(i)}}(\bar{z}_i,\bar{\tau}^{(i)})\right)^* \Theta^{(J+\alpha_{ba}^{(i)},\beta_{ba}^{(i)})}_{M_{ba}^{(i)},\bar{a}_{ba}^{(i)}}(\bar{z}_i,\bar{\tau}^{(i)}) = \delta_{IJ} \qquad (M_{ba}^{(i)} < 0). \tag{2.45}$$

The same holds for the other zero-mode wavefunctions. This is ensured by the following useful relation for $M_{ab}^{(i)} > 0$,

$$\left(\Theta^{(I+\alpha_{ab}^{(i)},\beta_{ab}^{(i)})}_{M_{ab}^{(i)},a_{ab}^{(i)}}(z_i,\tau^{(i)})\right)^* = \Theta^{(-I+\alpha_{ba}^{(i)},\beta_{ba}^{(i)})}_{M_{ba}^{(i)},\bar{a}_{ba}^{(i)}}(\bar{z}_i,\bar{\tau}^{(i)}). \tag{2.46}$$

This relation is applicable for $M_{ab}^{(i)} < 0$ in the same way. Now that there are three tori under consideration, then the total number of zero-modes in the 4D low energy effective theory is given by a product of the number of the zero-modes on each of tori, i.e.,

$$\prod_{i=1}^{3} |M_{ab}^{(i)}|, \tag{2.47}$$

except for $M_{ab}^{(i)} = 0$. Also, the same holds for a case of $M_{ab}^{(i)} < 0$ and the other cases. Thus, thanks to magnetic fluxes, family replications of matters, i.e., generation structures like three-generation quarks and leptons in the SM, are generated in the torus compactification with non-trivial magnetic fluxes.

Before finishing this section, we would like to show three-point interaction constants, called Yukawa coupling constants, on magnetized torus. The Yukawa coupling constants are completely free parameters from the 4D bottom-up point of view. However, in magnetized SYM theory, we can obtain analytical forms of the Yukawa couplings, whose forms are written by the functions of moduli parameters. First, let us consider the $U(8)$ gauge group as a gauge group which the SYM theory possesses. In the presence of non-vanishing three-block diagonal magnetic fluxes, we assume the gauge group symmetry breaking into the Pati–Salam gauge group as $U(8) \to U(4)_C \times U(2)_L \times U(2)_R$. Here, $U(4)_C$ corresponds to the Pati–Salam color gauge group and on the other hand, $U(2)_L$ and $U(2)_R$ correspond to the left and right gauge symmetries, respectively. It is very useful to use the Pati–Salam gauge group and its supermultiplets under the Pati–Salam group in order to obtain the matter contents of the minimal supersymmetric standard model (MSSM). Hence, this is why we focus on the Pati–Salam gauge group in the remainder of this section. On magnetized tori, we can analytically calculate the explicit form of the Yukawa couplings which are expressed as the overlap integrations of the zero-mode wavefunctions [29],

$$Y_{\mathcal{I},\mathcal{J},\mathcal{K}} = \prod_{i=1}^{3} \lambda^{(i)}_{I^{(i)},J^{(i)},K^{(i)}}, \tag{2.48}$$

$$\lambda^{(i)}_{I^{(i)},J^{(i)},K^{(i)}} = \int d^2 z_i \, \Theta^{(I^{(i)}+\alpha_I^{(i)},\beta_I^{(i)})}_{M_I^{(i)},a_I^{(i)}}(z_i,\tau^{(i)}) \Theta^{(J^{(i)}+\alpha_J^{(i)},\beta_J^{(i)})}_{M_J^{(i)},a_J^{(i)}}(z_i,\tau^{(i)}) \left(\Theta^{(K^{(i)}+\alpha_K^{(i)},\beta_K^{(i)})}_{M_K^{(i)},a_K^{(i)}}(z_i,\tau^{(i)})\right)^* . \tag{2.49}$$

Note that calligraphic index $\mathcal{I}$ runs from 0 to $\prod_{i=1}^{3} |M_{ab}^{(i)}| - 1$ and the same holds for the other calligraphic indices $\mathcal{J}$ and $\mathcal{K}$. Here and hereafter, the calligraphic indices denote family labels for the three sectors, and the italic symbols "I", "J" and "K" denote the three sectors which interact with each other via the three-point Yukawa couplings. As explained in the previous paragraphs, since the zero-mode wavefunctions are changed under the gauge transformations, there exists a condition that the above Yukawa couplings should not be projected out. The condition can be interpreted as the gauge invariance conditions for the magnetic fluxes, the Scherk–Schwartz phases and the Wilson line phase, i.e.,

$$M_I^{(i)} + M_J^{(i)} = M_K^{(i)}, \tag{2.50}$$

$$\alpha_I^{(i)} + \alpha_J^{(i)} = \alpha_K^{(i)}, \tag{2.51}$$

$$\beta_I^{(i)} + \beta_J^{(i)} = \beta_K^{(i)}, \tag{2.52}$$

$$M_I^{(i)} a_I^{(i)} + M_J^{(i)} a_J^{(i)} = M_K^{(i)} a_K^{(i)}. \tag{2.53}$$

A useful formula of the Jacobi's theta function is known as

$$\vartheta\begin{bmatrix} r/N_1 \\ 0 \end{bmatrix}(z_1, N_1\tau) \times \vartheta\begin{bmatrix} s/N_2 \\ 0 \end{bmatrix}(z_2, N_2\tau) = \sum_{m\in\mathbb{Z}_{N_1+N_2}} \vartheta\begin{bmatrix} \frac{r+s+N_1 m}{N_1+N_2} \\ 0 \end{bmatrix}(z_1+z_2, (N_1+N_2)\tau) \times\vartheta\begin{bmatrix} \frac{N_2 r - N_1 s + N_1 N_2 m}{N_1 N_2 (N_1+N_2)} \\ 0 \end{bmatrix}(N_2 z_1 - N_1 z_2, N_1 N_2 (N_1+N_2)\tau), \tag{2.54}$$

which is available under the above gauge invariance conditions (2.50)–(2.53). Here, we assume $r, s \in \mathbb{R}$, $N_1, N_2 \in \mathbb{Z}$ and $z_1, z_2, \tau \in \mathbb{C}$. By using this useful formula for the Jacobi theta function (2.54) and the orthogonality conditions, we consequently find that the analytical form of the Yukawa couplings on the two dimensional torus in terms of the Jacobi's theta functions needs as

$$\begin{aligned}\lambda^{(i)}_{I^{(i)},J^{(i)},K^{(i)}} = \exp\left(\frac{i\pi}{\mathrm{Im}\,\tau^{(i)}}(a_I^{(i)}\mathrm{Im}\,(M_I^{(i)}a_I^{(i)}) + a_J^{(i)}\mathrm{Im}\,(M_J^{(i)}a_J^{(i)}) - a_K^{(i)}\mathrm{Im}\,(M_K^{(i)}a_K^{(i)}))\right) \\ \times \sum_{m\in\mathbb{Z}_{M_K^{(i)}}} \delta_{I^{(i)}+\alpha_I^{(i)}+J^{(i)}+\alpha_J^{(i)}+mM_I^{(i)},K^{(i)}+\alpha_K^{(i)}+lM_K^{(i)}} \\ \times \vartheta\begin{bmatrix} \frac{M_J^{(i)}(I^{(i)}+\alpha_I^{(i)}) - M_I^{(i)}(J^{(i)}+\alpha_J^{(i)}) + mM_I^{(i)}M_J^{(i)}}{M_I^{(i)}M_J^{(i)}M_K^{(i)}} \\ 0 \end{bmatrix}(X, Y),\end{aligned} \tag{2.55}$$

where we define $X \equiv M_I^{(i)}\beta_J^{(i)} - M_J^{(i)}\beta_I^{(i)} + M_I^{(i)}M_J^{(i)}(a_I^{(i)} - a_J^{(i)})$ and $Y \equiv \tau^{(i)}M_I^{(i)}M_J^{(i)}M_K^{(I)}$, and l denotes a possible integer. Indeed, in the above expression of the Yukawa couplings, we can omit the Wilson line phases, because those can be absorbed into the Scherk–Schwartz phases without loss of generality, and vice versa [31]. Hereafter, we set all of the Wilson line phases to be zero, i.e., $a_X^{(i)} = 0$ for all of $i = 1, 2, 3$ and $X = I, J, K$.

2.2 Extensions to toroidal orbifolds

In this section, we investigate the SYM theory on magnetized toroidal orbifolds T^2/Z_N ($N = 2, 3, 4, 6$). Namely, we apply the discussions in the previous section to the orbifolded cases.

We add another identification of the orbifolding projections to the toroidal periodic boundary conditions, i.e., $z_i \sim z_i + 1 \sim z_i + \tau^{(i)}$. The toroidal orbifolds are defined by dividing the two dimensional torus by Z_N rotations,

$$z_i \sim \omega z_i, \tag{2.56}$$

with

$$\omega \equiv e^{2\pi i/N}. \tag{2.57}$$

With the orbifolding identifications, two-dimensional extra spaces are totally identified as

$$z_i \sim \omega z_i + m + n\tau^{(i)} \qquad (m, n \in \mathbb{Z}), \tag{2.58}$$

for $N = 2, 3, 4, 6$. It is known that for $N = 2$, the value of the complex structure modulus parameter is not constrained except for $\mathrm{Im}\,\tau > 0$, and also that for $N = 3, 4$ and 6 cases, $\tau = \omega$ must be satisfied due to the consistency condition of crystallography [47, 31]. In association with the orbifolding identification for $N = 2, 3, 4$ and 6, the Z_N twisting manipulation of the 10D gauge and gaugino fields in non-Abelian SYM gauge theories are assigned as

$$A_\mu(x, \{\omega z_i, \bar{\omega}\bar{z}_i\}) = PA_\mu(x, \{z_i, \bar{z}_i\})P^{-1}, \tag{2.59}$$
$$A_{z_i}(x, \{\omega z_i, \bar{\omega}\bar{z}_i\}) = \bar{\omega}PA_{z_i}(x, \{z_i, \bar{z}_i\})P^{-1}, \tag{2.60}$$
$$A_{\bar{z}_i}(x, \{\omega z_i, \bar{\omega}\bar{z}_i\}) = \omega PA_{\bar{z}_i}(x, \{z_i, \bar{z}_i\})P^{-1}, \tag{2.61}$$
$$\lambda_+(x, \{\omega z_i, \bar{\omega}\bar{z}_i\}) = P\lambda_+(x, \{z_i, \bar{z}_i\})P^{-1}, \tag{2.62}$$
$$\lambda_-(x, \{\omega z_i, \bar{\omega}\bar{z}_i\}) = \omega P\lambda_-(x, \{z_i, \bar{z}_i\})P^{-1}, \tag{2.63}$$

with a projection operator P. The operator P has to satisfy $P \in U(N)$ and $P^N = \mathbf{1}_N$. Since it is useful to treat the simple form of the orbifolding operator P without using the most general form, and we focus only on the following form,

$$P = \begin{pmatrix} \eta_1 \mathbf{1}_{N_1} & & \\ & \ddots & \\ & & \eta_n \mathbf{1}_n \end{pmatrix}, \tag{2.64}$$

where $\eta_j \in \{1, \omega, ..., \omega^{N-1}\}$ $(j = 1, 2, ..., n)$. In the two-block diagonal example as shown in the previous section, in accordance with the gauge symmetry breaking $U(N) \to U(N_a) \times U(N_b)$, the bi-fundamental matter fields $\psi_+^{(i)ab}$ and $\psi_+^{(i)ba}$ appear, for instance. Then, the bi-fundamental fields vary under the Z_N transformation (2.62) and (2.63), such as $\psi^{(i)ab} \to \eta_a\bar{\eta}_b\psi^{(i)ab}$ and $\psi^{(i)ba} \to \eta_b\bar{\eta}_a\psi^{(i)ba}$. Note that the diagonal adjoint parts, e.g., $\psi_+^{(i)aa}$ and $\psi_+^{(i)bb}$, receive no effects from the Z_N transformation. In the following, we call the transformation coefficient as the Z_N parity. On the toroidal orbifolds, the representations of the adjoint and bi-fundamental matter fields are the same as those on the torus. However, the family replication and the analytic form of the zero-mode wavefunctions are changed by the additional boundary conditions in Eqs. (2.59)–(2.63). Let us consider a sector in a positive-chirality spinor $\psi_+^{(i)}$ where we assume the magnetic flux $M^{(i)}$ (> 0), the Scherk–Schwartz phases $\alpha^{(i)}$ and $\beta^{(i)}$, and the Wilson line phase $a^{(i)}$ and the Z_N parity $\eta^{(i)}$ on the i-th torus, respectively. Then, the formal solution of the zero-mode equation (2.23) with the orbifolding identification (2.59)–(2.63) is easily found as

$$\psi^{(i)}_{+,\eta^{(i)}}(z_i) = \sum_{I^{(i)}=0}^{|M^{(i)}|-1} \tilde{\Theta}^{(I^{(i)}+\alpha^{(i)},\beta^{(i)})}_{M^{(i)},a^{(i)};\eta^{(i)}}(z_i, \tau^{(i)}), \tag{2.65}$$

where $\tilde{\Theta}^{(I^{(i)}+\alpha^{(i)},\beta^{(i)})}_{M^{(i)},a^{(i)};\eta^{(i)}}(z_i,\tau^{(i)})$ can be calculated easily by the general recipes as

$$\tilde{\Theta}^{(I^{(i)}+\alpha^{(i)},\beta^{(i)})}_{M^{(i)},a^{(i)};\eta^{(i)}}(z_i,\tau^{(i)}) = \frac{1}{N}\sum_{x=0}^{N-1}(\bar{\eta}^{(i)})^x \Theta^{(I^{(i)}+\alpha^{(i)},\beta^{(i)})}_{M^{(i)},a^{(i)}}(\omega^x z_i,\tau^{(i)}). \tag{2.66}$$

It is quite straightforward to confirm that this form of the formal solution is invariant under the orbifolding transformation $z_i \to \omega z_i$ up to the Z_N parity $\eta^{(i)}$, such that,

$$\tilde{\Theta}^{(I^{(i)}+\alpha^{(i)},\beta^{(i)})}_{M^{(i)},a^{(i)};\eta^{(i)}}(\omega z_i,\tau^{(i)}) = \eta^{(i)}\tilde{\Theta}^{(I^{(i)}+\alpha^{(i)},\beta^{(i)})}_{M^{(i)},a^{(i)};\eta^{(i)}}(z_i,\tau^{(i)}). \tag{2.67}$$

As well as in the case of $M^{(i)} > 0$, we can straightforwardly obtain the zero-mode wavefunctions in a case of $M^{(i)}_{ab} < 0$ only by replacing $z_i \to \bar{z}_i$, $\tau_i \to \bar{\tau}_i$ and $a^{(i)} \to \bar{a}^{(i)}$. In the following discussions, we set the Wilson line phase to be zero for simplicity. As pointed out in the above, the Wilson line phase is able to be absorbed into the Scherk–Schwartz (SS) phases. Without loss of generality, we select the basis as

$$a^{(i)} = 0. \tag{2.68}$$

In practice, Eq. (2.66) is not so useful. It is naively expected that some of zero-mode wavefunctions spanning a complete set is projected out by the Z_N orbifolding identification. However, from the formal solution (2.66), it is quite hard to count the number of independent zero-mode wavefunctions on the magnetized T^2/Z_N. Hence, we need to rewrite the formal solution in terms of the original coordinate z_i, not in terms of the Z_N manipulated coordinate $\omega^x z_i$. By using the orthogonal conditions of the zero-modes on the magnetized torus, in principle we can calculate expansion coefficients as

$$C^{(\omega^x)}_{I^{(i)}J^{(i)}} \equiv \int d^2 z_i \left(\Theta^{(I^{(i)}+\alpha^{(i)},\beta^{(i)})}_{M^{(i)},0}(z_i,\tau^{(i)})\right)^* \Theta^{(J^{(i)}+\alpha^{(i)},\beta^{(i)})}_{M^{(i)},0}(\omega^x z_i,\tau^{(i)}). \tag{2.69}$$

Indeed, it is almost impossible to analytically perform this integration of a product of the rotated and unrotated zero-modes from the technical point of view, since the definition of the Jacobi's theta function includes an infinite summation. Then, the authors in Ref. [32] utilized *"operator formalism"* where they treated the quantum mechanics in the 2D flat spaces compactified on a 2D torus and finally succeeded in obtaining the analytic forms of the expansion coefficients (2.69) [32].[3] The analytic formulae of the expansion coefficients are written in Appendix A. By utilizing the analytical formulae for the coefficient matrices, the rotated zero-mode wavefunctions can be expanded in terms of the unrotated zero-mode wavefunctions as

$$\Theta^{(I^{(i)}+\alpha^{(i)},\beta^{(i)})}_{M^{(i)},0}(\omega^x z_i,\tau^{(i)}) = \sum_{J^{(i)}=0}^{|M^{(i)}|-1} C^{(\omega^x)}_{I^{(i)}J^{(i)}}\Theta^{(J^{(i)}+\alpha^{(i)},\beta^{(i)})}_{M^{(i)},0}(z_i,\tau^{(i)}). \tag{2.70}$$

[3]Note that we can numerically obtain the expansion coefficients without performing analytic calculations. Indeed, by using such numerical results, the number of the zero-mode wavefunctions on T^2/Z_N ($N = 2,3,4,6$) was classified in Ref. [31].

By inserting this expression into the formal solution in Eq. (2.66), we consequently find the relation between the zero-mode wavefunctions on T^2 and those on T^2/Z_N ($N = 2, 3, 4, 6$),

$$\tilde{\Theta}^{(I^{(i)}+\alpha^{(i)},\beta^{(i)})}_{M^{(i)},0;\eta^{(i)}}(z_i,\tau^{(i)}) = \sum_{J^{(i)}=0}^{|M^{(i)}|-1} M^{(Z_N;\eta^{(i)})}_{I^{(i)}J^{(i)}} \Theta^{(J^{(i)}+\alpha^{(i)},\beta^{(i)})}_{M^{(i)},0}(z_i,\tau^{(i)}), \tag{2.71}$$

where we define a rotation matrix for the zero-mode wavefunctions as

$$M^{(Z_N;\eta^{(i)})}_{I^{(i)}J^{(i)}} \equiv \frac{1}{N}\sum_{x=0}^{N-1} (\bar{\eta}^{(i)})^x C^{(\omega^x)}_{I^{(i)}J^{(i)}}. \tag{2.72}$$

As one can easily find, the zero-mode wavefunctinons on T^2/Z_N are expressed by the linear combination of the zero-mode wavefunctions on T^2. It is important to mention how many zero-modes on the left-hand side are independent each other. According to the knowledge in the linear algebra, the degeneracy of the zero-mode wavefunctions is given as

$$\text{Rank}\left[M^{(Z_N;\eta^{(i)})}_{I^{(i)}J^{(i)}}\right], \tag{2.73}$$

since the zero-modes on T^2 can be regarded as the basis which forms a complete set. In general, the total number of linearly independent zero-modes on T^2/Z_N is reduced by the orbifold identification projection,

$$\text{Rank}\left[M^{(Z_N;\eta^{(i)})}_{I^{(i)}J^{(i)}}\right] \leq |M^{(i)}|. \tag{2.74}$$

In order to know the number of the zero-modes on T^2/Z_N, all we have to do is to investigate the matrix rank of $M^{(Z_N;\eta^{(i)})}_{I^{(i)}J^{(i)}}$. Indeed, the numbers of the zero-modes for T^2/Z_N were systematically investigated in Ref. [31]. We show the results in Appendix A. The number of the linearly independent zero-modes on T^2/Z_N can be regarded as the number of physical states for a matter field in the sector, after dimensional reduction. Thus, for T^2/Z_N cases, the matrix rank of $M^{(Z_N;\eta^{(i)})}_{I^{(i)}J^{(i)}}$ gives the family replication number of the matter field in the 4D low energy effective theory.

In addition to the family replication number, the operator formalism brings us with the information about the kinetic terms in the 4D low energy effective theory. On T^2, the kinetic terms are inevitably on a diagonal basis of kinetic terms due to the orthogonality condition in Eqs. (2.44) or (2.45). On the other hand, this is not correct on T^2/Z_N, since the zero-mode basis is non-trivially rotated into the physical basis with the non-trivial linear combination of the zero-modes. Accordingly, the kinetic mixing appears as

$$\mathcal{K}^{(Z_N;\eta^{(i)})}_{I^{(i)}J^{(i)}} = \int d^2 z_i \left(\tilde{\Theta}^{(I^{(i)}+\alpha^{(i)},\beta^{(i)})}_{M^{(i)},0;\eta^{(i)}}(z_i,\tau^{(i)})\right)^* \tilde{\Theta}^{(J^{(i)}+\alpha^{(i)},\beta^{(i)})}_{M^{(i)},0;\eta^{(i)}}(z_i,\tau^{(i)}). \tag{2.75}$$

Indeed, as shown in Ref. [32], the kinetic matrix $\mathcal{K}^{(Z_N;\eta^{(i)})}_{I^{(i)}J^{(i)}}$ can be rewritten as the coefficient matrix of the zero-mode eigenstates after some straightforward calculations,

$$\mathcal{K}^{(Z_N;\eta^{(i)})}_{I^{(i)}J^{(i)}} = M^{(Z_N;\eta^{(i)})}_{J^{(i)}I^{(i)}}. \tag{2.76}$$

This directly means that the kinetic terms are not diagonal at this step. Thus, when we investigate phenomenological observables, i.e., the Yukawa couplings on the magnetized T^2/Z_N, changing the basis also for the kinetic terms by means of a unitary matrix $U^{(Z_N;\eta^{(i)})}$ is required so as the kinetic terms to be diagonal,

$$\mathcal{K}^{(Z_N;\eta^{(i)})}_{I^{(i)}J^{(i)}} \to \left(U^{(Z_N;\eta^{(i)}}\right)^\dagger \mathcal{K}^{(Z_N;\eta^{(i)})}_{I^{(i)}J^{(i)}} U^{(Z_N;\eta^{(i)})} = \mathrm{diag}\,(\underbrace{1,...,1}_{\mathrm{Rank}\,[M^{(Z_N;\eta^{(i)})}]},0,...,0). \tag{2.77}$$

By taking into account the mixing effect from the non-diagonal kinetic matrix, we find the physical zero-mode eigenstates whose index is given by $I'^{(i)} = 0, 1, ..., \mathrm{Rank}\left[M^{(Z_N;\eta^{(i)})}_{I^{(i)}J^{(i)}}\right] - 1$ as

$$\sum_{I^{(i)}=0}^{|M^{(i)}|-1} \tilde{\Theta}^{(I^{(i)}+\alpha^{(i)},\beta^{(i)})}_{M^{(i)},0;\eta^{(i)}}(z_i,\tau^{(i)}) \left(U^{(Z_N;\eta^{(i)})}\right)_{I^{(i)}I'^{(i)}}. \tag{2.78}$$

Hereafter, we refer to the above expression of the zero-mode wavefunctions as the physical zero-modes or the physical eigenstates on T^2/Z_N and so forth.

We are ready to analytically write down the three-point Yukawa couplings for three matter sectors in the physical eigenstates. Now that we have the analytic forms of the physical zero-mode eigenstates (2.78), all we have to do is to calculate the overlapping of a product of the physical zero-mode wavefunctions. Some specific forms of the analytic Yukawa couplings are shown in the following chapters.

Chapter 3

Classification of three-generation models

3.1 Strategy for classification

This chapter and the following sections are mainly based on the results in Ref. [42].

In this part, we show the results of the classification for the possibility to construct three-generation models such as the SM of quarks and leptons, on the basis of the magnetized toroidal orbifolds. First of all, we explain a breaking pattern of the non-Abelian gauge group in detail in the 10D SYM theory. We start with the $U(N)$ SYM theory on the magnetized T^2/Z_N ($N = 2, 3, 4, 6$). Then, we turn on the three-block diagonal fluxes,

$$A^{(b)}(\{z_i, \bar{z}_i\}) = \sum_{i=1}^{3} \frac{\pi}{g\mathrm{Im}\,\tau^{(i)}} \times \begin{pmatrix} M_a^{(i)}\mathrm{Im}[(\bar{z}_i + \bar{C}_a^{(i)})dz_i]\,\mathbf{1}_{N_a} & 0 & 0 \\ 0 & M_b^{(i)}\mathrm{Im}[(\bar{z}_i + \bar{C}_b^{(i)})dz_i]\,\mathbf{1}_{N_b} & 0 \\ 0 & 0 & M_c^{(i)}\mathrm{Im}[(\bar{z}_i + \bar{C}_c^{(i)})dz_i]\,\mathbf{1}_{N_c} \end{pmatrix}. \tag{3.1}$$

As explained in the previous chapters, thanks to the (Abelian) three-block diagonal fluxes, the $U(N)$ gauge group is broken down into its subgroups as $U(N) \to U(N_a) \times U(N_b) \times U(N_c)$ with $N = N_a + N_b + N_c$. In accordance with the gauge symmetry breaking, the six off diagonal parts of the 10D gauge and gaugino fields appear except for the three diagonal parts under the Pati–Salam gauge group. The off diagonal parts are bi-fundamental matter fields, e.g., $\lambda_{ab}, \lambda_{bc}, \lambda_{ca}, \lambda_{ba}, \lambda_{cb}, \lambda_{ac}$, whose representations are $(N_a, \bar{N}_b), (N_b, \bar{N}_c), (\bar{N}_a, N_c), (\bar{N}_a, N_b), (\bar{N}_b, N_c), (N_a, \bar{N}_c)$, respectively. Here and hereafter, as treated before, we set $N = 8$, $N_a = 4$, $N_b = 2$ and $N_c = 2$, namely, the Pati–Salam gauge group $U(4)_C \times U(2)_L \times U(2)_R$. Then, λ_{ab} of the gaugino correspond to the left-handed quark and lepton doublets in the SM, λ_{ca} correspond to the right-handed quarks

and leptons and λ_{bc} correspond to the up-type and down-type Higgsinos as in the MSSM. Note that the superpartner scalars of $\lambda_{ab}, \lambda_{ca}$ and λ_{bc} via the 10D vector field and the superpartner fields λ_{bc} are nothing but the Higgs fields that acquire the vacuum expectation values via radiative electroweak symmetry breaking. As we will see in the following, we have to prepare three-generations of the matter fields in ab- and ca-sectors. Then, we focus only on the left-handed, right-handed matters and the up- and down-type Higgs fields $\lambda_{ab}, \lambda_{ca}$ and λ_{bc}, and assume that the zero-modes of $\lambda_{ab}, \lambda_{ca}$ and λ_{bc} are only normalizable and the other zero-modes are massive or non-normalizable.

Here, we reconsider the conditions that the Yukawa couplings on the toroidal orbifolds are non-vanishing. On the torus, the Yukawa couplings are non-vanishing and gauge invariant when the four conditions in Eqs. (2.50)–(2.53) are simultaneously satisfied. In addition to Eqs. (2.50)–(2.53), the Yukawa couplings on the toroidal orbifolds are constrained by an additional condition for the Z_N parities of each of zero-mode wavefunctions. Namely, the five conditions characterize the Yukawa couplings on the toroidal orbifolds,

$$M_I^{(i)} + M_J^{(i)} = M_K^{(i)}, \tag{3.2}$$

$$\alpha_I^{(i)} + \alpha_J^{(i)} = \alpha_K^{(i)}, \tag{3.3}$$

$$\beta_I^{(i)} + \beta_J^{(i)} = \beta_K^{(i)}, \tag{3.4}$$

$$M_I^{(i)} a_I^{(i)} + M_J^{(i)} a_J^{(i)} = M_K^{(i)} a_K^{(i)}, \tag{3.5}$$

$$\eta_{ab}^{(i)} \eta_{bc}^{(i)} \eta_{ca}^{(i)} = 1. \tag{3.6}$$

The case with the vanishing SS phases and Wilson line phases has been investigated in Ref. [33]. As pointed out in Refs. [31, 32], the degrees of freedom of the Wilson line phases are absorbed into the SS phases and vice versa. For example, the configuration of the vanishing Wilson line phase and the non-vanishing SS phases,

$$\alpha \neq 0, \qquad \beta \neq 0, \qquad Ma = 0, \tag{3.7}$$

corresponds to the case of the non-vanishing Wilson line phase and the vanishing SS phases,

$$\tilde{\alpha} = 0, \qquad \tilde{\beta} = 0, \qquad M\tilde{a} \neq 0. \tag{3.8}$$

This correspondence is given by the relationship between the Wilson line phase $\tilde{a}$, the SS phases α, β and the complex structure modulus τ,

$$M\tilde{a} = \alpha\tau - \beta. \tag{3.9}$$

Thus, in the following procedure, we consider only the non-vanishing SS phases, and set the Wilson line phases to be zero.

In the following, we denote the zero-mode wavefunctions of the left-handed and right-handed fermions and the Higgs bosons as $\psi_{L_i}(z), \psi_{R_j}(z)$ and $\phi_{H_k}(z)$. We symbolically

express the Yukawa coupling constants for three matters as the form of the overlapping zero-mode wavefunctions, Y_{ijk},

$$Y_{ijk} = \int d^2 z \psi_{L_i}(z) \psi_{R_j}(z) \phi_{H_k}(z), \tag{3.10}$$

up to an overall factor. Here, we allow multiple family replications of the Higgs fields in general. As we will understand in the following part, it tends to be seen that the multiple replication of the Higgs fields, e.g., two or five Higgs bosons, appears in the toroidal and orbifold compactification with magnetic fluxes. This is why we add the index $k = 0, 1, 2, ...$ to the symbol "H". When the zero-modes of the left-handed and right-handed matters are (quasi-)localized on two different tori, then, the Yukawa couplings are written by the factorized form,

$$Y_{ijk} = a_{ik} b_{jk}. \tag{3.11}$$

A Yukawa coupling matrix for this factorized form inevitably gives a zero eigenstate. Hence, this type of the Yukawa couplings is not suitable for quark and lepton mass matrices since they are massive. On the other hand, let us consider the case in which all of flavors, i.e., the left-handed, the right-handed matters and the Higgs fields, appear only on a single torus. Then, the Yukawa couplings are symbolically written as

$$Y_{ijk} = a^{(1)}_{ijk} a^{(2)} a^{(3)}. \tag{3.12}$$

In the above expression, $a^{(2)}$ and $a^{(3)}$ are just overall factors derived from the tori which do not affect the flavor structures of the left-handed, the right-handed matters and the Higgs fields. In this case, the Yukawa couplings generally lead to three non-zero eigenvalues, which are suitable for the mass matrices of quarks and leptons. It is easily found by Eq. (3.12) that the contribution from the first torus determines the properties of the total Yukawa couplings. In the following classification, we focus only on a single torus where all of flavors, i.e., the left-handed (ab-sector), the right-handed (ca-sector) matters and the Higgs fields (bc-sector), are generated by the effects of magnetic fluxes. We also focus on the ab-, bc- and ca-sectors which are characterized by the configurations of the several parameters and the five constraints in Eqs. (3.2) and (3.6). Then, the vector-like sectors, i.e., the ba-, cb- and ac-sectors are automatically determined by the corresponding configurations after the configurations of the main three sectors are fixed. We will not treat the vector-like sectors, and assume that the zero-modes in the vector-like sectors are all eliminated by the chiral projections of magnetic fluxes and/or the boundary conditions on the other two tori which we do not focus on. In the following part, we focus on the single torus associated with the flavors and suppress the torus index i.

We are now going to classify possibilities of obtaining three-generation models. In this respect, we would like to mention about the signs of magnetic fluxes in each of the three sectors. Equation (3.2) implies that the sign of one of magnetic fluxes is opposite to those

of the other two magnetic fluxes. In other words, two patterns of the signs are possible,

$$M_{ab} < 0, \quad M_{ca} < 0, \tag{3.13}$$
$$M_{ab} < 0, \quad M_{ca} > 0. \tag{3.14}$$

In the other two patterns with opposite signs of magnetic fluxes, i.e., $M_{ab} > 0$, $M_{ca} > 0$ and $M_{ab} > 0$, $M_{ca} < 0$, the possibilities of obtaining three-generation models are exactly the same as the above two patterns. Accordingly, we impose an additional condition,

$$|M_{ab}| \leq |M_{ca}|. \tag{3.15}$$

Note that the opposite case $|M_{ab}| \geq |M_{ca}|$ can be obtained just by changing the role of the two sectors. Hence, it is sufficient to focus on the case of Eq. (3.15). By imposing Eq. (3.15), we can evade double countings of the combinations of the magnetic fluxes. Therefore, we comprehensively search the combinations of the magnetic fluxes and the other free parameters under the Eqs. (3.2)–(3.6), (3.13) or (3.14), and (3.15).

As stated in the previous chapter, the Wilson line phases and the SS phases cannot take arbitrary continuous values. Indeed, the allowed values of them are limited in some discrete values [31]. This is originated from the connections between the boundary conditions associated with the orbifolding identifications and the gauge transformations derived from the input magnetic fluxes. In this thesis, we systematically search all the allowed discrete values of the SS phases.

According to Ref. [31], the numbers of the magnetic fluxes which can generate three replications of the matter field are given as

- $|M_{ab}|, |M_{ca}| = 4$ – 8 on T^2/Z_2,
- $|M_{ab}|, |M_{ca}| = 6$ – 12 on T^2/Z_3,
- $|M_{ab}|, |M_{ca}| = 8$ – 16 on T^2/Z_4,
- $|M_{ab}|, |M_{ca}| = 12$ – 24 on T^2/Z_6.

In addition, the allowed discrete values of the SS phases are similarly given as

- On T^2/Z_2, $(\alpha_{XY}, \beta_{XY}) = (0,0), (1/2,0), (0,1/2), (1/2,1/2)$,
- On T^2/Z_3, $(\alpha_{XY}, \beta_{XY}) = (0,0), (1/3,1/3), (2/3,2/3)$ for even numbers of the flux, $(\alpha_{XY}, \beta_{XY}) = (1/6,1/6), (1/2,1/2), (5/6,5/6)$ for odd numbers of the flux,
- On T^2/Z_4, $(\alpha_{XY}, \beta_{XY}) = (0,0), (1/2,1/2)$,
- On T^2/Z_6, $(\alpha_{XY}, \beta_{XY}) = (0,0)$ for even numbers of the flux, $(\alpha_{XY}, \beta_{XY}) = (1/2,1/2)$ for odd numbers of the flux,

where $XY = ab, bc, ca$. The Z_N parities are also similarly given as

- $\eta_{ab}, \eta_{ca} = \pm 1$ on T^2/Z_2,
- $\eta_{ab}, \eta_{ca} = 1, \omega, \omega^2$ for $\omega \equiv e^{2\pi i/3}$ on T^2/Z_3,
- $\eta_{ab}, \eta_{ca} = \pm i, \pm 1$ on T^2/Z_4,
- $\eta_{ab}, \eta_{ca} = 1, \omega, \omega^2, \omega^3, \omega^4, \omega^5$ for $\omega \equiv e^{2\pi i/6}$ on T^2/Z_6.

In the classification, we systematically take into account of all the values of the above parameters in the ab- and ca-sectors. Note that the parameters in the bc-sector (the Higgs sector) are automatically determined by the gauge invariant constraints (3.2)–(3.6). Also, this implies that on the magnetized orbifolds the number of the generations of the Higgs fields can be predicted by the requirements for three-generations of quarks and leptons.

3.2 Results of the classification

The results of the classification are shown in Tables 3.1 on T^2/Z_2, 3.2 on T^2/Z_3, 3.3 on T^2/Z_4, 3.4 on T^2/Z_6. Tables 3.1, 3.2, 3.3 and 3.4 show the numbers of the possible candidates for three-generation models after systematically searching the magnetic fluxes and the SS phases. Then, the numbers of the emerging Higgs pairs are also shown in the tables. We distinguish one Higgs pair with $M_{bc} \neq 0$ from that with $M_{bc} = 0$. The situation is that we distinguish a Higgs pair of the constant zero-mode wavefunctions which universally spread on T^2/Z_N from another Higgs pair of localized zero-mode wavefunctions. The discrimination of the former and latter cases is made by "1 (trivial)" and "1" in the column of Tables 3.1, 3.2, 3.3 and 3.4. The former and latter cases of one Higgs pair should be different from each other in the 4D effective theory. This is the reason why we count the cases of $M_{bc} = 0$. The label "Without the SS phases" represents the classification for all the vanishing SS phases, while the label "General cases" represents the exhaustive classification for both the vanishing and non-vanishing SS phases. It should be noted that the result in "Without the SS phases" on T^2/Z_2 in Table 3.1 has been already analyzed in Ref. [33]. Thus, there are $217 + 558 + 798 + 999 = 2572$ candidates for three-generation models on the magnetized toroidal orbifolds. We summarize the explicit combinations of the free parameters on T^2/Z_2 in Appendix B of this thesis, and those on T^2/Z_N $(N = 3, 4, 6)$ in Appendix B of Ref. [42].

We show the histogram for the numbers of the Higgs pairs on T^2/Z_N $(N = 2, 3, 4, 6)$ in Figure 3.1. The result on T^2/Z_2 (Z_3, Z_4, Z_6) is depicted by the blue (orange, gray, yellow) histogram bins, respectively. Figure 3.1 manifests that three-generations of the Higgs pairs can not be constructed on the magnetized orbifolds in any case. It is also concluded that two and four generations of the Higgs pairs are possible except for T^2/Z_2. We understand that one and multi (e.g., five or six) generations of the Higgs pairs are predominantly favored statistically. In the next chapters, we will argue whether the Yukawa couplings with the one- and multi-generation Higgs fields can lead to sufficient large mass hierarchies and suitable mixing angles simultaneously or not.

General cases			
$M_{ab} < 0, M_{ca} < 0$	# of the Higgs pairs	$M_{ab} < 0, M_{ca} > 0$	# of the Higgs pairs
41	5	16	1 (trivial)
56	6	65	1
30	7		
8	8		
1	9		
$136 + 81 = 217$ in total			

Without the SS phases			
$M_{ab} < 0, M_{ca} < 0$	# of the Higgs pairs	$M_{ab} < 0, M_{ca} > 0$	# of the Higgs pairs
5	5	4	1 (trivial)
2	6	5	1
2	8		
1	9		
$10 + 9 = 19$ in total			

Table 3.1: The numbers of the candidates for three-generation models and the Higgs pairs on T^2/Z_2. The result of "General cases" includes both the vanishing and non-vanishing SS phases, while the result of "Without the SS phases" is restricted to cases with the vanishing SS phases.

General cases			
$M_{ab} < 0, M_{ca} < 0$	# of the Higgs pairs	$M_{ab} < 0, M_{ca} > 0$	# of the Higgs pairs
11	4	17	1 (trivial)
83	5	142	1
190	6	21	2
83	7		
11	8		
$378 + 180 = 558$ in total			

Without the SS phases			
$M_{ab} < 0, M_{ca} < 0$	# of the Higgs pairs	$M_{ab} < 0, M_{ca} > 0$	# of the Higgs pairs
1	4	9	1 (trivial)
6	5	27	1
7	6		
6	7		
1	8		
$21 + 36 = 57$ in total			

Table 3.2: The numbers of the candidates for three-generation models and the Higgs pairs on T^2/Z_3. The result of "General cases" includes both the vanishing and non-vanishing SS phases, while the result of "Without the SS phases" is restricted to cases with the vanishing SS phases.

General cases			
$M_{ab} < 0, M_{ca} < 0$	# of the Higgs pairs	$M_{ab} < 0, M_{ca} > 0$	# of the Higgs pairs
9	4	24	1 (trivial)
128	5	228	1
254	6	18	2
120	7		
17	8		
$528 + 270 = 798$ in total			

Without the SS phases			
$M_{ab} < 0, M_{ca} < 0$	# of the Higgs pairs	$M_{ab} < 0, M_{ca} > 0$	# of the Higgs pairs
3	4	12	1 (trivial)
37	5	60	1
59	6	6	2
27	7		
10	8		
$136 + 78 = 214$ in total			

Table 3.3: The numbers of the candidates for three-generation models and the Higgs pairs on T^2/Z_4. The result of "General cases" includes both the vanishing and non-vanishing SS phases, while the result of "Without the SS phases" is restricted to cases with the vanishing SS phases.

General cases			
$M_{ab} < 0, M_{ca} < 0$	# of the Higgs pairs	$M_{ab} < 0, M_{ca} > 0$	# of the Higgs pairs
14	4	24	1 (trivial)
156	5	282	1
326	6	27	2
150	7		
20	8		
$666 + 333 = 999$ in total			

Without the SS phases			
$M_{ab} < 0, M_{ca} < 0$	# of the Higgs pairs	$M_{ab} < 0, M_{ca} > 0$	# of the Higgs pairs
4	4	12	1 (trivial)
45	5	73	1
76	6	8	2
36	7		
10	8		
$171 + 93 = 264$ in total			

Table 3.4: The numbers of the candidates for three-generation models and the Higgs pairs on T^2/Z_6. The result of "General cases" includes both the vanishing and non-vanishing SS phases, while the result of "Without the SS phases" is restricted to cases with the vanishing SS phases.

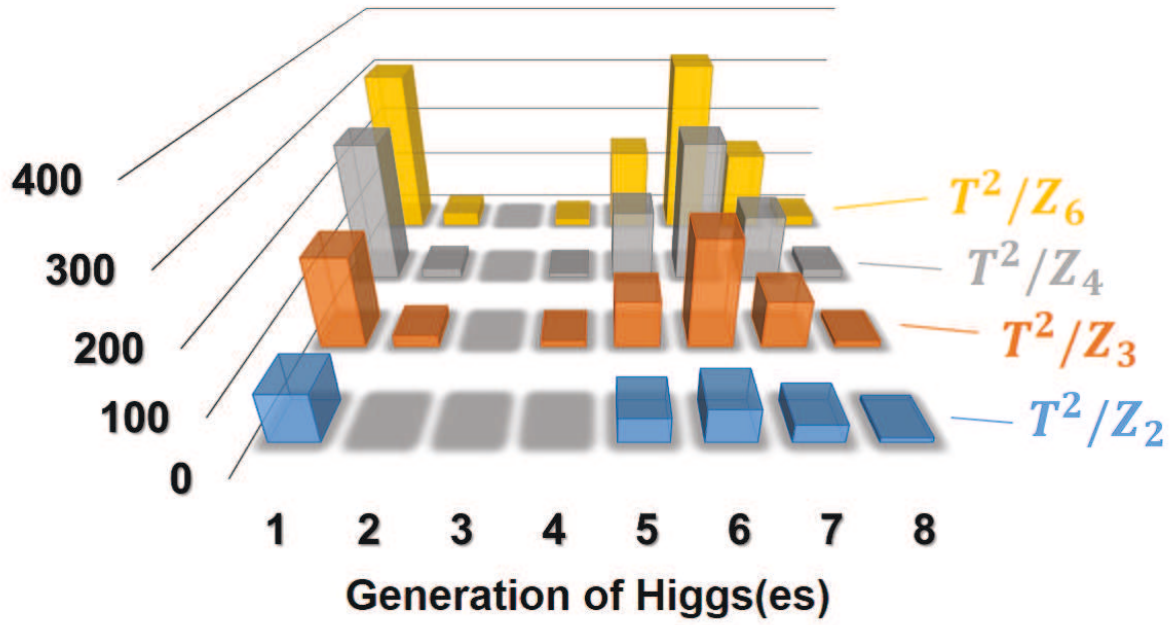

Figure 3.1: The histogram for the numbers of the Higgs pairs on T^2/Z_N $(N = 2, 3, 4, 6)$. The result on T^2/Z_2 (Z_3, Z_4, Z_6) is depicted by the blue (orange, gray, yellow) histogram bin.

Chapter 4

Systematic analysis of Yukawa hierarchies

4.1 Motivation for investigating Yukawa hierarchies

In the previous chapter, we analyzed the possibilities of obtaining three-generation models of the quarks and leptons in the framework of the magnetized orbifolds $T^2/Z_N\,(N = 2, 3, 4, 6)$. We see that there are quite many possibilities that such models appear with a single and multiple Higgs doublet pairs. Among such possibilities, how should we select promising combinations of the magnetic fluxes, the SS phases and the Z_N parities for the model buildings ? For realistic model buildings, in general we need to prepare the four sectors including the Yukawa couplings in the SM with the neutrino extension, i.e., the up- and down-quark sectors, the charged lepton sector and the neutrino sector. In particular, the up- and down-quark sectors and the charged lepton sector are required to have hierarchical eigenvalues of their mass matrices. To be more concrete, we know experimentally large hierarchies of the masses existing,

$$\frac{m_u}{m_t} = \mathcal{O}(10^{-5}), \qquad \frac{m_c}{m_t} = \mathcal{O}(10^{-2}), \tag{4.1}$$

for the up-type quark sector,

$$\frac{m_d}{m_b} = \mathcal{O}(10^{-3}), \qquad \frac{m_s}{m_d} = \mathcal{O}(10^{-2}), \tag{4.2}$$

for the down-type quark sector, and

$$\frac{m_e}{m_\tau} = \mathcal{O}(10^{-4}), \qquad \frac{m_\mu}{m_\tau} = \mathcal{O}(10^{-1}), \tag{4.3}$$

for the charged lepton sector, as shown in Ref. [3]. Thus, the large hierarchy of $\mathcal{O}(10^{-5})$ is at least required for the construction including the up-type quark sector. Hence, we systematically and comprehensively classify the hierarchies between the smallest and largest

eigenvalues in the effective mass matrices. Based on this classification, we will know the possible candidates of the Yukawa couplings for the realistic model buildings. For that reason, we focus on the hierarchies in the effective mass matrices in the 4D low energy effective theory after dimensional reductions.

In the comprehensive classifications, we focus on the one and two Higgs pairs in the three-generation models of the quarks and leptons which are exhaustively investigated in the previous chapter. The one and two Higgs pairs are always generated by the fluxes of the opposite sign ($M_{ab} < 0$ and $M_{ca} > 0$). On the other hand, the multiple Higgs with more than three pairs are given by the fluxes with the same sign ($M_{ab} < 0$ and $M_{ca} < 0$). In the latter case, the Gaussian form of the mass matrices are obtained by assuming suitable combinations of the non-vanishing Higgs VEVs. The multiple Higgs with more than three pairs are the main subject in the next chapter. In the multiple Higgs cases, there are many free parameters unless we concretely construct and analyze the Higgs potential among the multiple Higgs pairs. Then, the VEVs of the Higgs pairs are literally free input parameters in calculating the mass eigenvalues of the SM fermions. Namely, there are as many free parameters as the number of the Higgs doublets. The mass matrices dependent on many free parameters consequently reduce to the flavor puzzle, because of the ambiguity in the mass matrices.

In addition, we would like to comment on the contributions of the non-vanishing SS phases. In the pre-existing studies [33, 44], the Yukawa hierarchies are derived only by the proper configurations of the Higgs VEVs. In this chapter, we also treat the patterns including the non-vanishing SS phases. In particular, the SS phase in the sixth direction, i.e., β, appears in the argument "a" of the definition of the Jacobi theta function. This implies that there are possibilities in modifying the mass hierarchies of the mass matrices, thanks to the SS phases. As well as the one and two Higgs pairs, the multiple Higgs cases with more than three pairs are likely affected by them.

Before closing this section, we would like to refer to the values of the complex structure modulus τ. On T^2/Z_2, its value is arbitrary, as shown in the previous chapters. Hence, the complex structure modulus can be a free parameter on the T^2/Z_2 orbifold. However, on the other hand, the values of the complex modulus on the other orbifolds are restricted to specific values,

$$\tau = e^{2\pi i/N} \qquad (N = 3, 4, 6), \tag{4.4}$$

due to the consistency condition. Thus, we are not allowed to freely scatter the values of the complex modulus on the T^2/Z_N $(N = 3, 4, 6)$. It is easily found that the imaginary part of the complex structure modulus τ appears in the argument of the Jacobi theta function as

$$y_{ijk} \sim e^{-c_{ijk} \times \mathrm{Im}\, \tau} \tag{4.5}$$

with a constant c_{ijk} dependent on the indices i, j, k, where we roughly approximate the Jacobi theta function by extracting the term of $l = 0$. The magnitude of the imaginary part $\mathrm{Im}\, \tau$ directly affects the eigenvalues of the mass matrices. Therefore, the orbifolds

T^2/Z_N $(N = 3, 4, 6)$ have strong predictabilities for the mass eigenvalues from this point of view.

4.2 One-Higgs-pair case

At first, we focus on the one Higgs cases. For the one Higgs cases, the general form of the mass matrices is given in the 4D effective theory as

$$M_{ij} = y_{ij} v, \tag{4.6}$$

where $v = 174$ GeV is the VEV of the Higgs doublet and we suppress the index $k = 0$. As pointed out in the previous chapter, we have no parameter except for the T^2/Z_2 orbifold. Only on the T^2/Z_2 orbifold, we can treat the complex modulus parameter as a free parameter.

Before showing the results of the comprehensive analyses, we would like to show an illustrating pattern for T^2/Z_2 case and its predictions. On T^2/Z_2 with non-trivial orbifolding twists, namely with non-trivial SS phases, we show the analytic expression of the Yukawa couplings. Also in this chapter, we adopt the basis where the Wilson line phases are gauged out and only the SS phases are non-trivial. With respect to the zero-mode wavefunctions on T^2 and T^2/Z_2, we know the relationship between them. Thus, all we have to do is to rotate the basis of the zero-mode wavefunctions from T^2 to T^2/Z_2. Indeed, the analytic Yukawa couplings ($\lambda_{I,J,K}$ on T^2 and $\tilde{\lambda}_{I,J,K}$ on T^2/Z_2) obtained from the overlapping integral are given as

$$\lambda_{I,J,K} = \int d^2 z \, \Theta^{(I+\alpha_I,\beta_I)}_{M_I,0}(z,\tau) \Theta^{(J+\alpha_J,\beta_J)}_{M_J,0}(z,\tau) \left(\Theta^{(K+\alpha_K,\beta_K)}_{M_K,0}(z,\tau) \right)^* , \tag{4.7}$$

$$\tilde{\lambda}_{I,J,K} = \int d^2 z \, \tilde{\Theta}^{(I+\alpha_I,\beta_I)}_{M_I,0;\eta_I}(z,\tau) \tilde{\Theta}^{(J+\alpha_J,\beta_J)}_{M_J,0;\eta_J}(z,\tau) \left(\tilde{\Theta}^{(K+\alpha_K,\beta_K)}_{M_K,0;\eta_K}(z,\tau) \right)^* . \tag{4.8}$$

As explained before, the Yukawa couplings on T^2 are written by eliminating the Wilson line phases in Eq. (2.55) as

$$\begin{aligned} \lambda_{I,J,K} = \frac{\mathcal{N}_{M_I}\mathcal{N}_{M_J}}{\mathcal{N}_{M_K}} \sum_{m \in Z_{M_K}} & \delta_{I+\alpha_I+J+\alpha_J+mM_I,K+\alpha_K+lM_K} \\ & \times \vartheta \begin{bmatrix} \frac{M_J(I+\alpha_I)-M_I(J+\alpha_J)+M_IM_Jm}{M_IM_JM_K} \\ 0 \end{bmatrix} (X,Y), \end{aligned} \tag{4.9}$$

where we use the definitions $X \equiv M_I\beta_J - M_J\beta_I$ and $Y \equiv M_IM_JM_K\tau$. By taking into account of the diagonalization for the kinetic terms, we consequently find the desired Yukawa couplings,

$$\tilde{\lambda}'_{I',J',K'} = \sum_{I=0}^{|M_I|-1} \sum_{J=0}^{|M_J|-1} \sum_{K=0}^{|M_K|-1} \tilde{\lambda}_{I,J,K} \left(U^{Z_2;\eta_I} \right)_{I,I'} \left(U^{Z_2;\eta_J} \right)_{J,J'} \left(U^{Z_2;\eta_K} \right)^*_{K,K'} . \tag{4.10}$$

The index I' (J' and K') runs over $I' = 0, 1, ..., \mathrm{Rank}[M^{(Z_2;\eta_I)}]-1$ ($J' = 0, 1, ..., \mathrm{Rank}[M^{(Z_2;\eta_J)}]-1$ and $K' = 0, 1, ..., \mathrm{Rank}[M^{(Z_2;\eta_K)}] - 1$). In this basis, the kinetic terms are individually diagonalized for the three sectors which construct the Yukawa interactions. Consequently, the expression of the Yukawa couplings on T^2/Z_2 in Eq. (4.10) is exactly the desired one. In general, the diagonalizing matrices $U^{Z_N;\eta_I}$ on T^2/Z_N orbifolds, are not diagonal, and provide the Yukawa couplings with mixing effects. However, we can set the diagonalizing matrices on T^2/Z_2 case as a diagonal form,

$$\left(U^{Z_2;\eta_I}\right)_{I,I'} \to \delta_{I,I'}. \tag{4.11}$$

For the other orbifolds $T^2/Z_N\,(N = 3, 4, 6)$, some contributions from the non-diagonal unitary matrices are generated and it is plausible that their effects disturb the structures of the Yukawa couplings.[1] In the comprehensive analyses, we will take into account of such mixing effects on $T^2/Z_N\,(N = 3, 4, 6)$.

Let us consider the one-pair Higgs example on T^2/Z_2 which is generated by the following magnetic fluxes, SS twist phases and Z_2 parities,

$$(M_{bc}, M_{ca}, M_{ab}) = (-2, -4, +6), \tag{4.12}$$
$$(\alpha_{bc}, \alpha_{ca}, \alpha_{ab}) = (0, 0, 0), \tag{4.13}$$
$$(\beta_{bc}, \beta_{ca}, \beta_{ab}) = (1/2, 0, 1/2), \tag{4.14}$$
$$(\eta_{bc}, \eta_{ca}, \eta_{ab}) = (+1, +1, +1), \tag{4.15}$$

for the Yukawa couplings between the up-type quarks and the up-type Higgs doublet and

$$(M_{bc'}, M_{c'a}, M_{ab}) = (-1, -5, +6), \tag{4.16}$$
$$(\alpha_{bc'}, \alpha_{c'a}, \alpha_{ab}) = (0, 0, 0), \tag{4.17}$$
$$(\beta_{bc'}, \beta_{c'a}, \beta_{ab}) = (1/2, 0, 1/2), \tag{4.18}$$
$$(\eta_{bc'}, \eta_{c'a}, \eta_{ab}) = (+1, +1, +1), \tag{4.19}$$

for those between the down-type quarks and the down-type Higgs doublet, where we assume that the $U(2)_R$ is broken down to its subgroups. Note that here we set all the Wilson line phases to be vanishing, as chosen in the previous chapter. The bi-fundamental representation in the ab-sector corresponds to the left-handed quark doublets. Similarly, the matter fields in the ca-sector ($c'a$-, bc- and bc'-sectors) are the right-handed up-type quarks (right-handed down-type quarks, the up-type Higgs doublet and the down-type Higgs doublet). By plugging the above configurations of the fluxes, SS twists and Z_2 parities with specific replacements, e.g., $M_{ab} \to M_I$, we obtain the analytic expression of the Yukawa couplings. However, the analytic expression is quite clumsy. Hence, we focus only on the approximated form of the Yukawa matrices. At first, we define useful

[1] See, e.g., Ref. [43].

functions which will appear in the Yukawa matrices,

$$\eta_N^{(u)} \equiv \vartheta \begin{bmatrix} N/M_u \\ 0 \end{bmatrix} (-2, M_u\tau), \tag{4.20}$$

$$\eta_N^{(d)} \equiv \vartheta \begin{bmatrix} N/M_d \\ 0 \end{bmatrix} (-5/2, M_d\tau), \tag{4.21}$$

where $M_u \equiv M_{ab}M_{bc}M_{ca} = 48$ and $M_d \equiv M_{ab}M_{bc'}M_{c'a} = 30$. The definitions of these functions are slightly different from those defined in Refs. [33, 44]. In fact, the above definitions can be rewritten as

$$\eta_N^{(u)} = e^{2\pi i \frac{N}{M_u}(-2)} \times \vartheta \begin{bmatrix} N/M_u \\ 0 \end{bmatrix} (0, M_u\tau), \tag{4.22}$$

$$\eta_N^{(d)} = e^{2\pi i \frac{N}{M_d}(-5/2)} \times \vartheta \begin{bmatrix} N/M_d \\ 0 \end{bmatrix} (0, M_d\tau), \tag{4.23}$$

by using the formula of the Jacobi theta function (2.54). From these rewritten functions, we find that the non-vanishing SS twist phases just provide phase factors in front of $\eta_N^{(u)}$ and $\eta_N^{(d)}$. By plugging the above fluxes, SS twists and Z_2 parities into the Yukawa couplings in the Z_2 case, we finally obtain the Yukawa matrices for the up- and down-type quarks,

$$\tilde{\lambda}^{\prime(u)}_{I',J'} \sim \begin{pmatrix} \eta_0^{(u)} & 0 & \eta_{12}^{(u)} \\ 0 & \eta_2^{(u)} & 0 \\ \eta_8^{(u)} & 0 & \eta_4^{(u)} \end{pmatrix}, \tag{4.24}$$

$$\tilde{\lambda}^{\prime(d)}_{I',J'} \sim \begin{pmatrix} \eta_0^{(d)} & \eta_6^{(d)} & \eta_{12}^{(d)} \\ \eta_5^{(d)} & \eta_1^{(d)} & \eta_{23}^{(d)} \\ \eta_{10}^{(d)} & \eta_4^{(d)} & \eta_2^{(d)} \end{pmatrix}. \tag{4.25}$$

Here, we approximate each of the Yukawa coupling elements by using a formula of the Jacobi theta functions [33],

$$\eta_N^{(u,d)} < \eta_{N'}^{(u,d)} \qquad (N > N'). \tag{4.26}$$

By diagonalizing the above Yukawa matrices, we show sample values of the one-pair Higgs model in Table 4.1. In numerical calculation, we have only a single free parameter, i.e., an imaginary part of the complex structure modulus. In Table 4.1, theoretical sample values are given by $\mathrm{Im}\,\tau = 10$. It is found that the setup with the above magnetic fluxes, SS twist phases and Z_2 parities can lead to only the observed mass hierarchies among the up- and down-type quarks. However, the setup gives tiny mixing angles which are inconsistent with the observed mixing angles of the quarks. The other cases of the magnetic fluxes, SS phases and Z_2 parities are similar to the results in Table 4.1. Even if we can realize the suitable mass hierarchies of the quarks, we never obtain the largest mixing angles in the

CKM mixing matrix, i.e., $|(V_{\rm CKM})_{12}| \simeq 0.23$. We can conclude that the one-pair Higgs models on T^2/Z_2 are not suitable in constructing flavor models.

Indeed, there are other patterns of one-pair Higgs models on T^2/Z_2 besides the pattern in the previous paragraph. The Yukawa hierarchies in the patterns are corresponding to the mass hierarchies, because of the one-pair Higgs models. The ratios between three eigenvalues of the Yukawa matrices are shown in Figures 4.1, 4.2 and 4.3. The difference among Figures 4.1, 4.2 and 4.3 is the value of the complex structure modulus. We set $\mathrm{Im}\,\tau = 1$ in Figure 4.1, $\mathrm{Im}\,\tau = 5$ in Figure 4.2 and $\mathrm{Im}\,\tau = 10$ in Figure 4.3. Note that we can freely choose the values of the complex structure modulus in the T^2/Z_2 case, as pointed out previously. The yellow (blue) bins show the ratio between the smallest and largest (the smallest and second largest) eigenvalues, namely, m_1/m_3 (m_2/m_3). Then, the mass ordering is $m_1 \leq m_2 \leq m_3$. We find that the mass hierarchies become larger as $\mathrm{Im}\,\tau$ becomes larger. In some patterns with $\mathrm{Im}\,\tau = 10$, the sufficient hierarchy, i.e., $\mathcal{O}(10^{-5})$, can be realized by setting a large value of $\mathrm{Im}\,\tau$.

Next, we investigate the cases of the one-pair Higgs models on T^2/Z_N ($N = 3, 4, 6$). Note that the values of the complex structure modulus should be $\tau = e^{2\pi i/N}$ on T^2/Z_N ($N = 3, 4, 6$). This implies that we have no free parameter in the one-pair Higgs models on T^2/Z_N. In Figures 4.4, 4.5 and 4.6, we can not find the promising patterns which lead to the sufficient hierarchy ($\mathcal{O}(10^{-5})$). The reason is that we can not choose the large value of $\mathrm{Im}\,\tau$ in these cases. Although we need $\mathrm{Im}\,\tau \sim 10$ on T^2/Z_2, $\mathrm{Im}\,\tau = \sin(2\pi i/N) < 1$ on T^2/Z_N ($N = 3, 4, 6$) is too small to realize the sufficient hierarchy.

	Sample values	Observed values
$(m_u, m_c, m_t)/m_t$	$(9.9 \times 10^{-6}, 2.8 \times 10^{-2}, 1)$	$(1.5 \times 10^{-5}, 7.5 \times 10^{-3}, 1)$
$(m_d, m_s, m_b)/m_b$	$(5.0 \times 10^{-3}, 1.6 \times 10^{-2}, 1)$	$(1.2 \times 10^{-3}, 2.3 \times 10^{-2}, 1)$
$\lvert V_{\rm CKM}\rvert$	$\begin{pmatrix} 0.99 & 3.1 \times 10^{-8} & 0 \\ 3.1 \times 10^{-8} & 0.99 & 2.6 \times 10^{-13} \\ 0 & 2.6 \times 10^{-13} & 0.99 \end{pmatrix}$	$\begin{pmatrix} 0.97 & 0.23 & 0.0035 \\ 0.23 & 0.97 & 0.041 \\ 0.0087 & 0.040 & 1.0 \end{pmatrix}$

Table 4.1: Theoretical sample values of the one-pair Higgs model on T^2/Z_2.

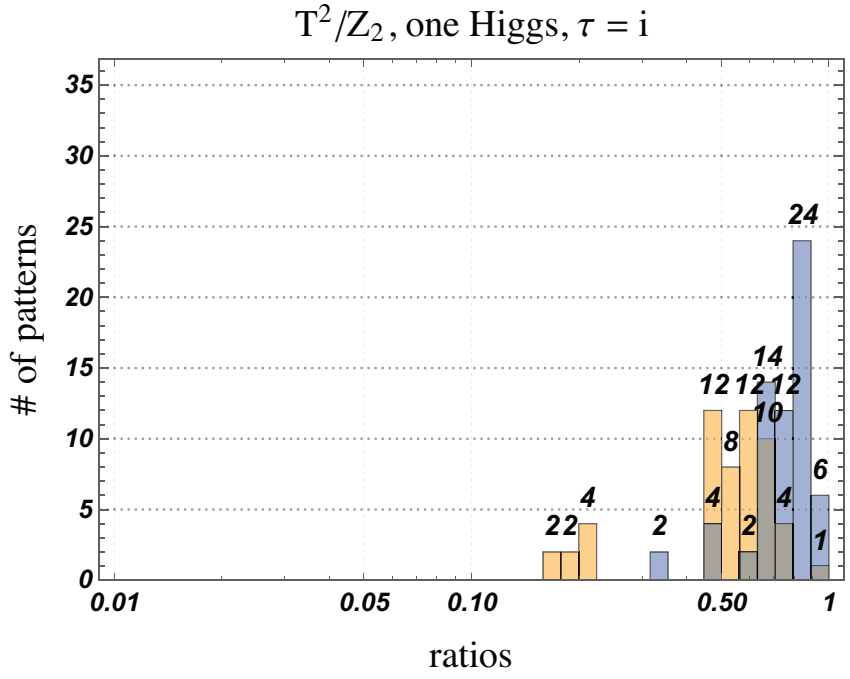

Figure 4.1: The ratios between three eigenvalues of the Yukawa matrices on T^2/Z_2. Here, we set $\mathrm{Im}\,\tau = 1$.

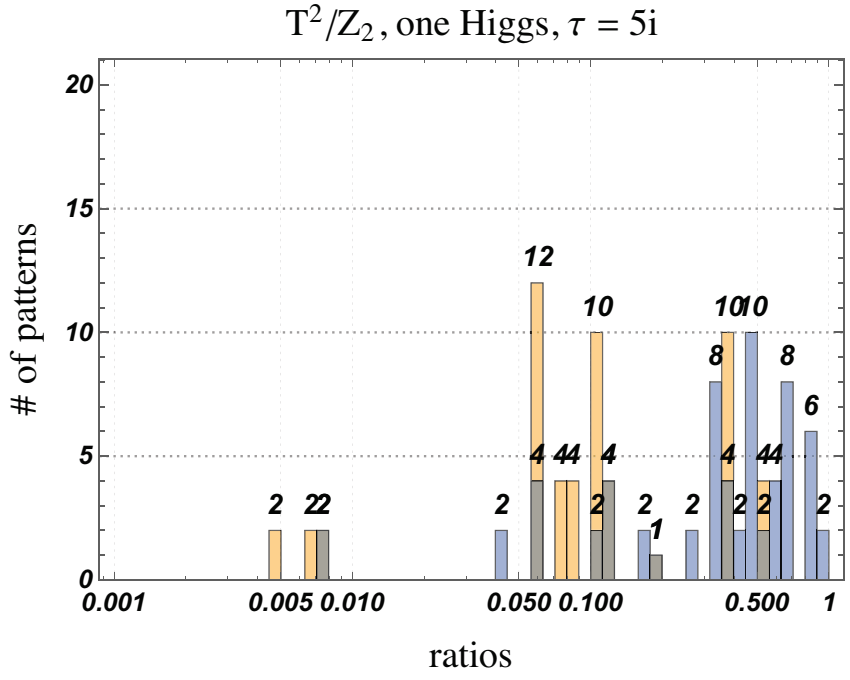

Figure 4.2: The ratios between three eigenvalues of the Yukawa matrices on T^2/Z_2. Here, we set $\mathrm{Im}\,\tau = 5$.

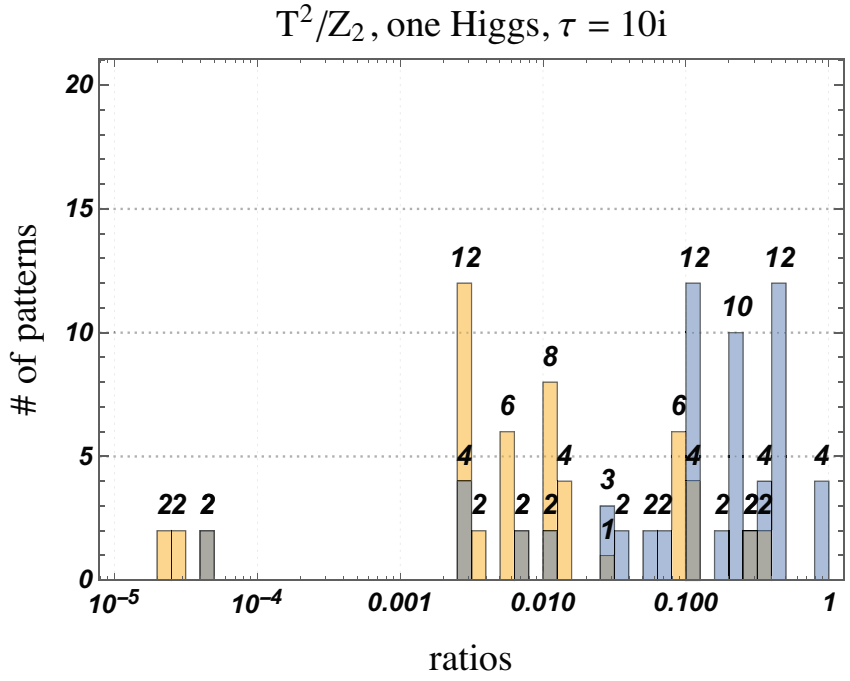

Figure 4.3: The ratios between three eigenvalues of the Yukawa matrices on T^2/Z_2. Here, we set $\mathrm{Im}\,\tau = 10$.

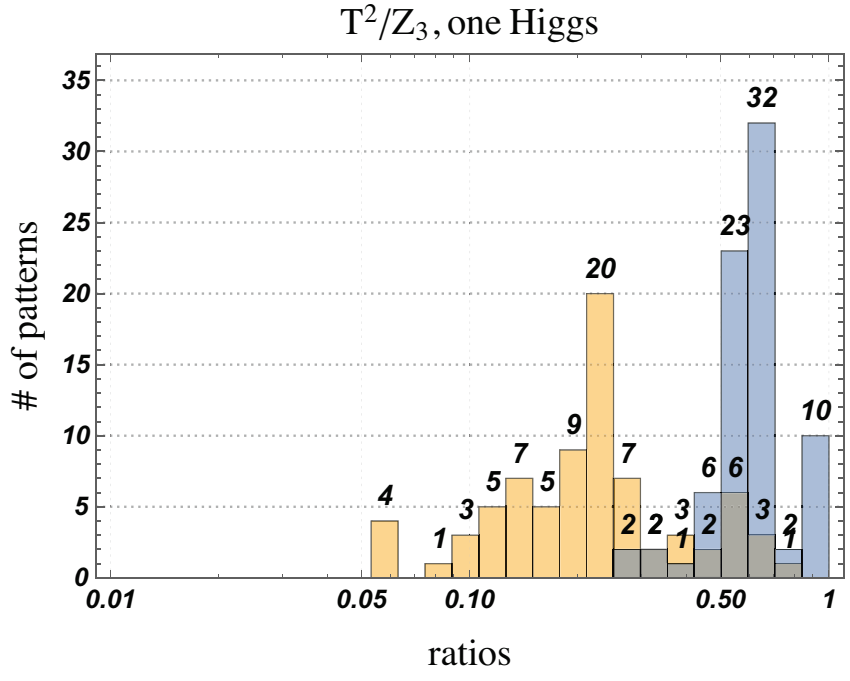

Figure 4.4: The ratios between three eigenvalues of the Yukawa matrices on T^2/Z_3

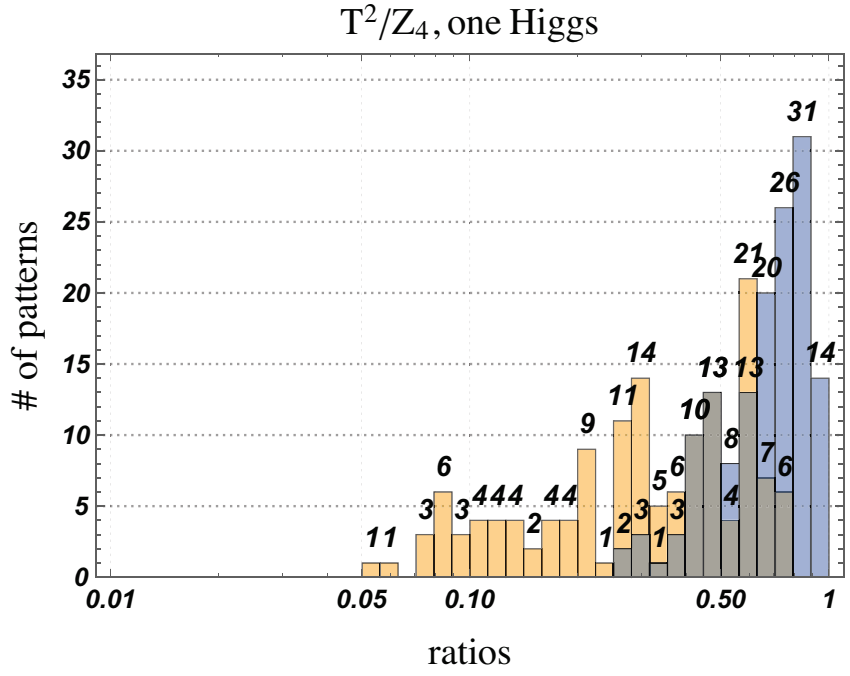

Figure 4.5: The ratios between three eigenvalues of the Yukawa matrices on T^2/Z_4

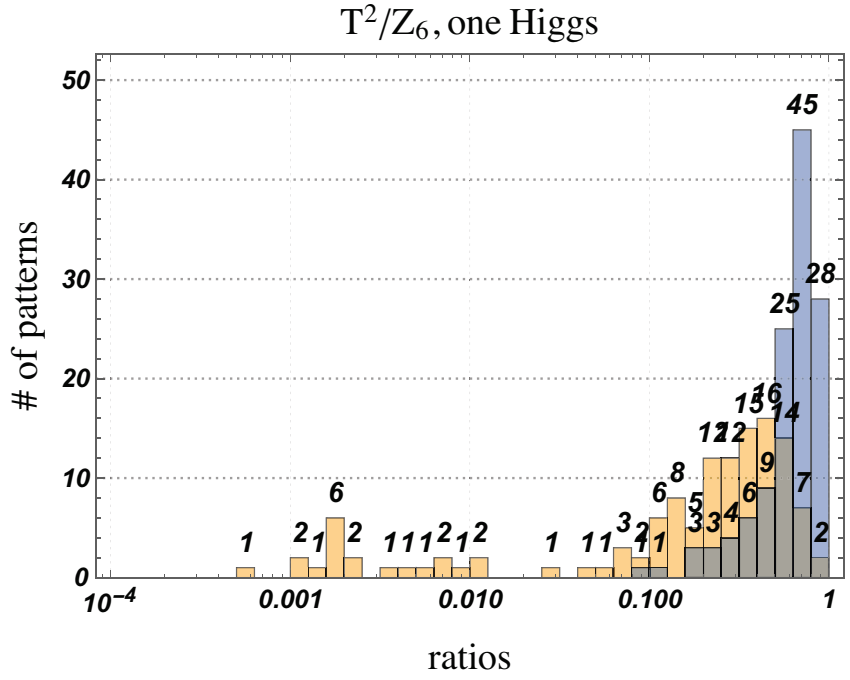

Figure 4.6: The ratios between three eigenvalues of the Yukawa matrices on T^2/Z_6

4.3 Two-Higgs-pair case

In this chapter, we try to investigate the mass hierarchy in the two-pair Higgs models. Note that the two generations of the Higgs doublets are possible except for T^2/Z_2. Then, values of the complex structure modulus must be discretized, as mentioned already. For the two Higgs doublet cases, the mass matrix is given in terms of the two VEVs as

$$M_{ij} = y_{ij1}v_1 + y_{ij2}v_2, \tag{4.27}$$

where v_1 and v_2 denote the VEVs of the two Higgs doublets. The VEVs satisfy

$$v_1^2 + v_2^2 = v^2 = (174\,\mathrm{GeV})^2. \tag{4.28}$$

In the two Higgs cases, the eigenvalues of the mass matrix in Eq. (4.27) are affected by the ratio of the two VEVs. Hence, the ratio of the VEVs, i.e., v_1/v_2, is considered as an only free parameter. In numerical studies, step sizes of the ratio v_1/v_2 are chosen as 0.001 from 0.001 to 1 and 0.1 from 1 to 1000.

Figure 4.7 shows distributions of the mass hierarchies on T^2/Z_3. We easily find that specific tunings of the VEV ratio can lead to mild hierarchies of the mass eigenvalues. However, a sufficient ratio $\mathcal{O}(10^{-5})$ can not be reached. Figures 4.8 and 4.9 also show the results on T^2/Z_4 and T^2/Z_6. By rough estimations, the hierarchies between eigenvalues as large as 5×10^{-2} for T^2/Z_2 and 5×10^{-3} for T^2/Z_4 and T^2/Z_6 are found. These hierarchies do not explain the observed mass ratio between the up and top quarks $m_u/m_t = \mathcal{O}(10^{-5})$. Thus, we can conclude that the two-pair Higgs models are not suitable for model buildings including the quark flavors.

Before closing this chapter, we would like to point out the reason of less hierarchical structures in the two-pair Higgs models. For example, let us consider an example of the following configuration of the magnetic fluxes, SS twist phases and Z_6 parities for T^2/Z_6,

$$\{M_{ab}, \alpha_{ab}, s_{ab}\} = \{-15, 1/2, 0\}, \tag{4.29}$$
$$\{M_{ca}, \alpha_{ca}, s_{ca}\} = \{+24, 0, 5\}, \tag{4.30}$$
$$\{M_{bc}, \alpha_{bc}, s_{bc}\} = \{-9, 1/2, 1\}. \tag{4.31}$$

Here, we use a charge of the Z_6 parity, e.g., $\eta_{ab} \equiv e^{2\pi i s_{ab}/6}$. The same holds for the ca- and bc-sectors. It is easily confirmed that this configuration leads to three generations of the left-handed and right-handed fermions and two generations of the Higgs doublets. (The mass ratios in this configuration are shown in the second panel from the upper right in Fig. 4.7.) By plugging the possible value of the complex modulus parameter $\tau = e^{2\pi i/6}$, we can eventually obtain the numerical expression of the mass matrix,

$$M_{ij} = y_{ij1}v_1 + y_{ij2}v_2, \tag{4.32}$$

where,

$$y_{ij1} = \begin{pmatrix} -0.204991 - 0.0796877i & 0.00942303 + 0.09068i & 0.0519518 + 0.0517703i \\ 0.0763198 + 0.0222452i & -0.00676905 - 0.017782i & -0.0077252 - 0.00374813i \\ -0.0507492 - 0.0180038i & 0.0683165 + 0.0433135i & -0.0157981 - 0.12252i \end{pmatrix}, \tag{4.33}$$

$$y_{ij2} = \begin{pmatrix} 0.00505039 + 0.0102538i & 0.00941751 - 0.180948i & -0.0776918 - 0.115464i \\ -0.00982989 - 0.00704602i & 0.00161259 + 0.0544036i & 0.0166123 + 0.0174854i \\ 0.0133678 - 0.0127981i & 0.0383659 - 0.114777i & -0.00590916 + 0.172257i \end{pmatrix}. \tag{4.34}$$

The hierarchy in each of the matrix elements in Eqs. (4.33) and (4.34) is found as $\mathcal{O}(10^{-2})$. This is due to the mixing effects from the kinetic mixing and the basis changing from the torus zero-mode eigenstates to the orbifold zero-mode eigenstates. Thus, such mixing effects disturb the hierarchical structure in the mass matrix on the original torus zero-mode basis. This smearing effect appears also in the other configuration of the fluxes and so on. Thus, we can conclude that the two-pair Higgs models are not suitable for the quark sector.

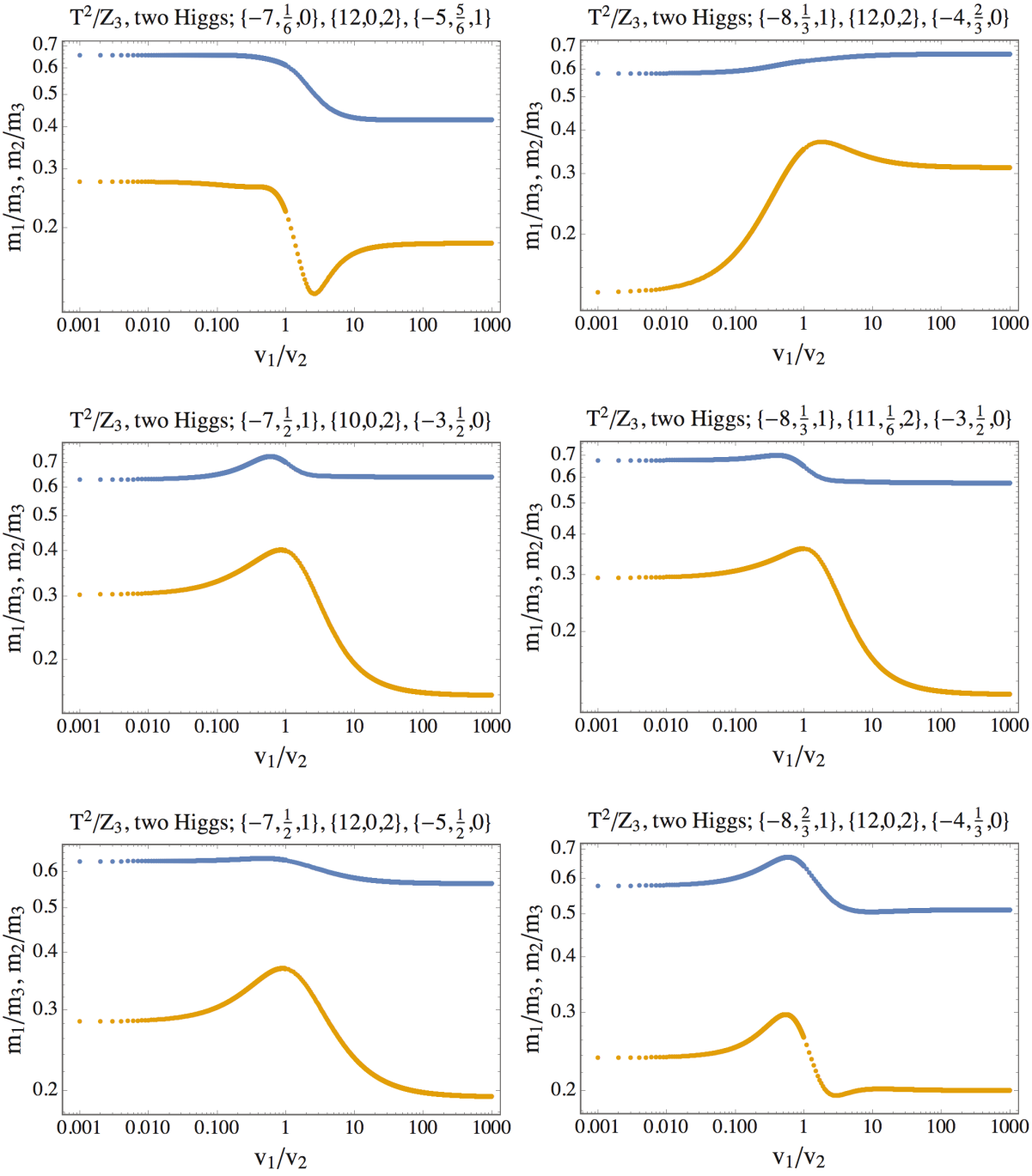

Figure 4.7: The values of the mass hierarchies on T^2/Z_3. In these figures, ratios of eigenvalues of the mass matrix, $m_1/m_3, m_2/m_3$, are plotted as functions of the ratio of Higgs VEVs v_1/v_2, which is varied with the step size 0.001 from 0.001 to 1 and with the step size 0.1 from 1 to 1000.

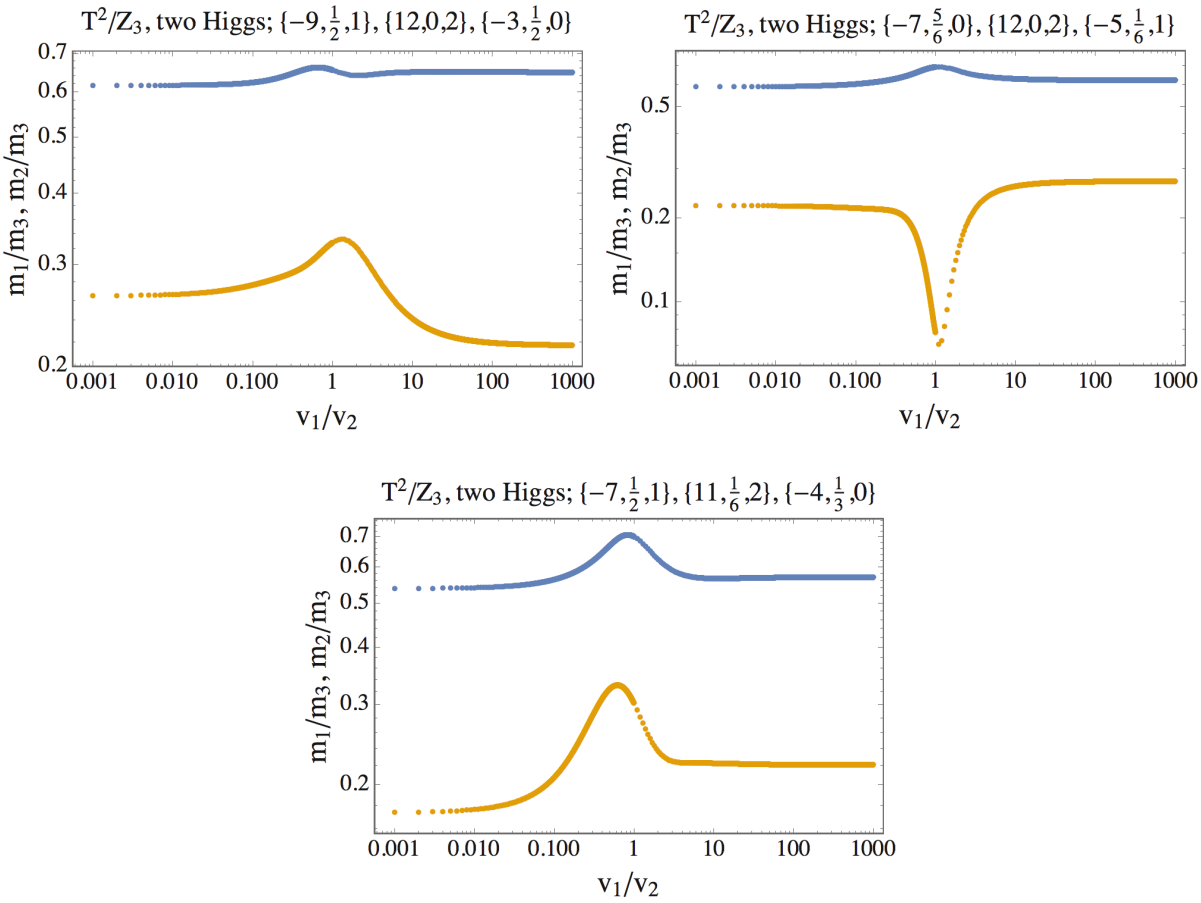

Figure 4.7: (Continued.) The values of the mass hierarchies on T^2/Z_3. In these figures, ratios of eigenvalues of the mass matrix, $m_1/m_3, m_2/m_3$, are plotted as functions of the ratio of Higgs VEVs v_1/v_2, which is varied with the step size 0.001 from 0.001 to 1 and with the step size 0.1 from 1 to 1000.

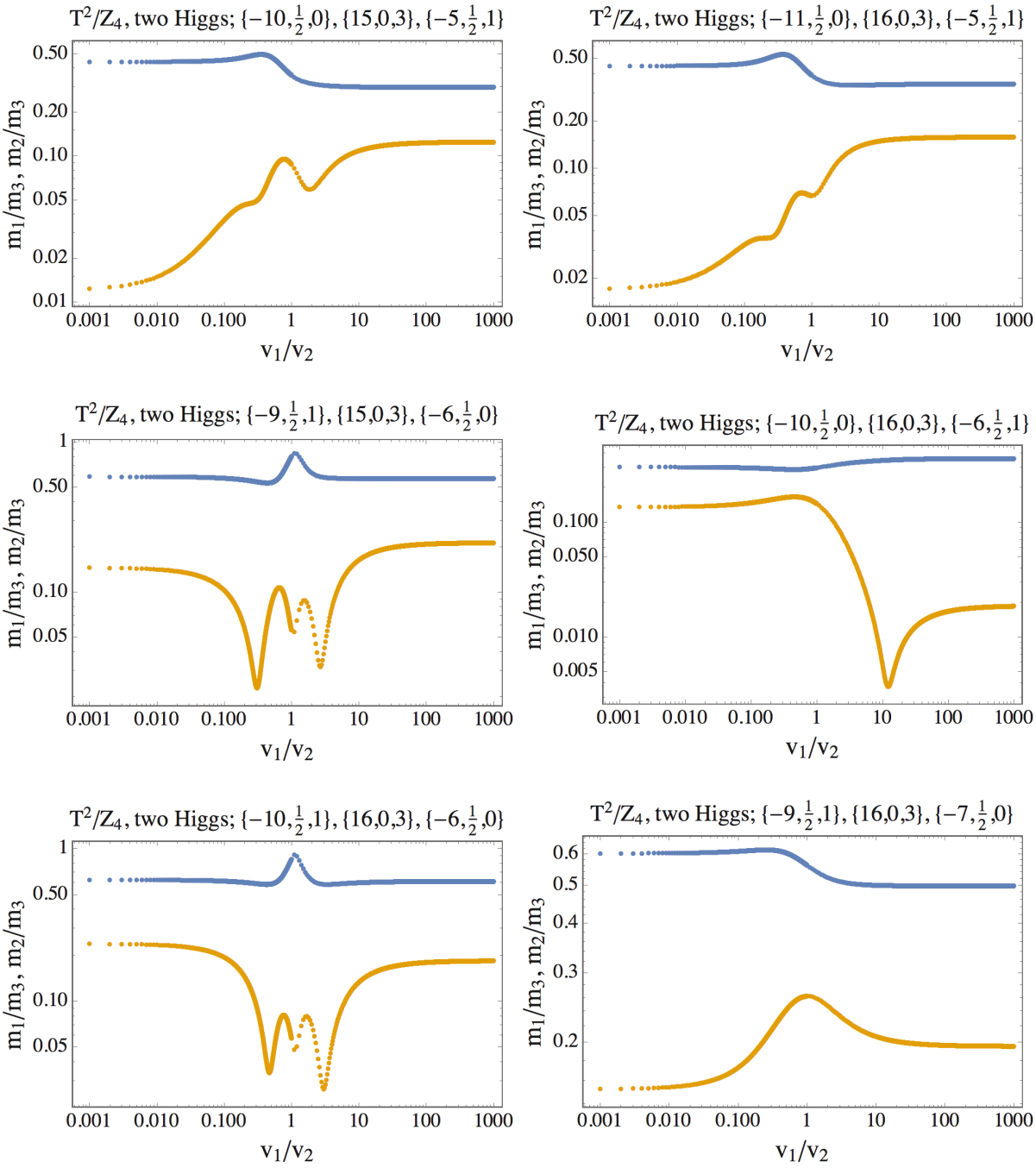

Figure 4.8: The values of the mass hierarchies on T^2/Z_4. In these figures, ratios of eigenvalues of the mass matrix, $m_1/m_3, m_2/m_3$, are plotted as functions of the ratio of Higgs VEVs v_1/v_2, which is varied with the step size 0.001 from 0.001 to 1 and with the step size 0.1 from 1 to 1000.

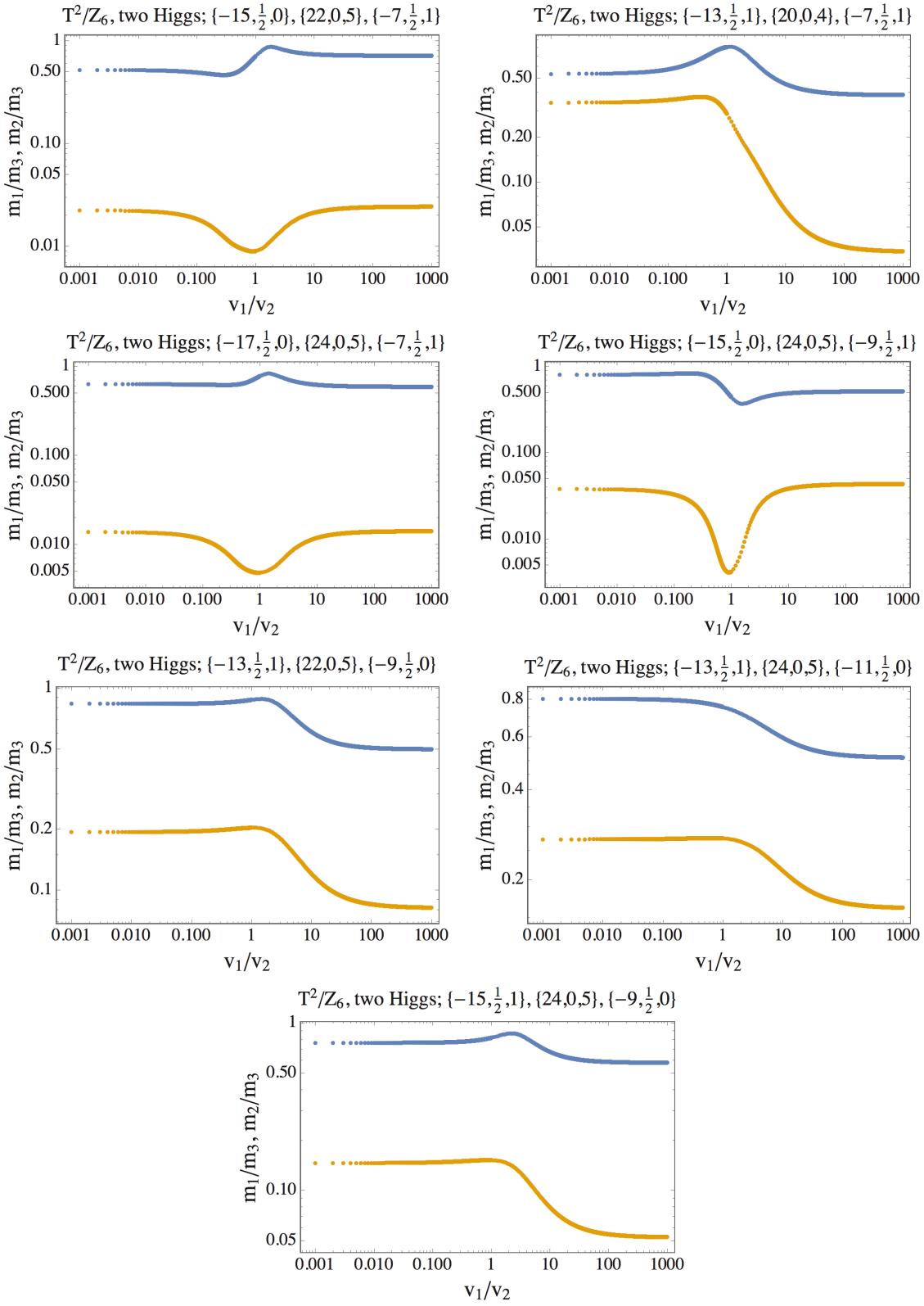

Figure 4.9: The values of the mass hierarchies on T^2/Z_6. In these figures, ratios of eigenvalues of the mass matrix, $m_1/m_3, m_2/m_3$, are plotted as functions of the ratio of Higgs VEVs v_1/v_2, which is varied with the step size 0.001 from 0.001 to 1 and with the step size 0.1 from 1 to 1000.

Chapter 5

Gaussian Froggatt–Nielsen mechanism

In this chapter, we propose a promising texture of mass matrices derived from the magnetized orbifold background [44]. We show that such a texture can realize some of the experimental data of quarks and charged leptons, i.e., mass hierarchies and quark mixing angles. Furthermore, we construct a concrete model with the promising texture on the basis of ten-dimensional supersymmetric Yang–Mills theory with non-vanishing magnetic fluxes.

5.1 Supersymmetry

The ten-dimensional SYM theory has $\mathcal{N} = 4$ 4D-supersymmetries (SUSY), that is, it contains four 4D supercharges. However, the flux configurations satisfying a certain condition can preserve only a part of supersymmetries, i.e., $\mathcal{N} = 1$ 4D SUSY. Then, we can derive the MSSM-like supersymmetric models from the 10D SYM theory. The SUSY preserving condition is given by

$$\frac{1}{\mathcal{A}^{(1)}}\langle F_{45}\rangle + \frac{1}{\mathcal{A}^{(2)}}\langle F_{67}\rangle + \frac{1}{\mathcal{A}^{(3)}}\langle F_{89}\rangle = 0, \tag{5.1}$$

as mentioned in Refs. [38, 46]. Here $\mathcal{A}^{(i)}$ denotes an area of the i-th torus. This condition restricts model-building strongly.

The authors of Ref. [38] tried to construct a model satisfying this condition. As a result, they obtained a single model that has realistic spectra with the low-scale SUSY breaking scenario on the 2D torus. In their model, three-generation structure is generated without an orbifold projection and the Pati–Salam magnetic fluxes break the $U(8)$ group down to $U(4) \times U(2) \times U(2)$, i.e., the Pati–Salam gauge group, which is usually broken by Wilson-lines. Without orbifoldings, the flux configuration which is adopted in the model is a unique ansatz to generate three-generations because of the strict SUSY condition.

If the three-generation structure is given by degenerate zero-modes reduced by orbifold projections, then, the four-block texture of fluxes is required to make a difference between the SM quarks and leptons. However, the SUSY preserving condition can not be satisfied with such flux configurations [40]. Magnetized orbifold models that entail to preserve $\mathcal{N} = 1$ SUSY can not be realized within the 10D SYM theory.

It may seem that various orbifold models can be realized with high-scale SUSY breaking scenario, where all the SUSY are broken entirely by magnetic fluxes at the compactification scale. However, that is not easy because we owe to Wilson-lines the success of the previous model in terms not only of gauge symmetry breaking but also of Yukawa hierarchies. The Wilson-lines shift the localization points of the zero-mode wavefunctions and we could control the magnitude of the overlaps of them, directly. Namely, the Wilson-lines were the key degrees of freedom to realize experimental data of masses of quarks and leptons and CKM mixings in the model.

In this chapter, we try to construct an SM-like non-supersymmetric model with a magnetized and orbifold background, which can realize mass hierarchies and mixings. Then, we also discuss the effects of high-scale SUSY breaking.

5.2 Model construction

The three-generation structures are necessarily generated only on a torus, since we require full-rank Yukawa matrices derived from such Yukawa couplings at the tree level in order to obtain three non-zero masses. The configurations of magnetic fluxes on the other two tori must be so determined to leave the MSSM field contents unchanged and to eliminate extra fields, i.e., so-called exotic-modes. As we mentioned in the previous chapter, the introduced magnetic fluxes are not restricted by the D-term SUSY preserving condition (5.1), because it is impossible to satisfy the condition (5.1) and we left the low-scale SUSY breaking scenario for that at the high-scale in the magnetized orbifold models. Since the structures of the other two tori must not change or spoil the three-generation structures of quarks and leptons, the second and third parts of Yukawa couplings, $a^{(2)}$ and $a^{(3)}$ in Eq. (3.12), can not possess the flavor index if the three-generation structures are generated on the first two-dimensional orbifold T^2/Z_2, that is, Yukawa couplings in the four-dimensional effective theory are given by

$$Y_{IJK} = \lambda^{(1)}_{IJK}\lambda^{(2)}\lambda^{(3)}, \tag{5.2}$$

where Yukawa couplings $\lambda^{(2)}$ and $\lambda^{(3)}$ are $\mathcal{O}(1)$ global factors.

For the moment, we concentrate on the orbifold T^2/Z_2 where three degenerate zero-modes are generated, and discuss the entire extra dimensions later. Three degenerate zero-modes are given by four types of magnetic fluxes in T^2/Z_2 orbifold models, i.e., $M = 4, 5$ for even-modes ($\eta = +1$) and $M = 7, 8$ for odd-modes ($\eta = -1$). The magnetic fluxes that a Higgs sector feels are automatically determined because of gauge symmetry and other consistency if the fluxes of the left-handed and the right-handed sectors are

fixed. Twenty configurations of magnetic fluxes yielding the three-generation models and the degeneracy of Higgs fields on such configurations are listed in Ref. [35], if there are no non-trivial SS twist phases. The authors also studied the quark masses and mixings numerically in a sample model. We focus on the other configuration of magnetic fluxes, and analyze the Yukawa-coupling textures obtained from such a flux configuration. In this section, we construct a model containing the three-generations of quarks and leptons, which can realize (semi-)realistic patterns of masses and mixings simultaneously, even though we do not use the Wilson-line phases in such orbifold models.

We start from a ten-dimensional $U(8)$ SYM theory with the following flux configuration on the first torus with the coordinates (y_4, y_5),

$$F_{45} \propto \begin{pmatrix} 0 \times \mathbf{1}_3 & & & \\ & 1 \times \mathbf{1}_1 & & \\ & & 5 \times \mathbf{1}_2 & \\ & & & -7 \times \mathbf{1}_2 \end{pmatrix}, \tag{5.3}$$

which is nothing but a four-block flux. The magnetic flux breaks the $U(8)$ gauge group down to $SU(3)_C \times SU(2)_L \times SU(2)_R$ up to $U(1)$s. There exists the remaining $SU(2)_R$ gauge group and it is difficult to break the $SU(2)_R$ gauge group by the the magnetic fluxes and orbifold projections. We show the configuration of the magnetic fluxes which each sector feels and the Z_2 boundary conditions in Table 5.1.

	left-handed field	right-handed field	Higgs field
quark-sector	-5 (even)	-7 (odd)	$+12$ (odd)
lepton-sector	-4 (even)	-8 (odd)	$+12$ (odd)

Table 5.1: The values of magnetic fluxes and the Z_2 boundary conditions for quarks and leptons on the first orbifold T^2/Z_2.

We can see that the flux configuration generates the three-generations of quarks and leptons and five-generations of Higgs multiplets from Table 5.1. The first column on the right in the table shows the magnetic fluxes and the Z_2 boundary conditions of the Higgs sector. It is important that the Z_2 boundary condition in the Higgs sector is determined by that in the left- and the right-handed sectors to obtain the non-vanishing Yukawa couplings. The integrand of non-vanishing Yukawa couplings, i.e., a product of three orbifold zero-modes is a totally even-function and the sum of three magnetic fluxes in each sector is zero because of the gauge invariance, i.e., $M_{ab} + M_{bc} + M_{ca} = 0$. We select different flux configurations between quark and lepton sectors in order to realize the experimental data of quarks and leptons. If we select the same configurations between quarks and leptons, i.e., we use the three-block (Pati–Salam) flux, theoretical sample values of quark and leptons are the same such that the model predicts the degenerate

masses of quarks and leptons. Taking into account of such a requirement, $SU(2)_R$ gauge group remains and the $SU(2)_R$ gauge group breaking sector (or mechanism) is required. We can always consider such an additional sector as an extension of our model. Since we are focusing on the structures of Yukawa matrices here, we just assume the $SU(2)_R$ gauge group breaking that gives the different vacuum expectation values to the up- and down-sector of Higgs fields. In the model, the four types of Yukawa matrices (the up- and down-sectors in quarks and those in leptons) possess different structures by introducing two different types of the magnetic fluxes, orbifold boundary conditions and the VEVs of Higgs fields.

We show all the zero-mode wavefunctions given by the above flux configurations in Table 5.2 and Table 5.3.

Generation	Q	u, d	H_u, H_d
0	$\psi^{0,5}$	$\frac{1}{\sqrt{2}}(\psi^{1,7}-\psi^{6,7})$	$\frac{1}{\sqrt{2}}(\phi^{1,12}-\phi^{11,12})$
1	$\frac{1}{\sqrt{2}}(\psi^{1,5}-\psi^{4,5})$	$\frac{1}{\sqrt{2}}(\psi^{2,7}-\psi^{5,7})$	$\frac{1}{\sqrt{2}}(\phi^{2,12}-\phi^{10,12})$
2	$\frac{1}{\sqrt{2}}(\psi^{2,5}-\psi^{3,5})$	$\frac{1}{\sqrt{2}}(\psi^{3,7}-\psi^{4,7})$	$\frac{1}{\sqrt{2}}(\phi^{3,12}-\phi^{9,12})$
3	—	—	$\frac{1}{\sqrt{2}}(\phi^{4,12}-\phi^{8,12})$
4	—	—	$\frac{1}{\sqrt{2}}(\phi^{5,12}-\phi^{7,12})$

Table 5.2: Zero-mode wavefunctions of the left-handed quarks Q, the right-handed quarks u, d and the up- and down- Higgs fields H_u, H_d.

Generation	L	e, ν	H_u, H_d
0	$\psi^{0,4}$	$\frac{1}{\sqrt{2}}(\psi^{1,8}-\psi^{7,8})$	$\frac{1}{\sqrt{2}}(\phi^{1,12}-\phi^{11,12})$
1	$\frac{1}{\sqrt{2}}(\psi^{1,4}-\psi^{3,4})$	$\frac{1}{\sqrt{2}}(\psi^{2,8}-\psi^{6,8})$	$\frac{1}{\sqrt{2}}(\phi^{2,12}-\phi^{10,12})$
2	$\psi^{2,4}$	$\frac{1}{\sqrt{2}}(\psi^{3,8}-\psi^{5,8})$	$\frac{1}{\sqrt{2}}(\phi^{3,12}-\phi^{9,12})$
3	—	—	$\frac{1}{\sqrt{2}}(\phi^{4,12}-\phi^{8,12})$
4	—	—	$\frac{1}{\sqrt{2}}(\phi^{5,12}-\phi^{7,12})$

Table 5.3: Zero-mode wavefunctions of the left-handed leptons L, the right-handed charged leptons e, the neutrinos ν and the up- and down- Higgs fields H_u, H_d.

We can calculate all the Yukawa couplings analytically. For a simple description, we

define the following function,

$$\eta_N = \vartheta \begin{bmatrix} N/M \\ 0 \end{bmatrix} (0, M\tau). \tag{5.4}$$

We use this function to represent the Jacobi theta function in the elements of the Yukawa couplings. A complex structure parameter τ in Eq. (5.4) denotes $\tau^{(1)}$ in the previous chapter and M is a product of three fluxes, $5 \times 7 \times 12 = 420$ for the quark-sector and $4 \times 8 \times 12 = 384$ for the lepton-sector.

We have five generations of Higgs fields, and the Yukawa couplings are written as

$$Y_{IJK} H_K (Q_L)_I (Q_R)_J = \left(Y_{IJ0} H_0 + Y_{IJ1} H_1 + Y_{IJ2} H_2 + Y_{IJ3} H_3 + Y_{IJ4} H_4\right) (Q_L)_I (Q_R)_J. \tag{5.5}$$

Note that mass matrices of quarks and leptons are given by a linear combination of the five Yukawa matrices. A certain linear combination of the five Higgs fields corresponds to the SM Higgs field. The five Yukawa matrices are written in terms of the η-function. For the quark-sector, we obtain

$$Y_{IJ0} = \frac{1}{\sqrt{2}} \begin{pmatrix} \sqrt{2}\left(\eta_5 - \eta_{65}\right) & \sqrt{2}\left(\eta_{185} - \eta_{115}\right) & \sqrt{2}(\eta_{55} + \eta_{125}) \\ \eta_{173} - \eta_{103} - \eta_{187} + \eta_{163} & \eta_{67} - \eta_{137} - \eta_{53} + \eta_{17} & \eta_{113} - \eta_{43} - \eta_{127} + \eta_{197} \\ \eta_{79} - \eta_{149} - \eta_{19} + \eta_{89} & \eta_{101} - \eta_{31} - \eta_{199} + \eta_{151} & \eta_{139} - \eta_{209} - \eta_{41} + \eta_{29} \end{pmatrix}, \tag{5.6}$$

$$Y_{IJ1} = \frac{1}{\sqrt{2}} \begin{pmatrix} \sqrt{2}\left(\eta_{170} - \eta_{110}\right) & \sqrt{2}\left(\eta_{10} - \eta_{130}\right) & \sqrt{2}(\eta_{50} + \eta_{190}) \\ \eta_2 - \eta_{142} - \eta_{58} + \eta_{82} & \eta_{178} - \eta_{38} - \eta_{122} + \eta_{158} & \eta_{62} - \eta_{202} - \eta_{118} + \eta_{22} \\ \eta_{166} - \eta_{26} - \eta_{194} + \eta_{94} & \eta_{74} - \eta_{206} - \eta_{46} + \eta_{94} & \eta_{106} - \eta_{34} - \eta_{134} + \eta_{146} \end{pmatrix}, \tag{5.7}$$

$$Y_{IJ2} = \frac{1}{\sqrt{2}} \begin{pmatrix} \sqrt{2}\left(\eta_{75} - \eta_{135}\right) & \sqrt{2}\left(\eta_{165} - \eta_{45}\right) & \sqrt{2}\left(\eta_{15} - \eta_{195}\right) \\ \eta_{173} - \eta_{33} - \eta_{117} + \eta_{93} & \eta_3 - \eta_{207} - \eta_{123} + \eta_{87} & \eta_{183} - \eta_{27} - \eta_{57} + \eta_{153} \\ \eta_9 - \eta_{201} - \eta_{51} + \eta_{81} & \eta_{171} - \eta_{39} - \eta_{129} + \eta_{81} & \eta_{69} - \eta_{141} - \eta_{111} + \eta_{99} \end{pmatrix}, \tag{5.8}$$

$$Y_{IJ3} = \frac{1}{\sqrt{2}} \begin{pmatrix} \sqrt{2}\left(\eta_{100} - \eta_{140}\right) & \sqrt{2}\left(\eta_{80} - \eta_{200}\right) & \sqrt{2}\left(\eta_{160} - \eta_{20}\right) \\ \eta_{68} - \eta_{208} - \eta_{128} + \eta_{152} & \eta_{172} - \eta_{32} - \eta_{52} + \eta_{88} & \eta_8 - \eta_{148} - \eta_{188} + \eta_{92} \\ \eta_{184} - \eta_{44} - \eta_{124} + \eta_{164} & \eta_4 - \eta_{136} - \eta_{116} + \eta_{164} & \eta_{176} - \eta_{104} - \eta_{64} + \eta_{76} \end{pmatrix}, \tag{5.9}$$

$$Y_{IJ4} = \frac{1}{\sqrt{2}} \begin{pmatrix} \sqrt{2}\left(\eta_{145} - \eta_{205}\right) & \sqrt{2}\left(\eta_{95} - \eta_{25}\right) & \sqrt{2}\left(\eta_{85} - \eta_{155}\right) \\ \eta_{107} - \eta_{37} - \eta_{47} + \eta_{23} & \eta_{73} - \eta_{143} - \eta_{193} + \eta_{157} & \eta_{167} - \eta_{97} - \eta_{13} + \eta_{83} \\ \eta_{61} - \eta_{131} - \eta_{121} + \eta_{11} & \eta_{179} - \eta_{109} - \eta_{59} + \eta_{11} & \eta_1 - \eta_{71} - \eta_{181} + \eta_{169} \end{pmatrix}. \tag{5.10}$$

Similarly, for the lepton-sector, we obtain

$$
\begin{aligned}
Y_{IJ0} &= \begin{pmatrix} y_b & 0 & -y_l \\ 0 & \frac{1}{\sqrt{2}}(y_e - y_i) & 0 \\ -y_f & 0 & y_h \end{pmatrix}, \\
Y_{IJ1} &= \begin{pmatrix} 0 & y_c - y_k & 0 \\ \frac{1}{\sqrt{2}}(y_b - y_h) & 0 & \frac{1}{\sqrt{2}}(y_f - y_l) \\ 0 & 0 & 0 \end{pmatrix}, \\
Y_{IJ2} &= \begin{pmatrix} -y_j & 0 & y_d \\ 0 & \frac{1}{\sqrt{2}}(y_a - y_m) & 0 \\ y_d & 0 & -y_j \end{pmatrix}, \\
Y_{IJ3} &= \begin{pmatrix} 0 & 0 & 0 \\ \frac{1}{\sqrt{2}}(y_f - y_l) & 0 & \frac{1}{\sqrt{2}}(y_b - y_h) \\ 0 & y_c - y_k & 0 \end{pmatrix}, \\
Y_{IJ4} &= \begin{pmatrix} y_h & 0 & -y_f \\ 0 & \frac{1}{\sqrt{2}}(y_e - y_i) & 0 \\ -y_l & 0 & y_b \end{pmatrix},
\end{aligned}
$$

where

$$
\begin{aligned}
y_a &= \eta_0 + \eta_{96} + \eta_{192} + \eta_{96}, \\
y_b &= \eta_4 + \eta_{100} + \eta_{188} + \eta_{92}, \\
y_c &= \eta_8 + \eta_{104} + \eta_{184} + \eta_{88}, \\
y_d &= \eta_{12} + \eta_{108} + \eta_{180} + \eta_{84}, \\
y_e &= \eta_{16} + \eta_{112} + \eta_{176} + \eta_{80}, \\
y_f &= \eta_{20} + \eta_{116} + \eta_{172} + \eta_{76}, \\
y_g &= \eta_{24} + \eta_{120} + \eta_{168} + \eta_{72}, \\
y_h &= \eta_{28} + \eta_{124} + \eta_{164} + \eta_{68}, \\
y_i &= \eta_{32} + \eta_{128} + \eta_{160} + \eta_{64}, \\
y_j &= \eta_{36} + \eta_{132} + \eta_{156} + \eta_{60}, \\
y_k &= \eta_{40} + \eta_{136} + \eta_{152} + \eta_{56}, \\
y_l &= \eta_{44} + \eta_{140} + \eta_{148} + \eta_{52}, \\
y_m &= \eta_{48} + \eta_{144} + \eta_{144} + \eta_{48}.
\end{aligned}
$$

Note that a difference between the up and down sectors is given by the VEVs of the two types of Higgs fields, H_u and H_d.

5.3 Gaussian Froggatt–Nielsen mechanism

The model under consideration can lead to a (semi-)realistic pattern, as we will see later. Then, it is necessary that the Y_{IJ3} and the Y_{IJ4} dominate the others, that is, the VEVs of the fourth and fifth Higgs fields, $\langle H_3 \rangle$ and $\langle H_4 \rangle$, are much larger than the others. The specific ratios are not so important, since such a (semi-)realistic pattern can be realized within a wide parameter region around the above input parameters. To explain this, we focus on the analytical structures of the Yukawa matrices. We go back to Eq. (5.4),

$$\eta_N = \vartheta \begin{bmatrix} N/M \\ 0 \end{bmatrix} (0, M\tau) = \sum_{l \in \mathbb{Z}} e^{-\pi (\mathrm{Im}\, \tau)(N^2/M + 2Ml + Ml^2)}, \tag{5.11}$$

where $M = 420$ for quarks and $M = 384$ for leptons. For such large Ms ($\sim \mathcal{O}(100)$), higher-modes with $l \neq 0$ are strongly suppressed and we can use the following approximation,

$$\eta_N \simeq e^{-\pi (\mathrm{Im}\, \tau) N^2/M}. \tag{5.12}$$

Then, we find that the function η_N is more dominant than $\eta_{N'}$ for $N < N'$. By using this approximation, we can rewrite the five Yukawa matrices up to overall factors. For the quark sector, we obtain

$$Y_{IJ0} \simeq \begin{pmatrix} \eta_5 & -\eta_{115} & \eta_{55} \\ -\eta_{103} & -\eta_{53} & -\eta_{43} \\ -\eta_{19} & -\eta_{31} & \eta_{29} \end{pmatrix}, \tag{5.13}$$

$$Y_{IJ1} \simeq \begin{pmatrix} -\eta_{110} & \eta_{10} & \eta_{50} \\ \eta_2 & -\eta_{38} & \eta_{22} \\ -\eta_{26} & -\eta_{46} & -\eta_{34} \end{pmatrix}, \tag{5.14}$$

$$Y_{IJ2} \simeq \begin{pmatrix} \eta_{75} & -\eta_{45} & \eta_{15} \\ -\eta_{33} & \eta_3 & -\eta_{27} \\ \eta_9 & -\eta_{39} & \eta_{69} \end{pmatrix}, \tag{5.15}$$

$$Y_{IJ3} \simeq \begin{pmatrix} \eta_{100} & \eta_{80} & -\eta_{20} \\ \eta_{68} & -\eta_{32} & \eta_8 \\ -\eta_{44} & \eta_4 & -\eta_{64} \end{pmatrix}, \tag{5.16}$$

$$Y_{IJ4} \simeq \begin{pmatrix} \eta_{145} & -\eta_{25} & \eta_{85} \\ \eta_{23} & \eta_{73} & -\eta_{13} \\ \eta_{11} & \eta_{11} & \eta_1 \end{pmatrix}, \tag{5.17}$$

and the dominant part of the Yukawa matrices in the above example is given by

$$y_{\mathrm{quark}} = Y_{IJ3} + Y_{IJ4} \simeq \begin{pmatrix} \eta_{100} & -\eta_{25} & \eta_{20} \\ \eta_{23} & -\eta_{32} & -\eta_8 \\ \eta_{11} & \eta_4 & \eta_1 \end{pmatrix}, \tag{5.18}$$

where η_N is given approximately in Eq. (5.12) and we find that the effective Yukawa matrix has a Froggatt–Nielsen-like (FN-like) structure with Gaussian functions. Although

it is different from the original FN structure [11] where the Yukawa couplings are given by exponential functions, it is important to note that the quantum numbers corresponding to the FN charges are already determined by the magnetic fluxes. Furthermore, the lighter a particle is, the larger the FN charges are. That is, $a_i > a_{i+1}$ and $b_j > b_{j+1}$ if the Yukawa couplings are given by the following form,

$$y_{ij} \sim e^{-(a_i+b_j)^2}, \tag{5.19}$$

where a_i and b_j are the FN charges [1]. Therefore, we obtain the FN-like texture of Yukawa couplings derived from the magnetized orbifold model. This type of the parameterization in the Yukawa matrix

$$Y_{ij}^{(\mathrm{G})} = e^{-c(a_i+b_j)^2}, \tag{5.20}$$

is similar to the FN parameterization [11],

$$Y_{ij}^{(\mathrm{FN})} = e^{-c'(a'_i+b'_j)}, \tag{5.21}$$

up to overall coefficients in front of the Yukawa elements. The FN parametrization has been exhaustively investigated for long years after the proposition.

In the remnant of this section, we consider the phenomenological aspects of the Gaussian FN mass matrices. First, we look at the FN case with the 2×2 matrix, for simplicity,

$$Y_{\mathrm{exmple}}^{(\mathrm{FN})} = \begin{pmatrix} Y_{22}^{(\mathrm{FN})} & Y_{23}^{(\mathrm{FN})} \\ Y_{32}^{(\mathrm{FN})} & Y_{33}^{(\mathrm{FN})} \end{pmatrix}. \tag{5.22}$$

Here, we assume $Y_{22}^{(\mathrm{FN})} \leq Y_{23}^{(\mathrm{FN})}, Y_{32}^{(\mathrm{FN})} \leq Y_{33}^{(\mathrm{FN})}$. Indeed, this is also justified by the Gaussian parametrization (5.20) if $a_2 + b_2 \leq a_2 + b_3$, for instance. By diagonalizing this 2×2 matrix

$$V^\dagger Y_{\mathrm{exmple}}^{(\mathrm{FN})} V = \mathrm{diag}(m_2, m_3), \tag{5.23}$$

the ratio of two mass eigenvalues is calculated approximately as

$$\frac{m_2}{m_3} \sim \frac{Y_{23}^{(\mathrm{FN})} Y_{32}^{(\mathrm{FN})}}{\left(Y_{33}^{(\mathrm{FN})}\right)^2}, \tag{5.24}$$

[1] We can identify the FN charges in the quark-sector,

$$y_{\mathrm{quark}} \sim e^{-\pi(\mathrm{Im}\,\tau)(a_i+b_j)^2/420},$$
$$a_i = \{20, 10, 0\},$$
$$b_j = \{10, 5, 0\}.$$

and the (2, 3) element in the diagonalization matrix (V) is also given as

$$V_{23} \sim \frac{Y_{23}^{(\mathrm{FN})}}{Y_{33}^{(\mathrm{FN})}}. \tag{5.25}$$

In the FN parametrization, since the elements in the Yukawa matrix are explicitly expressed by the FN charges $a'_i\,(i=2,3)$ and $b'_j\,(j=2,3)$, now we can estimate the suitable FN charges and an overall constant c'. In the CKM mixing matrix, the observed value is known as $V_{cb} \simeq 0.04$, and thus we require the first constraint,

$$\frac{Y_{23}^{(\mathrm{FN})}}{Y_{33}^{(\mathrm{FN})}} \sim 0.04. \tag{5.26}$$

In addition, we also need additional constraints on the mass ratios,

$$\frac{Y_{23}^{(\mathrm{FN})}Y_{32}^{(\mathrm{FN})}}{\left(Y_{33}^{(\mathrm{FN})}\right)^2} \sim V_{cb}\frac{Y_{32}^{(\mathrm{FN})}}{Y_{33}^{(\mathrm{FN})}} \sim \left(\frac{m_c}{m_t}\right)_{\text{observed}} \sim 0.007, \tag{5.27}$$

for the charm and top quarks, and

$$\frac{Y_{23}^{(\mathrm{FN})}Y_{32}^{(\mathrm{FN})}}{\left(Y_{33}^{(\mathrm{FN})}\right)^2} \sim V_{cb}\frac{Y_{32}^{(\mathrm{FN})}}{Y_{33}^{(\mathrm{FN})}} \sim \left(\frac{m_s}{m_b}\right)_{\text{observed}} \sim 0.03, \tag{5.28}$$

for the strange and bottom quarks. Thus, we eventually find $Y_{32}^{(\mathrm{FN})}/Y_{33}^{(\mathrm{FN})} \sim 0.2$ for the up sector and $Y_{32}^{(\mathrm{FN})}/Y_{33}^{(\mathrm{FN})} \sim 1$ for the down sector. These constraints on the Yukawa elements are splendidly satisfied by a well-known value, i.e., $\lambda = 0.225$. (This value can originate from the Cabbibo angle $\lambda = \sin\theta_{12}$.) Indeed, suitable parameterizations in both the up and down sectors are known as

$$Y_{\text{example}}^{(\mathrm{FN})} \sim \begin{pmatrix} \lambda^3 & \lambda^2 \\ \lambda & 1 \end{pmatrix}, \tag{5.29}$$

for the up sector and

$$Y_{\text{example}}^{(\mathrm{FN})} \sim \begin{pmatrix} \lambda^2 & \lambda^2 \\ 1 & 1 \end{pmatrix}, \tag{5.30}$$

for the down sector up to $\mathcal{O}(1)$ coefficients in front of each element. The extension to realistic 3×3 Yukawa matrices among totally six quarks is straightforward. It is known that the quark sector can be well parametrized by the Cabbibo angle through the FN mechanism, even if we add the first generation of the quarks, that is, the up and down quarks.

Next, we focus on the Gaussian FN case. It is important to note that there is a different point between the usual FN and the Gaussian FN mechanisms. In the usual FN case, a (rough) relationship

$$\frac{Y_{ii}^{(\mathrm{FN})} Y_{33}^{(\mathrm{FN})}}{Y_{i3}^{(\mathrm{FN})} Y_{3i}^{(\mathrm{FN})}} \sim 1, \tag{5.31}$$

is found for $i = 1, 2$. This relationship is easily seen in the above example (5.29) and (5.30). However, in the Gaussian FN case, such a relationship does not hold:

$$\frac{Y_{ii}^{(\mathrm{G})} Y_{33}^{(\mathrm{G})}}{Y_{i3}^{(\mathrm{G})} Y_{3i}^{(\mathrm{G})}} \ll 1, \tag{5.32}$$

for $i = 1, 2$. Except for this point, the Gaussian FN case is almost the same as the usual FN case. Before considering the concrete mass matrices via the Gaussian FN mechanism, we consider the $SU(2)_R$ gauge symmetry. As stated in the previous section, the model possesses an additional $SU(2)_R$ gauge symmetry in addition to the SM gauge symmetry. The $SU(2)_R$ gauge symmetry forces the same VEVs for the up- and down-type Higgs fields. Then, the diagonalizing matrices in the up- and down-type quark mass matrices are equivalent to each other, and the CKM mixings are vanishing. In this chapter, we assume that an existence of non-perturbative effects or higher-dimensional corrections which may be derived from the superstring theories can break the $SU(2)_R$ gauge symmetry. If the existence of such effects breaks the $SU(2)_R$ symmetry, it is naively expected that the VEVs of the five generations of the Higgs fields are differently configured. In the following part, the Higgs VEVs are denoted by $v_{ui} \equiv \langle H_{ui} \rangle$ $(i = 0, 1, ..., 4)$ and $v_{dj} \equiv \langle H_{dj} \rangle$ $(j = 0, 1, ..., 4)$. As explained in the above paragraph, the Yukawa matrices for the fourth and fifth Higgs fields are used to work the Gaussian FN mechanism. Thus, we assume that the fourth and fifth non-vanishing VEVs of the Higgs fields are dominant compared with the other ones. In addition, we need an additional non-vanishing VEV in the down Higgs sector because of a realization of the mass hierarchy for the charged leptons. Hence, we assume the following configuration of the non-vanishing Higgs VEVs in total,

$$v_{u3} \sim v_{u4}, \qquad v_{d3} \sim v_{d4}, \qquad v_{d2} \ll v_{d4}. \tag{5.33}$$

In terms of these Higgs VEVs, the mass matrices of the up and down type quarks are

written as

$$M^{(u)} \simeq \begin{pmatrix} \eta_{100}v_{u3} & -\eta_{25}v_{u4} & -\eta_{20}v_{u3} \\ \eta_{23}v_{u4} & -\eta_{32}v_{u3} & \eta_8 v_{u3} \\ \eta_{11}v_{u4} & \eta_4 v_{u3} & \eta_1 v_{u4} \end{pmatrix} \tag{5.34}$$

$$= v_{u4}\begin{pmatrix} \eta_{100}\rho_u & -\eta_{25} & -\eta_{20}\rho_u \\ \eta_{23} & -\eta_{32}\rho_u & \eta_8\rho_u \\ \eta_{11} & \eta_4\rho_u & \eta_1 \end{pmatrix}, \tag{5.35}$$

$$M^{(d)} \simeq \begin{pmatrix} \eta_{100}v_{d3} & -\eta_{25}v_{d4} & \eta_{15}v_{d2} - \eta_{20}v_{d3} \\ \eta_{23}v_{d4} & \eta_3 v_{d2} - \eta_{32}v_{d3} & \eta_8 v_{d3} \\ \eta_9 v_{d2} + \eta_{11}v_{d4} & \eta_4 v_{d3} & \eta_1 v_{d4} \end{pmatrix} \tag{5.36}$$

$$= v_{d4}\begin{pmatrix} \eta_{100}\rho_d & -\eta_{25} & \eta_{15}\rho'_d - \eta_{20}\rho_d \\ \eta_{23} & \eta_3\rho'_d - \eta_{32}\rho_d & \eta_8\rho_d \\ \eta_9\rho'_d + \eta_{11} & \eta_4\rho_d & \eta_1 \end{pmatrix}, \tag{5.37}$$

where we define three VEV ratios,

$$\rho_u \equiv \frac{v_{u3}}{v_{u4}}, \qquad \rho_d \equiv \frac{v_{d3}}{v_{d4}}, \qquad \rho'_d \equiv \frac{v_{d2}}{v_{d4}}. \tag{5.38}$$

Let us focus on the (2×2) lower right parts of the mass matrices. We will see that $\rho_u \not\simeq \rho_d$ is required. When $\rho_u \simeq \rho_d$ with a negligibly small value of ρ'_d, the mass ratios are expected to be almost similar, $m_c/m_t \simeq m_s/m_b$. Actually, in the above (2×2) example, the mass ratios and mixing angle are estimated as

$$\frac{m_c}{m_t} \sim \eta_4\eta_8(\rho_u)^2, \tag{5.39}$$

$$\frac{m_s}{m_b} \sim \eta_3\rho'_d, \tag{5.40}$$

$$V_{cb} \sim \eta_8(\rho_u - \rho_d). \tag{5.41}$$

Here we know $\eta_1 \simeq 1$. In addition to this, we numerically estimate $\eta_{32} = 1.0 \times 10^{-5}$, $\eta_3 \sim 0.9, \eta_4 \sim 0.8$ and $\eta_8 \sim 0.5$ for $\tau = 1.5i$. By plugging these numerical values, the realistic patterns of the mass ratios and mixing angle can be realized by the following VEV ratios,

$$\rho'_d = \mathcal{O}(0.01) - \mathcal{O}(0.1), \qquad \rho_u = \mathcal{O}(0.1), \qquad \rho_u - \rho_d = \mathcal{O}(0.01) - \mathcal{O}(0.1). \tag{5.42}$$

Similary, we focus on all the other matrix elements. Suppose that $\eta_{15}\rho'_d - \eta_{20}\rho_d$ is positive, then the mixing angle V_{us} including the Cabbibo angle is given by

$$V_{us} \sim \frac{\eta_{15}}{\eta_8}\frac{\rho'_d}{\rho_d}. \tag{5.43}$$

In terms of numerical values $\eta_8 \sim 0.5$ and $\eta_{15} \sim 0.08$, $V_{us} = \mathcal{O}(0.1)$ can be realized for

$$\frac{\rho'_d}{\rho_d} = \mathcal{O}(0.1) - \mathcal{O}(1). \tag{5.44}$$

Moreover, we consider the determinants of the quark mass matrices, and then obtain two mass constraints,

$$\det M^{(u)} \sim (v_{u4})^2 \eta_{23}\eta_{25} = (m_u m_c m_t)_{\text{observed}}, \tag{5.45}$$
$$\det M^{(d)} \sim (v_{d4})^2 \eta_3\eta_{11}\eta_{15}(\rho'_d) = (m_d m_s m_b)_{\text{observed}}. \tag{5.46}$$

Thus, we find

$$\frac{m_u}{m_t} \sim \frac{\eta_{23}\eta_{25}}{\eta_4\eta_8(\rho_u)^2}, \tag{5.47}$$
$$\frac{m_d}{m_b} \sim \eta_{11}\eta_{15}\rho'_d. \tag{5.48}$$

With $\eta_{25} \sim 0.0009$, $\eta_{23} \sim 0.003$, $\eta_{15} \sim 0.08$ and $\eta_{11} \sim 0.3$ for $\tau = 1.5i$, the realistic mass ratios require $(\rho_u)^2 = \mathcal{O}(0.1)$ and $\rho'_d = \mathcal{O}(0.1)$. The promising parameter ranges of ρ_u, ρ_d and ρ'_d are found.

Now, we can numerically calculate the above Yukawa matrices, depending on the values of Higgs VEVs and an imaginary part of complex structure parameter, $\mathrm{Im}\,\tau$ [2]. In particular, we calculate the mass ratios of the quarks and charged leptons and the CKM mixing matrix at the compactification scale, e.g. GUT scale. If we try to realize the tiny neutrino masses simultaneously, the Majorana mass terms are required. The Majorana mass terms are expected to be induced by the non-perturbative effects of Euclidean-branes [48, 49]. However, we do not treat the Majorana masses. The reason is that the Pontecorvo–Maki–Nakagawa–Sakata (PMNS) mixing matrix depends on the texture of the Majorana masses. Although we can take account of the renormalization group equation (RGE) flows, the effects depend on the models including the $SU(2)_R$ breaking sector and we study it here without them.[3] We show sample spectra in Table 5.4 where $\mathrm{Im}\,\tau = 1.5$ and the VEVs of five Higgs fields are chosen as

$$\rho_u = 0.29. \qquad \rho_d = 0.38, \qquad \rho'_d = 0.1. \tag{5.49}$$

In Table 5.4, the sample values of the mass ratios and mixing angles in the quarks are shown.

[2] A real part of τ gives physical phases and we do not study them in this thesis. Other parameters give $\mathcal{O}(1)$ global factors.

[3] Indeed, the RGE changes the values of mass hierarchies and the elements of CKM matrix slightly [50].

	sample values	observed
$(m_u, m_c, m_t)/m_t$	$(1.7 \times 10^{-5}, 5.7 \times 10^{-3}, 1)$	$(1.5 \times 10^{-5}, 7.5 \times 10^{-3}, 1)$
$(m_d, m_s, m_b)/m_b$	$(2.0 \times 10^{-3}, 6.8 \times 10^{-2}, 1)$	$(1.2 \times 10^{-3}, 2.3 \times 10^{-2}, 1)$
$(m_e, m_\mu, m_\tau)/m_\tau$	$(2.7 \times 10^{-4}, 5.9 \times 10^{-2}, 1)$	$(2.9 \times 10^{-4}, 6.0 \times 10^{-2}, 1)$
$\lvert V_{\rm CKM}\rvert$	$\begin{pmatrix} 0.96 & 0.29 & 0.01 \\ 0.29 & 0.96 & 0.07 \\ 0.01 & 0.07 & 1.0 \end{pmatrix}$	$\begin{pmatrix} 0.97 & 0.23 & 0.0035 \\ 0.23 & 0.97 & 0.041 \\ 0.0087 & 0.040 & 1.0 \end{pmatrix}$

Table 5.4: Mass ratios of the quarks and the charged leptons and values of the CKM matrix $V_{\rm CKM}$ elements. The experimental data are quoted from Ref. [3].

Similarly, for the lepton sector, we obtain

$$Y_{IJ0} \simeq \begin{pmatrix} \eta_0 & 0 & -\eta_{44} \\ 0 & \eta_{16} & 0 \\ -\eta_{20} & 0 & \eta_{28} \end{pmatrix}, \tag{5.50}$$

$$Y_{IJ1} \simeq \begin{pmatrix} 0 & \eta_8 & 0 \\ \eta_4 & 0 & \eta_{20} \\ 0 & 0 & 0 \end{pmatrix}, \tag{5.51}$$

$$Y_{IJ2} \simeq \begin{pmatrix} -\eta_{36} & 0 & \eta_{12} \\ 0 & \eta_0 & 0 \\ \eta_{12} & 0 & -\eta_{36} \end{pmatrix}, \tag{5.52}$$

$$Y_{IJ3} \simeq \begin{pmatrix} 0 & 0 & 0 \\ \eta_{20} & 0 & \eta_4 \\ 0 & \eta_8 & 0 \end{pmatrix}, \tag{5.53}$$

$$Y_{IJ4} \simeq \begin{pmatrix} \eta_{28} & 0 & -\eta_{20} \\ 0 & \eta_{16} & 0 \\ -\eta_{44} & 0 & \eta_4 \end{pmatrix}. \tag{5.54}$$

Then, by assuming the non-vanishing VEV ratios ρ_d and ρ'_d like in the down-type quarks, we find the charged lepton mass matrix via the Gaussian FN mechanism,

$$M^{(l)} \simeq v_{d4} \begin{pmatrix} \eta_{28} & 0 & \eta_{12}\rho'_d - \eta_{20} \\ \eta_{20}\rho_d & \rho'_d + \eta_{16} & \eta_4\rho_d \\ \eta_{12}\rho'_d - \eta_{44} & \eta_8\rho_d & \eta_4 \end{pmatrix}. \tag{5.55}$$

The numerical results in the charged leptons are shown also in Table 5.4. We can see a

similar charge relation (except for $(1,2)$ and $(3,1)$ elements) as in the quark sector.[4]

We would like to mention about the stability for the input VEV parameters. The results are shown in Figures 5.1 and 5.2. In Figure 5.1, the input VEV ratio parameters ρ_u and ρ_d are randomly chosen in the range from 0 to 0.5. In the top (middle and bottom) panel of Figure 5.1, ρ'_d is set to be 0.01 (0.05 and 0.1). Six colors among the dots distinguish the values of the complex modulus parameter τ, that is, $\mathrm{Im}\,\tau$ =1.5 (red), 1.6 (orange), 1.7 (yellow), 1.8 (green), 1.9 (blue) and 2.0 (purple), respectively. The dots in the figures represent promising ratios of our numerical samples that brings us with the experimentally observed (center) values within a range from 1/5 to 5. These figures tell that a relatively wide parameter range for ρ_d is allowed. The promising parameter sets are within $\mathcal{O}(0.1)$ ranges of widths. This implies that the corresponding VEVs for the Higgs fields are allowed over $\mathcal{O}(1)$ [GeV] or more larger for

$$\tan\beta = \frac{v_u^{\mathrm{MSSM}}}{v_d^{\mathrm{MSSM}}} \equiv \sqrt{\frac{v_{u3}^2 + v_{u4}^2}{v_{d2}^2 + v_{d3}^2 + v_{d4}^2}} = 1. \tag{5.56}$$

Even for $\tan\beta = 50$, the allowed range of the VEVs can be distributed within a range of $\mathcal{O}(0.1)$ [GeV] widths. The number of trials for each parameter set $(\rho_d, \mathrm{Im}\,\tau)$ is 10^4. For $\mathrm{Im}\,\tau = 1.4$ and 2.1, we did not find any allowed region for two VEV ratio parameters (ρ_u, ρ_d).

Next, we would like to show another plane of the allowed parameter space. In Figure 5.2, a horizontal axis corresponds to the value of ρ'_d and a vertical axis corresponds to the value of ρ_d. The values of ρ_d and ρ'_d are also randomly chosen in a range from 0 to 0.5 with 10^4 trials. We draw the dots when the parameter set can provide the promising ratios of our numerical samples with the experimentally observed values within a range from 1/5 to 5, similarly to Figure 5.1. The other parameters are chosen as $(\rho_u, \mathrm{Im}\,\tau) = (0.3, 1.45)$ in the top panel and $(\rho_u, \mathrm{Im}\,\tau) = (0.2, 1.95)$ in the bottom panel. These figures tell that the Gaussian FN mechanism with input VEV parameters can provide more realistic flavor patterns among the quarks and charged leptons without any fine tuning.

[4]The FN charges are obtained by the following expression,

$$\begin{aligned} y_{\mathrm{lepton}} &\sim e^{-\pi(\mathrm{Im}\,\tau)(c_i+d_j)^2/384}, \\ c_i &= \{20, 5, 0\}, \\ d_j &= \{15, 5, 0\}. \end{aligned}$$

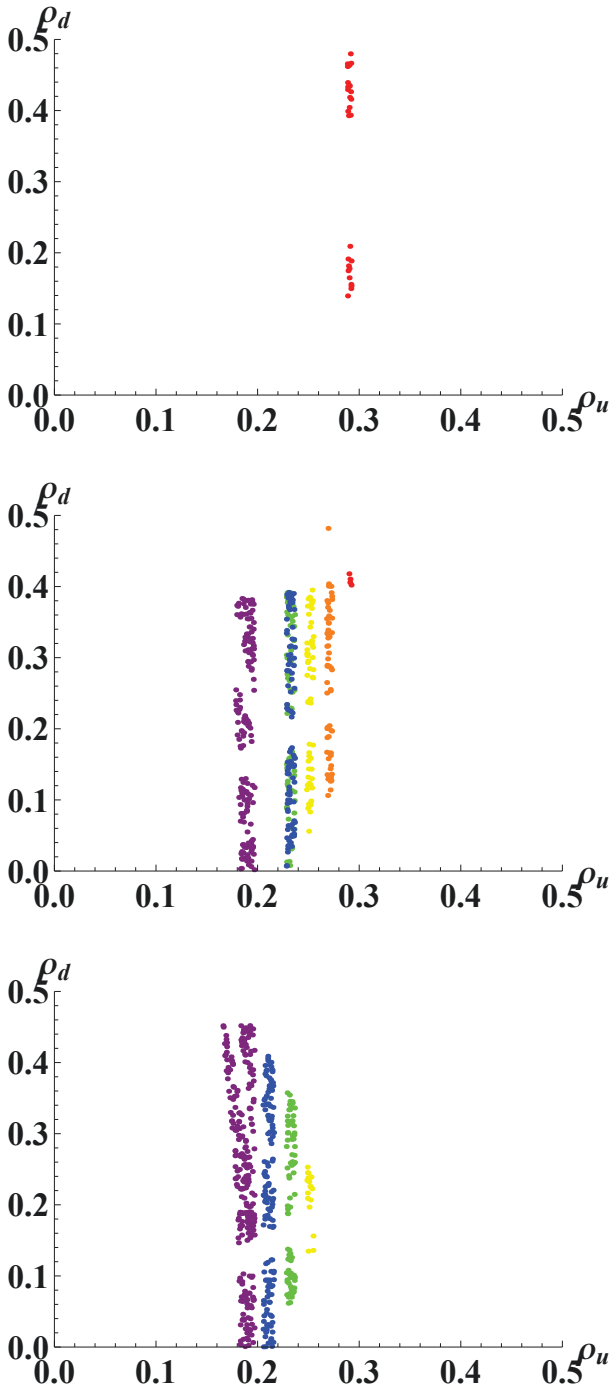

Figure 5.1: Allowed parameter regions of theoretical VEV input parameters. In the top (middle and bottom) panel ρ'_d is set to be 0.01 (0.05 and 0.1). Six colors among the dots distinguish the values of the complex modulus parameter τ, that is, $\mathrm{Im}\,\tau$ =1.5 (red), 1.6 (orange), 1.7 (yellow), 1.8 (green), 1.9 (blue) and 2.0 (purple), respectively. The dots in the figures provide the promising ratios of our numerical samples with the experimentally observed (center) values within a range from 1/5 to 5.

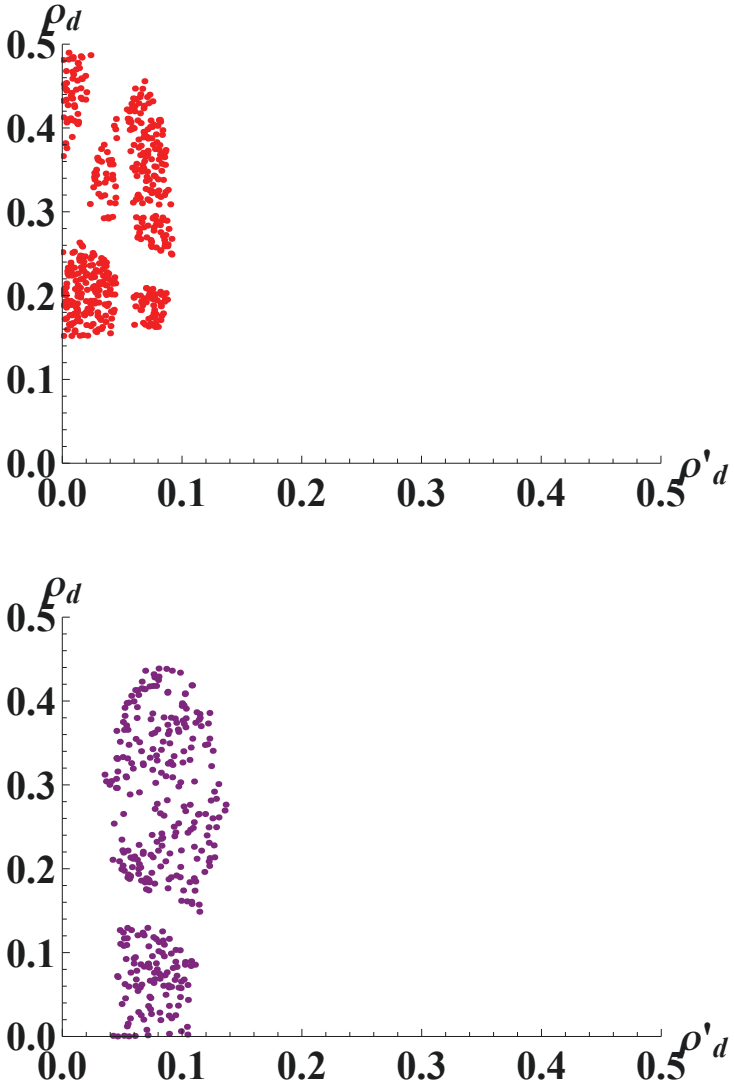

Figure 5.2: Allowed parameter regions of theoretical VEV input parameters. The other parameters are chosen as $(\rho_u, \mathrm{Im}\,\tau) = (0.3, 1.45)$ in the top panel and $(\rho_u, \mathrm{Im}\,\tau) = (0.2, 1.95)$ in the bottom panel.

5.4 10D embedding and D-term contributions

There are the 10D vector field and the 10D Majorana–Weyl spinor field in the 10D SYM theory. We can decompose the 10D vector field into the 4D vector field and three complex fields. Each of the three complex fields has a vector index on one of three tori $(T^2)^3$. Also, the 10D Majorana–Weyl spinor field is decomposed into four 4D Weyl spinor fields, i.e., $\lambda_{+++}, \lambda_{+--}, \lambda_{-+-}$ and λ_{--+}, where $\pm$ denotes the chirality on each torus. We will derive

the SM contents from them while eliminating extra massless modes, i.e., so-called exotic-modes, by the magnetic fluxes and orbifold projections.

The chirality projection caused by magnetic fluxes is as follows. On a torus, the positive chirality spinor fields and the vector fields have (normalizable) well-defined wave-functions with positive fluxes $M_{ab} > 0$. Then, the conjugate representations are vanishing. There is a constant zero-mode in the case with $M_{ab} = 0$. Then, the chirality projection does not work and the conjugate representation also remains.

On the orbifold T^2/Z_2, the fields are transformed as follows under the Z_2 orbifold twist, $z_1 \to -z_1$,

$$A_\mu(-z_1) = +PA_\mu(z_1)P^{-1}, \tag{5.57}$$
$$A_m(-z_1) = -PA_m(z_1)P^{-1}, \tag{5.58}$$
$$\psi_\pm(-z_1) = \pm P\psi_\pm(z_1)P^{-1}, \tag{5.59}$$

for $m = 4, 5$, where P is a projection operator ($P^2 = \mathbf{1}_8$). The number of degenerate zero-modes is reduced (or vanished), corresponding to the parity.

We show a sample embedding of our Yukawa coupling textures into the 10D SYM theory, taking the two types of orbifold projections into consideration. We introduce the following magnetic fluxes on the second and the third tori as

$$F_{67} = 2\pi \begin{pmatrix} 0 \times \mathbf{1}_4 & 0 & 0 \\ 0 & -1 \times \mathbf{1}_2 & 0 \\ 0 & 0 & -1 \times \mathbf{1}_2 \end{pmatrix}, \tag{5.60}$$
$$F_{89} = 2\pi \begin{pmatrix} 0 \times \mathbf{1}_4 & 0 & 0 \\ 0 & 1 \times \mathbf{1}_2 & 0 \\ 0 & 0 & 1 \times \mathbf{1}_2 \end{pmatrix}. \tag{5.61}$$

One can easily find that the SUSY condition (5.1) can not be satisfied with the fluxes Eqs. (5.3), (5.60) and (5.61). Here, we impose the two Z_2 projections. The first one is defined as,

$$(z_1, z_2, z_3) \to (-z_1, -z_2, z_3), \tag{5.62}$$

with the projection operator,

$$P = \begin{pmatrix} -1 \times \mathbf{1}_4 & 0 & 0 \\ 0 & 1 \times \mathbf{1}_2 & 0 \\ 0 & 0 & 1 \times \mathbf{1}_2 \end{pmatrix}. \tag{5.63}$$

The second one is defined as,

$$(z_1, z_2, z_3) \to (z_1, -z_2, -z_3), \tag{5.64}$$

with the same projection operator as Eq. (5.63). The magnetic background is consistent with the Table 5.1, and does not change the promising flavor structures mentioned in

the previous section. We summarize all the matter contents induced by the magnetic background in Table 5.5.

particles	SM contents	superpartners	assignment
gluons, W/B bosons	one generation	massless	A_μ, λ_{+++}
Q	three generations	massive (heavy)	A_6, A_7, λ_{-+-}
u, d	three generations	massive (heavy)	A_8, A_9, λ_{--+}
L	three generations	massive (heavy)	A_6, A_7, λ_{-+-}
ν, e	three generations	massive (heavy)	A_8, A_9, λ_{--+}
H_u, H_d	five generations	massive	A_4, A_5, λ_{+--}
exotics	none	none	—

Table 5.5: All the contents included in the model.

We obtain all the SM contents. Amazingly, we can eliminate all the extra fields, e.g., exotic modes, vector-like matters and diagonal adjoint fields, so-called open string moduli. The existence of such extra massless fields is known as a notorious open problem in the string phenomenology. Indeed, there necessarily remain some extra massless fields in the previous works [38, 40]. Since the magnetic background as we mentioned corresponds to the D-term SUSY breaking, the soft scalar mass terms arise while fermionic superpartners remain massless. These shift the spectra of scalars and zero-modes become massive or even tachyonic. Here, we give a short review of spectra of scalars and vectors on a magnetized torus [51]. Note that, if we consider on the first T^2/Z_2 orbifold, the coordinates of which are (y_4, y_5), parts of the 10D vector A_M $M = 6, 7, 8, 9$ are scalar fields and A_M $M = 4, 5$ are vector fields on the orbifold. In Ref. [51], the squared mass of a scalar field on the orbifold is given by

$$M^2_{\text{scalar}} = 2\pi \frac{|M_{ab}|}{\mathcal{A}^{(1)}}. \tag{5.65}$$

As for the vector fields, there are additional mass terms between A_4 and A_5. Their masses are given by

$$M^2_{\pm} = 2\pi \frac{|M_{ab}|}{\mathcal{A}^{(1)}} \pm 4\pi \frac{M_{ab}}{\mathcal{A}^{(1)}}. \tag{5.66}$$

We can easily find that one becomes massive with the compactification scale and the other

is tachyonic with the same scale. Accordingly, we can calculate the scalar masses,

$$m^2_{\tilde{Q}} = 2\pi\left(\frac{5}{\mathcal{A}^{(1)}} + \frac{1}{\mathcal{A}^{(2)}} \pm 2\frac{1}{\mathcal{A}^{(2)}} + \frac{1}{\mathcal{A}^{(3)}}\right), \tag{5.67}$$

$$m^2_{\tilde{L}} = 2\pi\left(\frac{4}{\mathcal{A}^{(1)}} + \frac{1}{\mathcal{A}^{(2)}} \pm 2\frac{1}{\mathcal{A}^{(2)}} + \frac{1}{\mathcal{A}^{(3)}}\right), \tag{5.68}$$

$$m^2_{\tilde{u},\,\tilde{d}} = 2\pi\left(\frac{7}{\mathcal{A}^{(1)}} + \frac{1}{\mathcal{A}^{(2)}} + \frac{1}{\mathcal{A}^{(3)}} \pm 2\frac{1}{\mathcal{A}^{(3)}}\right), \tag{5.69}$$

$$m^2_{\tilde{e},\,\tilde{\nu}} = 2\pi\left(\frac{7}{\mathcal{A}^{(1)}} + \frac{1}{\mathcal{A}^{(2)}} + \frac{1}{\mathcal{A}^{(3)}} \pm 2\frac{1}{\mathcal{A}^{(3)}}\right). \tag{5.70}$$

We find that they can become massive with proper ratios of the volumes of three tori. Finally, we calculate the Higgs masses at the compactification scale,

$$m^2_H = 2\pi\left(\frac{12}{\mathcal{A}^{(1)}} \pm 2\frac{12}{\mathcal{A}^{(1)}}\right). \tag{5.71}$$

The lightest scalar mode of the Higgs sector becomes tachyonic at the compactification scale. In any models with various 10D embeddings which do not induce the extra massless fields, at least one tachyonic mode inevitably remains. Then, we have to assume non-perturbative effects or higher-dimensional operators to make them massive. As another possibility, it is known that Wilson lines without magnetic fluxes also induce the massive modes. We can introduce the Wilson lines on the third torus if we undo the second Z_2 projection (5.64) in the above 10D embedding. The Higgs sector has non-vanishing Wilson lines without magnetic fluxes and obtains a certain mass on the third torus. They make the Higgs fields heavy or probably massless. Although the (MS)SM contents shown in Table 5.5 are unchanged, there also remains the massless Wilson line moduli. Furthermore, we have to make them massive somehow.

5.5 The other configurations for the Gaussian FN mechanism

In this model, we use the four-block flux given as

$$F_{45} \propto \begin{pmatrix} M_C\mathbf{1}_3 & 0 & 0 & 0 \\ 0 & M_{C'}\mathbf{1}_1 & 0 & 0 \\ 0 & 0 & M_L\mathbf{1}_2 & 0 \\ 0 & 0 & 0 & M_R\mathbf{1}_2 \end{pmatrix}. \tag{5.72}$$

Indeed, we can extend this block structure into more segmentalized one, i.e., a five-block flux,

$$F_{45} \propto \begin{pmatrix} M_C\mathbf{1}_4 & 0 & 0 & 0 & 0 \\ 0 & M_{C'}\mathbf{1}_1 & 0 & 0 & 0 \\ 0 & 0 & M_L\mathbf{1}_2 & 0 & 0 \\ 0 & 0 & 0 & M_R\mathbf{1}_1 & 0 \\ 0 & 0 & 0 & 0 & M_{R'}\mathbf{1}_1 \end{pmatrix}, \tag{5.73}$$

where $M_C, M_{C'}, M_L, M_R, M_{R'}$ take different values from each other. If we consider the case with $M_R^{(i)} = M_{R'}^{(i)}$, the five-block flux reduces to the four-block flux. It is easily seen that the five-block flux breaks the gauge symmetry as $U(8) \to U(3) \times U(2) \times U(1)^3$. As mentioned in the beginning of this chapter, there are two equations for magnetic fluxes, and two free parameters, i.e., the ratios of the volumes of tori. Hence, in general the SUSY preserving condition can be satisfied, if we choose the rations of the volumes. However, for segmentalized fluxes, i.e., four-block and five-block fluxes, in general the supersymmetry preserving condition can not be satisfied without an accidental compatibility of the magnetic fluxes.

In the five-block fluxes, the quantized fluxes $M_C, M_{C'}, M_L, M_R$ and $M_{R'}$ are different from each other. This is apparently difficult, however, in practice this is possible. We find four patterns in the five-block fluxes without the SS twist phases,

$$\begin{pmatrix} 0\times\mathbf{1}_4 & 0 & 0 & 0 & 0 \\ 0 & -1\times\mathbf{1}_1 & 0 & 0 & 0 \\ 0 & 0 & 4\times\mathbf{1}_2 & 0 & 0 \\ 0 & 0 & 0 & -5\times\mathbf{1}_1 & 0 \\ 0 & 0 & 0 & 0 & -8\times\mathbf{1}_1 \end{pmatrix},$$

$$\begin{pmatrix} 0\times\mathbf{1}_4 & 0 & 0 & 0 & 0 \\ 0 & 1\times\mathbf{1}_1 & 0 & 0 & 0 \\ 0 & 0 & 5\times\mathbf{1}_2 & 0 & 0 \\ 0 & 0 & 0 & -4\times\mathbf{1}_1 & 0 \\ 0 & 0 & 0 & 0 & -7\times\mathbf{1}_1 \end{pmatrix},$$

$$\begin{pmatrix} 0\times\mathbf{1}_4 & 0 & 0 & 0 & 0 \\ 0 & -1\times\mathbf{1}_1 & 0 & 0 & 0 \\ 0 & 0 & 4\times\mathbf{1}_2 & 0 & 0 \\ 0 & 0 & 0 & -8\times\mathbf{1}_1 & 0 \\ 0 & 0 & 0 & 0 & -5\times\mathbf{1}_1 \end{pmatrix},$$

$$\begin{pmatrix} 0\times\mathbf{1}_4 & 0 & 0 & 0 & 0 \\ 0 & 1\times\mathbf{1}_1 & 0 & 0 & 0 \\ 0 & 0 & 5\times\mathbf{1}_2 & 0 & 0 \\ 0 & 0 & 0 & -7\times\mathbf{1}_1 & 0 \\ 0 & 0 & 0 & 0 & -4\times\mathbf{1}_1 \end{pmatrix}.$$

When we use these five-block fluxes for the model construction, there appear three-generation structures of the quarks and leptons and their superpartners in addition to five generations of the MSSM-like Higgs pair. The concrete model construction in terms of the five-block flux is left for the future work.

Chapter 6

Coda

In this thesis, we have arranged an infrastructure for phenomenological model buildings. First, we have considered the higher-dimensional SYM theory compactified on a two-dimensional torus where a non-trivial magnetic background is assumed. Then, there appear several phenomenologically important ingredients for realistic model constructions. For example, the chiral matter spectra, the family replications of bi-fundamental matters and the interaction constants among the quarks or leptons to the Higgs boson (called Yukawa interactions) were actually realized in the framework of SYM on magnetized two-dimensional torus.

The varieties of such phenomenological properties have been confirmed on the toroidal orbifolds T^2/Z_N $(N = 2, 3, 4, 6)$ involving the Abelian magnetic fluxes. We have explored the phenomenological aspects of the magnetized toroidal orbifolds by comprehensively investigating the flavor structures of quarks and charged leptons. Indeed, the magnetic fluxes quantized by the Dirac quantization condition, the Scherk–Schwartz twist phases and the Z_N parities under the Z_N orbifold identifications explicitly characterize the detailed proprieties of the Yukawa coupling constants after naive dimensional reduction. By focusing on this, we developed systematic classifications for the possible configurations where the three generations of (general) left-handed and right-handed bi-fundamental matter fields can survive in the low energy effective theory. Then, it turned out that there are approximately 2600 possibilities of realizing the three-generation quarks and leptons, and also that there can exist multiply degenerate Higgs doublet models as well as single Higgs doublet models like in the SM of particle physics.

Among such enormous possibilities, we have tried to pick up promising candidates which we can use to construct the flavor models that allow to derive the experimental quark and lepton observables. We gave a theoretical proof that single Higgs doublet models, i.e., models with one generation of the Higgs doublet and two Higgs doublet models can not be suitable for the flavor model constructions. The reason is that slightly overlapped zero-mode wavefunctions localized on the toroidal orbifolds lead to degenerate values in the Yukawa coupling elements, and then mass eigenvalues are also degenerate, leading to unhierarchical to each other. We have found that the multiple-generations of the Higgs fields more than two are required to describe the quark mass hierarchies in the

framework of the magnetized toroidal orbifolds.

In addition, we have concretely constructed the model which is similar to the standard model (where almost all of the superpartner fields of the standard model particles become much heavier than the standard model particles with the Kaluza–Klein compactification momentum). In the model, we have discovered a certain mechanism which can generate large mass hierarchies and small mixing angles simultaneously. The mechanism is that the effective mass matrices after the Higgs doublets acquiring their non-zero vacuum expectation values are explicitly written by Gaussian functions of the sum of "effective flavor charges" assigned to three generations of quarks and leptons. It is found that the Gaussian structures are suitable for describing the flavor properties of the quarks and the charged leptons, and are considerably stable under the variation of input vacuum expectation values of the Higgs fields. In order to derive realistic Gaussian mass textures, we assumed the favorable Higgs potentials by hand. I hope to revisit such an assumption in the near future.

Appendix A

Explicit expressions of the expansion coefficients

In this chapter, we show the analytic forms of the expansion coefficients in Eq. (2.69), based on Ref. [32]. The expansion coefficients are obtained by so-called *"operator formalism"* where the relationship between quantized (KK) momenta and wavefunction localization points in the extra directions by means of the 2D quantum mechanics.

A T^2/Z_2

First of all, we show the T^2/Z_2 case and define $\eta \equiv \pm 1$ for later convenience. On the magnetized T^2/Z_2, the SS phases are restricted and their allowed values are only four combinations,

$$(\alpha, \beta) = (0,0), (\tfrac{1}{2}, 0), (0, \tfrac{1}{2}), (\tfrac{1}{2}, \tfrac{1}{2}). \tag{A.1}$$

The elements of expanson coefficients are analytically written as

$$C^{(\omega)}_{jk} = e^{2\pi i \cdot \frac{2\beta}{M}(j+\alpha)} \delta_{-2\alpha-j,k}. \tag{A.2}$$

The expansion matrix which rotates the torus zero-mode basis into the orbifold physical zero-mode basis is also given as

$$M^{(Z_2;\eta)}_{jk} = \frac{1}{2}\left(\delta_{j,k} + \eta C^{(\omega)}_{jk}\right). \tag{A.3}$$

On T^2/Z_2 orbifold with or without the SS twist phases, the independent zero-mode physical states on the orbifold can be easily counted by means of the floor function $[x]$ [32]. Here, the floor function is defined as

$$[x] \equiv \max\{n \in \mathbb{Z} \mid n \leq x\}. \tag{A.4}$$

A.1 $(\alpha, \beta) = (0, 0)$ case

In this case, the number of the independent zero-mode physical states on the orbifold is expressed as

$$(\#\text{ of the independent zero-mode physical states for } \eta = +1) = \left[\frac{M}{2}\right] + 1, \tag{A.5}$$

$$(\#\text{ of the independent zero-mode physical states for } \eta = +1) = \left[\frac{M-1}{2}\right], \tag{A.6}$$

A.2 $(\alpha, \beta) = (\frac{1}{2}, 0)$ case

In this case, the number of the independent zero-mode physical states on the orbifold is expressed as

$$(\#\text{ of the independent zero-mode physical states for } \eta = +1) = \left[\frac{M+1}{2}\right], \tag{A.7}$$

$$(\#\text{ of the independent zero-mode physical states for } \eta = +1) = \left[\frac{M}{2}\right], \tag{A.8}$$

A.3 $(\alpha, \beta) = (0, \frac{1}{2})$ case

In this case, the number of the independent zero-mode physical states on the orbifold is expressed as

$$(\#\text{ of the independent zero-mode physical states for } \eta = +1) = \left[\frac{M+1}{2}\right], \tag{A.9}$$

$$(\#\text{ of the independent zero-mode physical states for } \eta = +1) = \left[\frac{M}{2}\right], \tag{A.10}$$

A.4 $(\alpha, \beta) = (\frac{1}{2}, \frac{1}{2})$ case

In this case, the number of the independent zero-mode physical states on the orbifold is expressed as

$$(\#\text{ of the independent zero-mode physical states for } \eta = +1) = \left[\frac{M}{2}\right], \tag{A.11}$$

$$(\#\text{ of the independent zero-mode physical states for } \eta = +1) = \left[\frac{M+1}{2}\right], \tag{A.12}$$

B T^2/Z_3

On T^2/Z_3, the allowed discrete values of the SS twist phases are known as

$$\alpha = \beta = \begin{cases} 0, \frac{1}{3}, \frac{2}{3} & (M = \text{even}), \\ \frac{1}{6}, \frac{1}{2}, \frac{5}{6} & (M = \text{odd}). \end{cases} \tag{A.13}$$

The expansion matrix is given as

$$M_{jk}^{(Z_3;\eta)} = \frac{1}{3}\sum_{x=0}^{2} \bar{\eta}^2 C_{jk}^{(\omega^x)}, \tag{A.14}$$

by means of

$$C_{jk}^{(\omega)} = \frac{1}{\sqrt{M}} e^{-i\frac{\pi}{12}+i\frac{3\pi\alpha^2}{M}} e^{i\frac{\pi}{M}k(k+6)+2\pi i\frac{j\cdot k}{M}}, \tag{A.15}$$

$$C_{jk}^{(\omega^2)} = \frac{1}{\sqrt{M}} e^{i\frac{\pi}{12}-i\frac{3\pi\alpha^2}{M}} e^{-i\frac{\pi}{M}j(j+6)-2\pi i\frac{j\cdot k}{M}}. \tag{A.16}$$

The complex modulus parameter is fixed as $\omega = e^{2\pi i/3}$.

The number of the independent zero-mode physical states on the orbifold is shown in Tables A.1, A.2, A.3 and A.4. Hereafter, we assume $M > 0$.

M		2	4	6	8	10	12	14
η	1	1	1	3	3	3	5	5
	ω	0	2	2	2	4	4	4
	$\bar{\omega}$	1	1	1	3	3	3	5

Table A.1: The relation between the number of the independent zero-modes on T^2/Z_3 and the magnetic flux M = even, the SS phases $(\alpha, \beta) = (0, 0)$ and the Z_3 parity η.

M		2	4	6	8	10	12	14
η	1	1	2	2	3	4	4	5
	ω	1	1	2	3	3	4	5
	$\bar{\omega}$	0	1	2	2	3	4	4

Table A.2: The relation between the number of the independent zero-modes on T^2/Z_3 and the magnetic flux M = even, the SS phases $(\alpha, \beta) = (\frac{1}{3}, \frac{1}{3}), (\frac{2}{3}, \frac{2}{3})$ and the Z_3 parity η.

M		1	3	5	7	9	11	13
η	1	1	1	2	3	3	4	5
	ω	0	1	2	2	3	4	4
	$\bar{\omega}$	0	1	1	2	3	3	4

Table A.3: The relation between the number of the independent zero-modes on T^2/Z_3 and the magnetic flux $M =$ odd, the SS phases $(\alpha, \beta) = (\frac{1}{6}, \frac{1}{6}), (\frac{5}{6}, \frac{5}{6})$ and the Z_3 parity η.

M		1	3	5	7	9	11	13
η	1	0	2	2	2	4	4	4
	ω	1	1	1	3	3	3	5
	$\bar{\omega}$	0	0	2	2	2	4	4

Table A.4: The relation between the number of the independent zero-modes on T^2/Z_3 and the magnetic flux $M =$ odd, the SS phases $(\alpha, \beta) = (\frac{1}{2}, \frac{1}{2})$ and the Z_3 parity η.

C T^2/Z_4

On T^2/Z_4, the allowed discrete values of the SS twist phases are kwown as

$$\alpha = \beta = 0, \tfrac{1}{2}. \tag{A.17}$$

The expansion matrix is given as

$$M_{jk}^{(Z_4;\eta)} = \frac{1}{4}\sum_{x=0}^{3} \bar{\eta}^x C_{jk}^{(\omega^x)}, \tag{A.18}$$

by means of

$$C_{jk}^{(\omega)} = \frac{1}{\sqrt{M}} e^{2\pi i \frac{\alpha^2}{M}} e^{2\pi i \frac{j\cdot k}{M} + 2\pi i \frac{2\alpha}{M} k}, \tag{A.19}$$

$$C_{jk}^{(\omega^2)} = e^{-2\pi i \frac{2\alpha}{M}(\alpha+j)} \delta_{-2\alpha-j,k}, \tag{A.20}$$

$$C_{jk}^{(\omega^3)} = \frac{1}{\sqrt{M}} e^{-2\pi i \frac{\alpha^2}{M}} e^{-2\pi i \frac{j\cdot k}{M} - 2\pi i \frac{2\alpha}{M} k}. \tag{A.21}$$

The complex modulus parameter is fixed as $\omega = e^{2\pi i/4}$.

The number of the independent zero-mode physical states on the orbifold is shown in Tables A.5 and A.6. Hereafter, we assume $M > 0$.

M		1	2	3	4	5	6	7	8	9	10	11	12	13	14	15	16	17
η	$+1$	1	1	1	2	2	2	2	3	3	3	3	4	4	4	4	5	5
	$+i$	0	0	1	1	1	1	2	2	2	2	3	3	3	3	4	4	4
	-1	0	1	1	1	1	2	2	2	2	3	3	3	3	4	4	4	4
	$-i$	0	0	0	0	1	1	1	1	2	2	2	2	3	3	3	3	4

Table A.5: The relation between the number of the independent zero-modes on T^2/Z_4 and the magnetic flux M, the SS phases $(\alpha, \beta) = (\frac{1}{2}, \frac{1}{2})$ and the Z_4 parity η.

M		1	2	3	4	5	6	7	8	9	10	11	12	13	14	15	16
η	$+1$	0	1	1	1	1	2	2	2	2	3	3	3	3	4	4	4
	$+i$	1	1	1	1	2	2	2	2	3	3	3	3	4	4	4	4
	-1	0	0	0	1	1	1	1	2	2	2	2	3	3	3	3	4
	$-i$	0	0	1	1	1	1	2	2	2	2	3	3	3	3	4	4

Table A.6: The relation between the number of the independent zero-modes on T^2/Z_4 and the magnetic flux M, the SS phases $(\alpha, \beta) = (\frac{1}{2}, \frac{1}{2})$ and the Z_4 parity η.

D T^2/Z_6

On T^2/Z_6, the allowed discrete values of the SS twist phases are kwown as

$$\alpha = \beta = \begin{cases} 0 & (M = \text{even}) \\ \frac{1}{2} & (M = \text{odd}). \end{cases} \tag{A.22}$$

The expansion matrix is given as

$$M_{jk}^{(Z_6;\eta)} = \frac{1}{6} \sum_{x=0}^{5} \bar{\eta}^x C_{jk}^{(\omega^x)}, \tag{A.23}$$

by means of

$$C_{jk}^{(\omega)} = \frac{1}{\sqrt{M}} e^{i\frac{\pi}{12} + i\frac{\pi}{M}\alpha^2} e^{-i\frac{\pi}{M}k^2 + 2\pi i\frac{\alpha}{M}k + 2\pi i\frac{j\cdot k}{M}}, \tag{A.24}$$

$$C_{jk}^{(\omega^2)} = \frac{1}{\sqrt{M}} e^{-\frac{\pi}{12} + i\frac{3\pi\alpha^2}{M} + i\frac{\pi}{M}j^2 + 2\pi i\frac{\alpha}{M}} e^{i\frac{4\pi\alpha}{M}k + 2\pi i\frac{j\cdot k}{M}}, \tag{A.25}$$

$$C_{jk}^{(\omega^3)} = e^{-i\frac{4\pi\alpha^2}{M} - i\frac{4\pi\alpha}{M}} \delta_{-2\alpha-j,k}, \tag{A.26}$$

$$C_{jk}^{(\omega^4)} = \frac{1}{\sqrt{M}} e^{\frac{\pi}{12} - i\frac{3\pi\alpha^2}{M} - i\frac{\pi}{M}k^2 - 2\pi i\frac{\alpha}{M}} e^{-i\frac{4\pi\alpha}{M}k - 2\pi i\frac{j\cdot k}{M}}, \tag{A.27}$$

$$C_{jk}^{(\omega^5)} = \frac{1}{\sqrt{M}} e^{-i\frac{\pi}{12} - i\frac{\pi}{M}\alpha^2} e^{i\frac{\pi}{M}j^2 - 2\pi i\frac{\alpha}{M}j - 2\pi i\frac{j\cdot k}{M}}. \tag{A.28}$$

The complex modulus parameter is fixed as $\omega = e^{2\pi i/6}$.

The number of the independent zero-mode physical states on the orbifold is shown in Tables A.7 and A.8. Hereafter, we assume $M > 0$.

M		2	4	6	8	10	12	14	16	18	20	22	24	26
η	1	1	1	2	2	2	3	3	3	4	4	4	5	5
	ω	0	1	1	1	2	2	2	3	3	3	4	4	4
	ω^2	1	1	1	2	2	2	3	3	3	4	4	4	5
	ω^3	0	0	1	1	1	2	2	2	3	3	3	4	4
	ω^4	0	1	1	1	2	2	2	3	3	3	4	4	4
	ω^5	0	0	0	1	1	1	2	2	2	3	3	3	4

Table A.7: The relation between the number of the independent zero-modes on T^2/Z_6 and the magnetic flux M = even, the SS phases $(\alpha, \beta) = (0, 0)$ and the Z_6 parity η.

M		1	3	5	7	9	11	13	15	17	19	21	23	25
η	1	0	1	1	1	2	2	2	3	3	3	4	4	4
	ω	1	1	1	2	2	2	3	3	3	4	4	4	5
	ω^2	0	0	1	1	1	2	2	2	3	3	3	4	4
	ω^3	0	1	1	1	2	2	2	3	3	3	4	4	4
	ω^4	0	0	0	1	1	1	2	2	2	3	3	3	4
	ω^5	0	0	1	1	1	2	2	2	3	3	3	4	4

Table A.8: The relation between the number of the independent zero-modes on T^2/Z_6 and the magnetic flux M = odd, the SS phases $(\alpha, \beta) = (\frac{1}{2}, \frac{1}{2})$ and the Z_6 parity η.

Appendix B

The full results of systematic search on the T^2/Z_2 orbifold

In this Appendix, we show the full results of the systematic search on T^2/Z_2. The following table tells all the information of allowed configurations of the magnetic fluxes, SS twist phases and Z_2 parities. As mentioned in the main chapters, we use the "SS basis" where the Scherk–Schwartz twist phases are non-trivial, while all the Wilson lines are vanishing. The basis where all the Scherk–Schwartz twist phases are vanishing, while all the Wilson line phases are non-trivial can be straightforwardly obtained by the field definitions [43].

In the following results, we abbreviate the information of the bc-sector (the Higgs sector), since they can be straightforwardly extracted by the other sectors and the gauge invariance conditions,

$$\begin{aligned} M_{ab} + M_{ca} &= M_{bc}, \\ \alpha_{ab} + \alpha_{ca} &= \alpha_{bc}, \\ \beta_{ab} + \beta_{ca} &= \beta_{bc}, \\ \eta_{ab} + \eta_{ca} &= \eta_{bc}. \end{aligned}$$

as used in the systematic analyses. We separately show the two kinds of the full results,

$$M_{ab} < 0, \qquad M_{ca} < 0, \tag{B.1}$$

or

$$M_{ac} < 0, \qquad M_{ca} > 0, \tag{B.2}$$

Note that the symbol "$\boxed{1}$" denotes the one-generation of the Higgs doublet field (in the bc-sector) generated by a vanishing magnetic flux $M_{bc} = 0$. On the other hand, the plain number "1" denotes the one-generation of the Higgs double field generated by $M_{bc} \neq 0$.

Table B.1: The results of parameter configurations on T^2/Z_2 with $M_{ab} < 0$, $M_{ca} < 0$.

T^2/Z_2 with $M_{ab} < 0$, $M_{ca} < 0$								
ab-sector				ca-sector				bc-sector
M_{ab}	ω^i_{ab}	α_{ab}	β_{ab}	M_{ca}	ω^i_{ca}	α_{ca}	β_{ca}	# of Higgs
-4	0	0	0	-4	0	0	0	5
-4	0	0	0	-5	0	0	0	5
-4	0	0	0	-5	0	0	1/2	5
-4	0	0	0	-5	0	1/2	0	5
-4	0	0	0	-5	1	1/2	1/2	5
-5	0	0	0	-5	0	0	0	6
-5	0	0	0	-5	0	0	1/2	5
-5	0	0	0	-5	0	1/2	0	5
-5	0	0	1/2	-5	0	0	1/2	6
-5	0	0	1/2	-5	0	1/2	0	5
-5	0	1/2	0	-5	0	1/2	0	6
-5	0	0	0	-5	1	1/2	1/2	5
-5	0	0	1/2	-5	1	1/2	1/2	5
-5	0	1/2	0	-5	1	1/2	1/2	5
-5	1	1/2	1/2	-5	1	1/2	1/2	6
-4	0	0	0	-6	0	0	1/2	5
-4	0	0	0	-6	0	1/2	0	5
-4	0	0	0	-6	0	1/2	1/2	5
-4	0	0	0	-6	1	0	1/2	5
-4	0	0	0	-6	1	1/2	0	5
-4	0	0	0	-6	1	1/2	1/2	5
-5	0	0	0	-6	0	0	1/2	6
-5	0	0	0	-6	0	1/2	0	6
-5	0	0	0	-6	0	1/2	1/2	5
-5	0	0	1/2	-6	0	0	1/2	6
-5	0	0	1/2	-6	0	1/2	0	5
-5	0	0	1/2	-6	0	1/2	1/2	6
-5	0	1/2	0	-6	0	0	1/2	5
-5	0	1/2	0	-6	0	1/2	0	6
-5	0	1/2	0	-6	0	1/2	1/2	6
-5	0	0	0	-6	1	0	1/2	5
-5	0	0	0	-6	1	1/2	0	5
-5	0	0	0	-6	1	1/2	1/2	6
-5	0	0	1/2	-6	1	0	1/2	5
-5	0	0	1/2	-6	1	1/2	0	6
-5	0	0	1/2	-6	1	1/2	1/2	5
-5	0	1/2	0	-6	1	0	1/2	6

T^2/Z_2 with $M_{ab} < 0$, $M_{ca} < 0$								
ab-sector				ca-sector				bc-sector
M_{ab}	ω^i_{ab}	α_{ab}	β_{ab}	M_{ca}	ω^i_{ca}	α_{ca}	β_{ca}	# of Higgs
-5	0	1/2	0	-6	1	1/2	0	5
-5	0	1/2	0	-6	1	1/2	1/2	5
-5	1	1/2	1/2	-6	0	0	1/2	5
-5	1	1/2	1/2	-6	0	1/2	0	5
-5	1	1/2	1/2	-6	0	1/2	1/2	5
-5	1	1/2	1/2	-6	1	0	1/2	6
-5	1	1/2	1/2	-6	1	1/2	0	6
-5	1	1/2	1/2	-6	1	1/2	1/2	6
-6	0	0	1/2	-6	0	0	1/2	7
-6	0	0	1/2	-6	0	1/2	0	6
-6	0	0	1/2	-6	0	1/2	1/2	6
-6	0	1/2	0	-6	0	1/2	0	7
-6	0	1/2	0	-6	0	1/2	1/2	6
-6	0	1/2	1/2	-6	0	1/2	1/2	7
-6	0	0	1/2	-6	1	0	1/2	5
-6	0	0	1/2	-6	1	1/2	0	6
-6	0	0	1/2	-6	1	1/2	1/2	6
-6	0	1/2	0	-6	1	0	1/2	6
-6	0	1/2	0	-6	1	1/2	0	5
-6	0	1/2	0	-6	1	1/2	1/2	6
-6	0	1/2	1/2	-6	1	0	1/2	6
-6	0	1/2	1/2	-6	1	1/2	0	6
-6	0	1/2	1/2	-6	1	1/2	1/2	5
-6	1	0	1/2	-6	1	0	1/2	7
-6	1	0	1/2	-6	1	1/2	0	6
-6	1	0	1/2	-6	1	1/2	1/2	6
-6	1	1/2	0	-6	1	1/2	0	7
-6	1	1/2	0	-6	1	1/2	1/2	6
-6	1	1/2	1/2	-6	1	1/2	1/2	7
-4	0	0	0	-7	0	1/2	1/2	5
-4	0	0	0	-7	1	0	0	5
-4	0	0	0	-7	1	0	1/2	5
-4	0	0	0	-7	1	1/2	0	5
-5	0	0	0	-7	0	1/2	1/2	6
-5	0	0	1/2	-7	0	1/2	1/2	6
-5	0	1/2	0	-7	0	1/2	1/2	6
-5	0	0	0	-7	1	0	0	5
-5	0	0	0	-7	1	0	1/2	6

T^2/Z_2 with $M_{ab} < 0$, $M_{ca} < 0$								
ab-sector				ca-sector				bc-sector
M_{ab}	ω^i_{ab}	α_{ab}	β_{ab}	M_{ca}	ω^i_{ca}	α_{ca}	β_{ca}	# of Higgs
-5	0	0	0	-7	1	1/2	0	6
-5	0	0	1/2	-7	1	0	0	6
-5	0	0	1/2	-7	1	0	1/2	5
-5	0	0	1/2	-7	1	1/2	0	6
-5	0	1/2	0	-7	1	0	0	6
-5	0	1/2	0	-7	1	0	1/2	6
-5	0	1/2	0	-7	1	1/2	0	5
-5	1	1/2	1/2	-7	0	1/2	1/2	5
-5	1	1/2	1/2	-7	1	0	0	6
-5	1	1/2	1/2	-7	1	0	1/2	6
-5	1	1/2	1/2	-7	1	1/2	0	6
-6	0	0	1/2	-7	0	1/2	1/2	7
-6	0	1/2	0	-7	0	1/2	1/2	7
-6	0	1/2	1/2	-7	0	1/2	1/2	7
-6	0	0	1/2	-7	1	0	0	6
-6	0	0	1/2	-7	1	0	1/2	6
-6	0	0	1/2	-7	1	1/2	0	7
-6	0	1/2	0	-7	1	0	0	6
-6	0	1/2	0	-7	1	0	1/2	7
-6	0	1/2	0	-7	1	1/2	0	6
-6	0	1/2	1/2	-7	1	0	0	7
-6	0	1/2	1/2	-7	1	0	1/2	6
-6	0	1/2	1/2	-7	1	1/2	0	6
-6	1	0	1/2	-7	0	1/2	1/2	6
-6	1	1/2	0	-7	0	1/2	1/2	6
-6	1	1/2	1/2	-7	0	1/2	1/2	6
-6	1	0	1/2	-7	1	0	0	7
-6	1	0	1/2	-7	1	0	1/2	7
-6	1	0	1/2	-7	1	1/2	0	6
-6	1	1/2	0	-7	1	0	0	7
-6	1	1/2	0	-7	1	0	1/2	6
-6	1	1/2	0	-7	1	1/2	0	7
-6	1	1/2	1/2	-7	1	0	0	6
-6	1	1/2	1/2	-7	1	0	1/2	7
-6	1	1/2	1/2	-7	1	1/2	0	7
-7	0	1/2	1/2	-7	0	1/2	1/2	8
-7	0	1/2	1/2	-7	1	0	0	7
-7	0	1/2	1/2	-7	1	0	1/2	7

T^2/Z_2 with $M_{ab} < 0$, $M_{ca} < 0$								
ab-sector				ca-sector				bc-sector
M_{ab}	ω^i_{ab}	α_{ab}	β_{ab}	M_{ca}	ω^i_{ca}	α_{ca}	β_{ca}	# of Higgs
-7	0	$1/2$	$1/2$	-7	1	$1/2$	0	7
-7	1	0	0	-7	1	0	0	8
-7	1	0	0	-7	1	0	$1/2$	7
-7	1	0	0	-7	1	$1/2$	0	7
-7	1	0	$1/2$	-7	1	0	$1/2$	8
-7	1	0	$1/2$	-7	1	$1/2$	0	7
-7	1	$1/2$	0	-7	1	$1/2$	0	8
-4	0	0	0	-8	1	0	0	5
-5	0	0	0	-8	1	0	0	6
-5	0	0	$1/2$	-8	1	0	0	6
-5	0	$1/2$	0	-8	1	0	0	6
-5	1	$1/2$	$1/2$	-8	1	0	0	6
-6	0	0	$1/2$	-8	1	0	0	7
-6	0	$1/2$	0	-8	1	0	0	7
-6	0	$1/2$	$1/2$	-8	1	0	0	7
-6	1	0	$1/2$	-8	1	0	0	7
-6	1	$1/2$	0	-8	1	0	0	7
-6	1	$1/2$	$1/2$	-8	1	0	0	7
-7	0	$1/2$	$1/2$	-8	1	0	0	8
-7	1	0	0	-8	1	0	0	8
-7	1	0	$1/2$	-8	1	0	0	8
-7	1	$1/2$	0	-8	1	0	0	8
-8	1	0	0	-8	1	0	0	9

Table B.2: The results of parameter configurations on T^2/Z_2 with $M_{ab} < 0$, $M_{ca} > 0$.

T^2/Z_2 with $M_{ab} < 0$, $M_{ca} > 0$								
ab-sector				ca-sector				bc-sector
M_{ab}	ω^i_{ab}	α_{ab}	β_{ab}	M_{ca}	ω^i_{ca}	α_{ca}	β_{ca}	# of Higgs
-4	0	0	0	4	0	0	0	$\boxed{1}$
-4	0	0	0	5	0	0	0	1
-4	0	0	0	5	0	0	1/2	1
-4	0	0	0	5	0	1/2	0	1
-4	0	0	0	5	1	1/2	1/2	1
-5	0	0	0	5	0	0	0	$\boxed{1}$
-5	0	0	1/2	5	0	0	1/2	$\boxed{1}$
-5	0	1/2	0	5	0	1/2	0	$\boxed{1}$
-5	1	1/2	1/2	5	1	1/2	1/2	$\boxed{1}$
-4	0	0	0	6	0	0	1/2	1
-4	0	0	0	6	0	1/2	0	1
-4	0	0	0	6	0	1/2	1/2	1
-4	0	0	0	6	1	0	1/2	1
-4	0	0	0	6	1	1/2	0	1
-4	0	0	0	6	1	1/2	1/2	1
-5	0	0	0	6	0	0	1/2	1
-5	0	0	0	6	0	1/2	0	1
-5	0	0	1/2	6	0	0	1/2	1
-5	0	0	1/2	6	0	1/2	1/2	1
-5	0	1/2	0	6	0	1/2	0	1
-5	0	1/2	0	6	0	1/2	1/2	1
-5	0	0	0	6	1	1/2	1/2	1
-5	0	0	1/2	6	1	1/2	0	1
-5	0	1/2	0	6	1	0	1/2	1
-5	1	1/2	1/2	6	1	0	1/2	1
-5	1	1/2	1/2	6	1	1/2	0	1
-5	1	1/2	1/2	6	1	1/2	1/2	1
-6	0	0	1/2	6	0	0	1/2	$\boxed{1}$
-6	0	1/2	0	6	0	1/2	0	$\boxed{1}$
-6	0	1/2	1/2	6	0	1/2	1/2	$\boxed{1}$
-6	1	0	1/2	6	1	0	1/2	$\boxed{1}$
-6	1	1/2	0	6	1	1/2	0	$\boxed{1}$
-6	1	1/2	1/2	6	1	1/2	1/2	$\boxed{1}$
-4	0	0	0	7	0	1/2	1/2	1
-4	0	0	0	7	1	0	0	1
-4	0	0	0	7	1	0	1/2	1
-4	0	0	0	7	1	1/2	0	1

T^2/Z_2 with $M_{ab} < 0$, $M_{ca} > 0$								
ab-sector				ca-sector				bc-sector
M_{ab}	ω^i_{ab}	α_{ab}	β_{ab}	M_{ca}	ω^i_{ca}	α_{ca}	β_{ca}	# of Higgs
-5	0	0	0	7	0	1/2	1/2	1
-5	0	0	1/2	7	0	1/2	1/2	1
-5	0	1/2	0	7	0	1/2	1/2	1
-5	0	0	0	7	1	0	1/2	1
-5	0	0	0	7	1	1/2	0	1
-5	0	0	1/2	7	1	0	0	1
-5	0	0	1/2	7	1	1/2	0	1
-5	0	1/2	0	7	1	0	0	1
-5	0	1/2	0	7	1	0	1/2	1
-5	1	1/2	1/2	7	1	0	0	1
-5	1	1/2	1/2	7	1	0	1/2	1
-5	1	1/2	1/2	7	1	1/2	0	1
-6	0	0	1/2	7	0	1/2	1/2	1
-6	0	1/2	0	7	0	1/2	1/2	1
-6	0	1/2	1/2	7	0	1/2	1/2	1
-6	0	0	1/2	7	1	1/2	0	1
-6	0	1/2	0	7	1	0	1/2	1
-6	0	1/2	1/2	7	1	0	0	1
-6	1	0	1/2	7	1	0	0	1
-6	1	0	1/2	7	1	0	1/2	1
-6	1	1/2	0	7	1	0	0	1
-6	1	1/2	0	7	1	1/2	0	1
-6	1	1/2	1/2	7	1	0	1/2	1
-6	1	1/2	1/2	7	1	1/2	0	1
-7	0	1/2	1/2	7	0	1/2	1/2	$\boxed{1}$
-7	1	0	0	7	1	0	0	$\boxed{1}$
-7	1	0	1/2	7	1	0	1/2	$\boxed{1}$
-7	1	1/2	0	7	1	1/2	0	$\boxed{1}$
-4	0	0	0	8	1	0	0	1
-5	0	0	0	8	1	0	0	1
-5	0	0	1/2	8	1	0	0	1
-5	0	1/2	0	8	1	0	0	1
-5	1	1/2	1/2	8	1	0	0	1
-6	0	0	1/2	8	1	0	0	1
-6	0	1/2	0	8	1	0	0	1
-6	0	1/2	1/2	8	1	0	0	1
-6	1	0	1/2	8	1	0	0	1
-6	1	1/2	0	8	1	0	0	1

T^2/Z_2 with $M_{ab} < 0$, $M_{ca} > 0$								
ab-sector				ca-sector				bc-sector
M_{ab}	ω^i_{ab}	α_{ab}	β_{ab}	M_{ca}	ω^i_{ca}	α_{ca}	β_{ca}	# of Higgs
-6	1	$1/2$	$1/2$	8	1	0	0	1
-7	0	$1/2$	$1/2$	8	1	0	0	1
-7	1	0	0	8	1	0	0	1
-7	1	0	$1/2$	8	1	0	0	1
-7	1	$1/2$	0	8	1	0	0	1
-8	1	0	0	8	1	0	0	$\boxed{1}$

Bibliography

[1] **ATLAS** Collaboration, G. Aad *et al.*, *Observation of a new particle in the search for the Standard Model Higgs boson with the ATLAS detector at the LHC*, *Phys.Lett.* **B716** (2012) 1–29, [1207.7214].

[2] **CMS** Collaboration, S. Chatrchyan *et al.*, *Observation of a new boson at a mass of 125 GeV with the CMS experiment at the LHC*, *Phys.Lett.* **B716** (2012) 30–61, [1207.7235].

[3] **Particle Data Group** Collaboration, K. A. Olive *et al.*, *Review of Particle Physics*, *Chin. Phys.* **C38** (2014) 090001.

[4] H. Fritzsch, *Weak Interaction Mixing in the Six - Quark Theory*, *Phys. Lett.* **B73** (1978) 317–322.

[5] H. Fritzsch, *Quark Masses and Flavor Mixing*, *Nucl. Phys.* **B155** (1979) 189–207.

[6] M. Fukugita, M. Tanimoto, and T. Yanagida, *Phenomenological lepton mass matrix*, *Prog. Theor. Phys.* **89** (1993) 263–268.

[7] M. Fukugita, M. Tanimoto, and T. Yanagida, *Atmospheric neutrino oscillation and a phenomenological lepton mass matrix*, *Phys. Rev.* **D57** (1998) 4429–4432, [hep-ph/9709388].

[8] M. Fukugita, M. Tanimoto, and T. Yanagida, *Predictions from the Fritzsch type lepton mass matrices*, *Phys. Lett.* **B562** (2003) 273–278, [hep-ph/0303177].

[9] M. Fukugita, Y. Shimizu, M. Tanimoto, and T. T. Yanagida, θ_{13} *in neutrino mass matrix with the minimal texture*, *Phys. Lett.* **B716** (2012) 294–297, [1204.2389].

[10] M. Fukugita, Y. Kaneta, Y. Shimizu, M. Tanimoto, and T. T. Yanagida, *CP violating phase from minimal texture neutrino mass matrix: Test of the phase relevant to leptogenesis*, *Phys. Lett.* **B764** (2017) 163–166, [1609.01864].

[11] C. D. Froggatt and H. B. Nielsen, *Hierarchy of Quark Masses, Cabibbo Angles and CP Violation*, *Nucl. Phys.* **B147** (1979) 277–298.

[12] M. Kobayashi and T. Maskawa, *CP Violation in the Renormalizable Theory of Weak Interaction*, *Prog. Theor. Phys.* **49** (1973) 652–657.

[13] H. Ishimori, T. Kobayashi, H. Ohki, Y. Shimizu, H. Okada, and M. Tanimoto, *Non-Abelian Discrete Symmetries in Particle Physics*, *Prog. Theor. Phys. Suppl.* **183** (2010) 1–163, [1003.3552].

[14] P. F. Harrison, D. H. Perkins, and W. G. Scott, *Tri-bimaximal mixing and the neutrino oscillation data*, *Phys. Lett.* **B530** (2002) 167, [hep-ph/0202074].

[15] S. F. King, A. Merle, S. Morisi, Y. Shimizu, and M. Tanimoto, *Neutrino Mass and Mixing: from Theory to Experiment*, *New J. Phys.* **16** (2014) 045018, [1402.4271].

[16] **Daya Bay** Collaboration, F. P. An *et al.*, *Observation of electron-antineutrino disappearance at Daya Bay*, *Phys. Rev. Lett.* **108** (2012) 171803, [1203.1669].

[17] P. Ramond, R. G. Roberts, and G. G. Ross, *Stitching the Yukawa quilt*, *Nucl. Phys.* **B406** (1993) 19–42, [hep-ph/9303320].

[18] K. Harigaya, M. Ibe, and T. T. Yanagida, *Seesaw Mechanism with Occam's Razor*, *Phys. Rev.* **D86** (2012) 013002, [1205.2198].

[19] M. Tanimoto and T. T. Yanagida, *Occam's Razor in Quark Mass Matrices*, *PTEP* **2016** (2016), no. 4 043B03, [1601.04459].

[20] Y. Kaneta, Y. Shimizu, M. Tanimoto, and T. T. Yanagida, *Occam's Razor in Lepton Mass Matrices - The Sign of Universe's Baryon Asymmetry* -, 1604.03315.

[21] Y. Shimizu and Y. Tatsuta, *Edge of a cliff*, *JHEP* **10** (2016) 040, [1608.00200].

[22] G. Altarelli, F. Feruglio, I. Masina, and L. Merlo, *Repressing Anarchy in Neutrino Mass Textures*, *JHEP* **11** (2012) 139, [1207.0587].

[23] L. Randall and R. Sundrum, *A Large mass hierarchy from a small extra dimension*, *Phys. Rev. Lett.* **83** (1999) 3370–3373, [hep-ph/9905221].

[24] N. Arkani-Hamed, S. Dimopoulos, and G. R. Dvali, *The Hierarchy problem and new dimensions at a millimeter*, *Phys. Lett.* **B429** (1998) 263–272, [hep-ph/9803315].

[25] N. Arkani-Hamed, S. Dimopoulos, G. R. Dvali, and J. March-Russell, *Neutrino masses from large extra dimensions*, *Phys. Rev.* **D65** (2002) 024032, [hep-ph/9811448].

[26] K. Agashe, G. Perez, and A. Soni, *Flavor structure of warped extra dimension models*, *Phys. Rev.* **D71** (2005) 016002, [hep-ph/0408134].

[27] G. Altarelli and F. Feruglio, *Tri-bimaximal neutrino mixing from discrete symmetry in extra dimensions*, *Nucl. Phys.* **B720** (2005) 64–88, [hep-ph/0504165].

[28] L. E. Ibanez and A. M. Uranga, *String theory and particle physics: An introduction to string phenomenology*. Cambridge University Press, 2012.

[29] D. Cremades, L. E. Ibanez, and F. Marchesano, *Computing Yukawa couplings from magnetized extra dimensions*, *JHEP* **05** (2004) 079, [hep-th/0404229].

[30] H. Abe, T. Kobayashi, and H. Ohki, *Magnetized orbifold models*, *JHEP* **09** (2008) 043, [0806.4748].

[31] T.-H. Abe, Y. Fujimoto, T. Kobayashi, T. Miura, K. Nishiwaki, and M. Sakamoto, *Z_N twisted orbifold models with magnetic flux*, *JHEP* **01** (2014) 065, [1309.4925].

[32] T.-h. Abe, Y. Fujimoto, T. Kobayashi, T. Miura, K. Nishiwaki, and M. Sakamoto, *Operator analysis of physical states on magnetized T^2/Z_N orbifolds*, *Nucl. Phys.* **B890** (2014) 442–480, [1409.5421].

[33] H. Abe, K.-S. Choi, T. Kobayashi, and H. Ohki, *Three generation magnetized orbifold models*, *Nucl. Phys.* **B814** (2009) 265–292, [0812.3534].

[34] H. Abe, T. Kobayashi, H. Ohki, A. Oikawa, and K. Sumita, *Phenomenological aspects of 10D SYM theory with magnetized extra dimensions*, *Nucl. Phys.* **B870** (2013) 30–54, [1211.4317].

[35] H. Abe, K.-S. Choi, T. Kobayashi, and H. Ohki, *Non-Abelian Discrete Flavor Symmetries from Magnetized/Intersecting Brane Models*, *Nucl. Phys.* **B820** (2009) 317–333, [0904.2631].

[36] H. Abe, T. Kobayashi, H. Ohki, K. Sumita, and Y. Tatsuta, *Non-Abelian discrete flavor symmetries of 10D SYM theory with magnetized extra dimensions*, *JHEP* **06** (2014) 017, [1404.0137].

[37] H. Abe, K.-S. Choi, T. Kobayashi, and H. Ohki, *Higher Order Couplings in Magnetized Brane Models*, *JHEP* **06** (2009) 080, [0903.3800].

[38] H. Abe, T. Kobayashi, H. Ohki, and K. Sumita, *Superfield description of 10D SYM theory with magnetized extra dimensions*, *Nucl. Phys.* **B863** (2012) 1–18, [1204.5327].

[39] Y. Fujimoto, T. Kobayashi, T. Miura, K. Nishiwaki, and M. Sakamoto, *Shifted orbifold models with magnetic flux*, *Phys. Rev.* **D87** (2013), no. 8 086001, [1302.5768].

[40] H. Abe, T. Kobayashi, H. Ohki, K. Sumita, and Y. Tatsuta, *Flavor landscape of 10D SYM theory with magnetized extra dimensions*, *JHEP* **04** (2014) 007, [1307.1831].

[41] H. Abe, T. Kobayashi, K. Sumita, and Y. Tatsuta, *Supersymmetric models on magnetized orbifolds with flux-induced Fayet-Iliopoulos terms*, *Phys. Rev.* **D95** (2017), no. 1 015005, [1610.07730].

[42] T.-h. Abe, Y. Fujimoto, T. Kobayashi, T. Miura, K. Nishiwaki, M. Sakamoto, and Y. Tatsuta, *Classification of three-generation models on magnetized orbifolds*, *Nucl. Phys.* **B894** (2015) 374–406, [1501.02787].

[43] Y. Fujimoto, T. Kobayashi, K. Nishiwaki, M. Sakamoto, and Y. Tatsuta, *Comprehensive analysis of Yukawa hierarchies on T^2/Z_N with magnetic fluxes*, *Phys. Rev.* **D94** (2016), no. 3 035031, [1605.00140].

[44] H. Abe, T. Kobayashi, K. Sumita, and Y. Tatsuta, *Gaussian Froggatt-Nielsen mechanism on magnetized orbifolds*, *Phys. Rev.* **D90** (2014), no. 10 105006, [1405.5012].

[45] N. Marcus, A. Sagnotti, and W. Siegel, *Ten-dimensional Supersymmetric Yang-Mills Theory in Terms of Four-dimensional Superfields*, *Nucl. Phys.* **B224** (1983) 159.

[46] N. Arkani-Hamed, T. Gregoire, and J. G. Wacker, *Higher dimensional supersymmetry in 4-D superspace*, *JHEP* **03** (2002) 055, [hep-th/0101233].

[47] K.-S. Choi and J. E. Kim, *Quarks and leptons from orbifolded superstring*, *Lect. Notes Phys.* **696** (2006) 1–406.

[48] L. E. Ibanez and A. M. Uranga, *Neutrino Majorana Masses from String Theory Instanton Effects*, *JHEP* **03** (2007) 052, [hep-th/0609213].

[49] R. Blumenhagen, M. Cvetic, and T. Weigand, *Spacetime instanton corrections in 4D string vacua: The Seesaw mechanism for D-Brane models*, *Nucl. Phys.* **B771** (2007) 113–142, [hep-th/0609191].

[50] Z.-z. Xing, H. Zhang, and S. Zhou, *Updated Values of Running Quark and Lepton Masses*, *Phys. Rev.* **D77** (2008) 113016, [0712.1419].

[51] Y. Hamada and T. Kobayashi, *Massive Modes in Magnetized Brane Models*, *Prog. Theor. Phys.* **128** (2012) 903–923, [1207.6867].

早稲田大学　博士（理学）　学位申請　研究業績書

氏 名　　龍田　佳幸　　印

（2017 年　1 月　現在）

種 類 別	題名、　発表・発行掲載誌名、　発表・発行年月、　連名者（申請者含む）
○論文	Comprehensive analysis of Yukawa hierarchies on T^2/Z_N with magnetic fluxes, Phys. Rev. D 94 (2016) no.3, 035031, Yukihiro Fujimoto, Tatsuo Kobayashi, Kenji Nishiwaki, Makoto Sakamoto, Yoshiyuki Tatsuta
○論文	Classification of three-generation models on magnetized orbifolds, Nucl. Phys. B 894 (2015) 374-406, Tomo-hiro Abe, Yukihiro Fujimoto, Tatsuo Kobayashi, Takashi Miura, Kenji Nishiwaki, Makoto Sakamoto, Yoshiyuki Tatsuta
○論文	Gaussian Froggatt-Nielsen mechanism on magnetized orbifolds, Phys. Rev. D 90 (2014), 105006, Hiroyuki Abe, Tatsuo Kobayashi, Keigo Sumita, Yoshiyuki Tatsuta
論文	Supersymmetric models on magnetized orbifolds with flux-induced Fayet-Iliopoulos terms, Phys. Rev. D 95 (2016), 015005, Hiroyuki Abe, Tatsuo Kobayashi, Keigo Sumita, Yoshiyuki Tatsuta
論文	Edge of a cliff, JHEP 1610 (2016) 040, Yusuke Shimizu, Yoshiyuki Tatsuta
論文	Double Froggatt-Nielsen mechanism, Prog. Theor. Exp. Phys. (2016) 083B05, Kenji Nishiwaki, Yusuke Shimizu, Yoshiyuki Tatsuta
論文	Majorana neutrino mass structure induced by rigid instantons on toroidal orbifold, Phys. Rev. D 93 (2016) no.6, 065029, Tatsuo Kobayashi, Yoshiyuki Tatsuta, Shohei Uemura
論文	D-brane instanton induced μ-terms and their hierarchical structure, Phys. Rev. D 92 (2015) no.2, 026001, Hiroyuki Abe, Tatsuo Kobayashi, Yoshiyuki Tatsuta, Shohei Uemura
論文	Non-Abelian discrete flavor symmetries of 10D SYM theory with magnetized extra dimensions, JHEP 1406 (2014) 017, Hiroyuki Abe, Tatsuo Kobayashi, Hiroshi Ohki, Keigo Sumita, Yoshiyuki Tatsuta
論文	Flavor landscape of 10D SYM theory with magnetized extra dimensions, JHEP 1404 (2014) 007, Hiroyuki Abe, Tatsuo Kobayashi, Hiroshi Ohki, Keigo Sumita, Yoshiyuki Tatsuta

早稲田大学　博士（理学）　学位申請　研究業績書

種 類 別	題名、　発表・発行掲載誌名、　発表・発行年月、　連名者（申請者含む）
講演	Yoshiyuki Tatsuta, Testabilities of Occam's razor approaches in lepton mass matrices, HU-IBS Sapporo Summer Institute on Particle Physics and Cosmology, Sapporo, Aug 2016
講演	Yoshiyuki Tatsuta, Majorana neutrino mass matrices induced by rigid E-brane instantons, PASCOS 2016, Quy Nhon, Jul 2016
講演	Yoshiyuki Tatsuta, Elliptic inflation from intersecting/magnetized brane models, Particle Cosmology and beyond 2015, Kanazawa, Nov 2015
講演	Yoshiyuki Tatsuta , Inflation through Yukawa couplings in magnetized extra dimensions , KIAS-CFHEP Workshop and the 5th KIAS Workshop on Particle Physics and Cosmology, Seoul, Nov 2015
講演	龍田佳幸, Getting just the minimal supersymmetric standard model from magnetized D-branes, 日本物理学会　2015 年秋季大会，大阪，2015 年 9 月
講演	龍田佳幸, Yukawa couplings and phenomenological implications on magnetized orbifolds, 日本物理学会　第 70 回年次大会，東京，2015 年 3 月
講演	Yoshiyuki Tatsuta , Three-generations and Yukawa couplings on magnetized orbifolds, Ibaraki, Jan 2015
講演	龍田佳幸, Flavor structures in magnetized orbifold models, 日本物理学会　2014 年秋季大会，佐賀，2014 年 9 月
講演	Yoshiyuki Tatsuta, Gaussian Froggatt-Nielsen mechanism from magnetized extra dimensions, SI 2014, Yamanashi, Aug 2014
講演	Yoshiyuki Tatsuta, Non-Abelian discrete flavor symmetries on general magnetized background, PASCOS 2014, Poland, Jul 2014
講演	Keigo Sumita , Gaussian Froggatt-Nielsen mechanism from magnetized extra dimensions, PASCOS 2014, Poland, Jul 2014

早稲田大学　博士（理学）　学位申請　研究業績書

種 類 別	題名、　発表・発行掲載誌名、　発表・発行年月、　連名者（申請者含む）
講演	龍 田 佳 幸 , Gaussian textures of Yukawa couplings from magnetized extra dimensions, 日本物理学会　第 69 回年次大会, 神奈川, 2014 年 3 月
講演	龍田佳幸, 磁場をもつ 10 次元 SYM 理論におけるフレーバー対称性, 卓越した大学院拠点形成支援補助金事業シンポジウム, 東京, 2013 年 12 月
講演	龍田佳幸, Non-Abelian discrete flavor symmetry from magnetized extra dimensions, 日本物理学会　2013 年秋季大会, 高知, 2013 年 9 月
講演	Yoshiyuki Tatsuta, Non-Abelian discrete flavor symmetry from magnetized extra dimensions, SI 2013, Pusan, Aug 2013
講演	龍田佳幸, Flavor landscape of 10D SYM theory with general magnetic fluxes, 日本物理学会　第 68 回年次大会, 広島, 2013 年 3 月